NON-SIMILAR SOLUTION OF MIXED CONVECTION FROM A TRIANGULAR FIN EMBEDDED IN POROUS MEDIUM

By

NABEEL MOUSA AHMAD ABU-RUMMAN

Supervised By

Dr. NASRI J. RABADI

Submitted in partial fulfillment of the requirements for the degree of

Master of Science in Mechanical Engineering
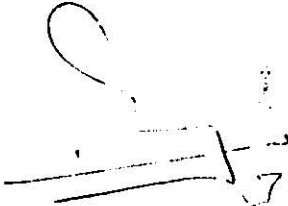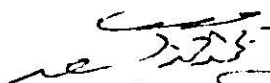
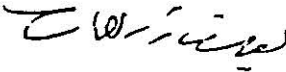Faculty of Graduate Studies

University of Jordan

Amman, Jordan

May, 1991

نوقشت هذه الرسالة بتاريخ ١٩٩١/٥/١٤م وأجيزت .

لجنة المناقشة
----

١) د. نصري جبرائيل الربضي / مقرراً

٢) اُ.د. محمد أحمد السعد / عضواً

٣) د. محمود سليم عوده / عضواً

٤) د. يوسف حسن زريقات / عضواً

To the people of Iraq

To all the unknown people who work faithfully hard toward the reunion and progress of this great nation

Acknowledgement

I would like to express my deep gratitude to my supervisor Dr. Nasri Rabadi who through his guidance, encouragement and support this work is enabled to be accomplished.

My special thanks and appreciation to my parents who raised me to this point that I am able to perform this research. Also, I would like to thank all my friends for their encouragement. I will not forget here to thank Miss . H. Khadrou at the mechanical engineering department, Mr. A. Abu-Rumman at the library, Dr. B. Kahalleh and Mr. Abu-Mustafa at the computer laboratory.

Contents

List of Figures

Nomenclature

A,   constant defined in Equation (3.6 b);

AF,   aiding flows;

B,   constant defined in Equation (3.7a);

c,   constant of integration;

C,   specific heat of convicted fluid;

f,   dimensionless stream function defined by Equation (3.16);

f',   dimensionless velocity in streamwise direction;

g,   acceleration due to gravity;

g_x, g_y,   gravitational acceleration in x and y directions;

G,   auxiliary velocity function, $(= \partial f / \partial \zeta)$;

Gr,   Grashof number at L , $Gr = g|T_w - T_\infty|\beta K L / \nu^2$;

h,   local heat transfer coefficient;

IW,   isothermal walls;

K,   permeability of the porous medium;

k_f,   thermal conductivity of the convicted fluid;

k_m,   thermal conductivity of the saturated porous medium;

و بمقارنة هذا العمل مع اعمال سابقة حصل فيها على حفر

تشابهية لاسطح عمودية او مائلة او افقية و جد تشابثا ممتـــازا .

Abstract

The mixed convection boundary layer from inclined impermeable flat surfaces bounding saturated porous medium is studied. Two configurations are considered: One where the porous medium is located above the flat surface and the other the porous medium is located below the flat surface. The wall temperature and the free stream velocity are functions of the streamwise distance from the leading edge. Both components of the buoyancy forces are retained.

The momentum and thermal boundary layers are found to be non-similar. Non-similarity solutions using the local non-similarity method are obtained. The analysis admits the inclination to range from vertical to horizontal. The problem is found to involve a lot of parameters: The mixed convection; the inclination; the Rayleigh number; the Peclet number; the exponent of the wall temperature variation; the exponent of the free stream velocity variation and the streamwise location parameters.

Analytical expressions for the dimensionless heat flux, the dimensionless heat transfer coefficient, the local Nusselt number, the local dimensionless thermal boundary layer thickness, the average Nusselt number and the dimensionless total heat transfer rate are obtained. Distributions of the dimensionless velocity and temperature with the vertical to the wall coordinate are drawn. Distributions of the heat flux, the Nusselt number and the thermal boundary layer thickness with the dimensionless streamwise coordinate are drawn. Numeric values of the average Nusselt number and the total heat transfer rate are obtained. These distributions and numbers are obtained for selected parameter values

for two cases: One considering isothermal walls and the other considering linear wall temperature variations. Comparison with previous works shows excellent agreement.

Chapter 1

INTRODUCTION

1.1 Introduction

The problem of convection in porous medium has in the last two decades attracted the attention of many researchers for it's important applications in many engineering-related fields. The most important of these is the geothermal energy utilization.

Due to the increasing costs and rapid depletion of the resources of oil, man began searching for other energy resources. It is believed that if all the available geothermal resources being utilized, this can contribute significantly to the total world energy supply. Volcanic movements may cause in the formation of geothermal reservoirs where magmatic intrusion may occur. The intrusive magma may take the shape of inclined wall. If the intruded magma is trapped in an aquifer where permeable formations with a fluid (groundwater) both exist, the hot intrusive heats the meteoric water which is then driven upward by buoyancy to shallow depths of the earth's crust where the production wells exist [1].

Several body shapes immersed in porous medium have been considered by researchers. These are spheres, cylinders and flat plates. The last two may be horizontal, inclined or vertical. In addition, axi-symmetric and two- dimensional body shapes have also been considered. Many of the previous works considered free convection from these bodies and fewer considered mixed or forced convection. Also, most of the previous works obtained similarity solutions for special cases of similar boundary layers. For the general cases, solutions were obtained using the finite difference or the local non-similarity methods for non-similar boundary layers.

Most of the previous works which studied inclined walls had two main restrictions on their works. Special cases have been studied where similarity solutions are possible, and/or they neglected the buoyancy force component normal to the surface.

By neglecting the normal buoyancy force component, the momentum equation will be most applicable for vertical walls where the normal buoyancy vanishes and only the streamwise buoyancy force will exist. The applicability will decrease as the inclination from the vertical increases and will break down for horizontal walls. For horizontal walls only the normal buoyancy force component exists. So, the works which neglect the normal buoyancy and obtained similarity solutions, regardless of their ungenerality, are applicable only for vertical walls or walls with small inclinations from the vertical. By solving for non-similar boundary layers and retaining the normal buoyancy force component, these restrictions are removed. We are no more solving for special cases and the inclinations could range all the way from vertical to horizontal.

In this research the problem of mixed convection from the inclined impermeable walls of a triangular fin (wedge configuration) in saturated porous medium will be an-

alyzed. The mixed convection parameter (i.e. Gr/Re) will allow the convection to be forced for a (Gr/Re) value of zero, mixed as the value increases, or free at (Gr/Re) limit value of infinity. This analysis permits the inclinations of the inclined walls to range from 0° to 90° which includes vertical and horizontal walls besides inclined walls. Both the normal and the streamwise components of the buoyancy force will be retained which allows this range of inclination. The analysis assumes power law variations from leading edge of both wall temperature and free stream velocity. This is, to the author's knowledge, the first work that analyzes non-similar boundary layers of mixed convection from inclined walls in porous medium where both buoyancy components are retained.

It is very important to note that the applicability of this research applies for any configuration where inclined wall of any angle is embedded in saturated porous media. This wall is not for necessity being a fin.

1.2 Similar and Non-Similar Boundary-Layers

Many boundary layer problems do not admit similarity. The similarity or non-similarity concepts may occur in the momentum, the thermal boundary layers, or both. However, non-similarity in one field will cause non-similarity in the other field if the momentum and the energy equations are coupled. In the following we will discuss the concept of similarity.

It is said that the velocity and thermal boundary layers are similar if we can find two pairs of scale factors, one for each field, that upon applying them in the ordinate y and the abscissa u or $(T - T_\infty)$, the scaled velocity and temperature profiles, at any streamwise position x, are identical [2], where u is the streamwise velocity component; T is the temperature and T_∞ is the temperature at infinity. Hence, upon using the similarity transformation, the dimensionless velocity and temperature will both be only functions of the scaled (stretched) dimensionless coordinate.

Another way to describe similarity is to say that two velocity or temperature profiles located at different streamwise locations differ only by scale factors in u and y for the velocity field, or $(T - T_\infty)$ and y for the temperature field [3].

The requirement for similarity at two arbitrary streamwise positions x_1 and x_2 can be shown in the following relation

$$\frac{u(x_1, [y/g(x_1)])}{u_\infty(x_1)} = \frac{u(x_2, [y/g(x_2)])}{u_\infty(x_2)} \qquad (1.1)$$

for the velocity field, or

$$\frac{(T - T_\infty)(x_1, [y/g(x_1)])}{(T_w - T_\infty)(x_1)} = \frac{(T - T_\infty)(x_2, [y/g(x_2)])}{(T_w - T_\infty)(x_2)} \qquad (1.2)$$

for the temperature field, where $g(x)$ is the scale factor for y.

In the present problem both momentum and energy equations are coupled and non-similar boundary layers exist. The dimensionless velocity (i.e. $f'(\eta, \xi) = u/u_\infty$), and the dimensionless temperature (i.e. $\theta(\eta, \xi) = (T - T_\infty)/(T_w - T_\infty)$) are both functions of two independent variables (i.e η and ξ). Wherein, in the case of similarity, both the dimensionless velocity and temperature are functions of only one independent variable (i.e. η). So, the existence of ξ in the momentum or energy equations makes the velocity and the thermal boundary layers both non-similar (dependent on the streamwise location) through coupling.

The method of local non-similarity solutions for velocity boundary layers for several non-similar problems was described by Sparrow et al. [4]. They mentioned that non-similarities in velocity boundary layers stem from one or more of the following three factors: 1) Free stream velocity, 2) Surface mass flux and 3) Transverse curvature. An early study that describes the method of local non-similarity solutions for thermal boundary layers for several non-similar problems was published by Sparrow and Yu [5] . The reasons for non-similarity in thermal boundary layers may be caused by streamwise variation in surface temperature, surface heat flux, and/or volume heat generation. The works by Minkowycz and Sparrow [6] and Chen and Mucoglu [7] are two early examples of the numerous applications of the method.

1.3 Darcy's Law

It was found by Darcy in the year 1856 that the volume flow rate of water V, in a column of sand of length ΔL is proportional to the piezometric head Δh and the column cross sectional area A, and inversely proportional to the length of the column [1,8,9], that is

$$V \sim A\frac{\Delta h}{\Delta L} \tag{1.3}$$

In differential form

$$u = \frac{V}{A} = -K_c\frac{dh}{dL} = -K_c\frac{d}{dL}(p/\rho g + Z) \tag{1.4}$$

where K_c is the hydraulic conductivity, u is Darcy's velocity, Z is the distance measured vertically upward from an arbitrarily chosen datum level, p is the hydrostatic pressure, ρ is the density of the fluid, and g is the acceleration due to gravity. Further, it was found experimentally [1] that

$$K_c \sim \frac{\rho g}{\mu} \tag{1.5}$$

where μ is the dynamic viscosity of the fluid. So, Equation (1.4) can be put in a final form

$$\bar{u} = -(K/\mu)(\nabla p - \rho\bar{g}) \tag{1.6}$$

where K is the permeability of the saturated porous media, $\bar{u}$ is the velocity vector and $\bar{g}$ is the gravitational acceleration vector. Darcy's law is applicable for low permeability and porosity of the porous medium for which Reynold number, $Re = \rho u\sqrt{K}/\mu$, is less than unity [1].

Later, some researchers [10-15] used several modified equations based on Darcy's law in which the effects of inertia and boundary on convective flows in porous medium are included.

In the present work, Darcy's law will be applied.

الصفحة غير موجودة من أصل المصدر

Chapter 2

LITERATURE SURVEY

2.1 Introduction

Due to it's significant importance in geothermal energy and other engineering-related applications, the problem of convection in porous media has attracted a large volume of research. These problems range from free through mixed to forced convection. Different configurations bounding porous media have been subjected to study. These configurations range from vertical through inclined to horizontal flat plates. Also, cylindrical and spherical configurations have been examined. These surfaces may be permeable where injection or withdrawal of a fluid exists.

2.2 Numerical Solutions

Extensive numerical investigations of the convective heat transfer problems in porous medium have been conducted by a number of researchers during the last two decades. Two main approximate numerical methods have been used. These are finite-difference and local non-similarity. For the simplified similarity boundary layer analysis, direct integrations using Runge-Kutta methods are used.

399031

9

2.2.1 Free convection

Free convection in porous media has important applications in geothermal reservoirs. The bounding surfaces may be vertical, inclined, or horizontal flat plates. Also, curvature effects may be involved for cylindrical and spherical surfaces. These surfaces may be permeable or impermeable. The works considering vertical surfaces will first be reviewed .

Vertical surfaces

Cheng [16] considered permeable surfaces where the wall temperature and the injection or withdrawal velocities vary as power law functions of streamwise variable. Here, similarity solutions were obtained. The solutions were performed for a special case in which the prescribed wall temperature and the surface mass flux velocity vary as x^λ and $x^{(\lambda-1)/2}$, respectively . Velocity profiles, temperature profiles, heat transfer rate, and boundary layer thickness against the mass flux parameter are found for $\lambda = 0$, $1/3$, and 1.

Minkowycz and Cheng [17] considered the same problem in [16] but local non-similarity solutions for the non-similar boundary layer were obtained. The effects of the surface mass flux on temperature profiles, heat transfer rate, and thermal boundary layer thickness were studied. Comparison with previous works using the finite-difference method showed excellent agreement.

Conjugate free convection from vertical plate fins in porous media was studied by Pop et al. [18]. Similarity solutions were obtained for plate heat sources and circular heat sources. Stream function, temperature profiles, and temperature gradients were studied for both cases. Analytical expressions were also obtained for local Nusselt number, local

surface heat flux, and thermal boundary layer thickness.

Similar problem to [16] but considering conjugate problem was studied by Liu and Minkowycz [19]. The governing parameter for this problem were found to be the convection-conduction parameter (which represents the ratio of convective effects to fin conductance) and the lateral mass flux parameter. Non-similar solutions were obtained using the local non-similarity method. Effects of mass flux on fin temperature distributions, boundary layer thickness, local heat transfer coefficient, local heat flux, and total heat transfer rate were studied. It was found that injection of a fluid at the fin surface increases the boundary layer thickness, while increases fin temperature variation, local heat transfer coefficient, local heat flux, and total heat transfer rate. Withdrawal had reverse effects.

Inclined surfaces

Free convection over inclined isothermal walls were considered by Jang and Chang [20]. An implicit finite difference method was used to solve the governing equations. Both normal and streamwise components of buoyancy force were retained. Heat and mass buoyancies were assumed to exist. The range of applicability of inclination ranges from 0° to 90°. It was found that as inclination from horizontal increases, both heat and mass transfer rates increase. Comparison with previous works where similarity solutions were obtained, for normal buoyancy component neglected equations, showed these similarity solutions may under predict the heat and mass transfer rates for small inclination parameter values.

Horizontal surfaces

Horizontal surfaces in porous media where considered by Cheng and Chang [21]. Power law variation of wall temperature of the streamwise variable from leading edge was assumed. Similarity solutions were obtained for convective fluid over heated surfaces or under cooled surfaces. Analytical expressions were obtained for boundary layer thickness, local and overall surface heat flux.

Surfaces with curvature

Merkin [22] analyzed free convection from axi-symmetric and two- dimensional bodies of arbitrary shape. Constant wall temperature was considered and it was shown that the governing equations allow similarity solution for any body shape. The obtained ordinary differential equations has been solved previously.

Vertical cylinders in porous media with injection or withdrawal of a fluid was considered by Yucel [23]. Constant wall temperature and constant wall heat flux were assumed. Finite difference solutions were obtained for temperature profiles and heat transfer rates for various values of a parameter relating the injection or withdrawal of fluid to combined transverse curvature and surface mass flux.

Conjugate analysis for vertical cylindrical fin which is permeable was performed by Liu et al. [24]. Non-similar solutions were obtained by the local non-similarity method. Effects of the surface mass flux, the convection-conduction parameter and surface curvature on temperature distributions and heat transfer characteristics were studied. It was found that higher values of convection-conduction parameter result in nonmonotonical

local heat transfer distributions. Withdrawal of fluid increases the fin temperature variation, the local heat transfer coefficient , the average heat transfer coefficient, the local heat flux, and the total heat transfer rate. Injection had reverse effects.

Effects of surface mass flux and surface transverse curvature on natural convective boundary layers were studied by Minkowycz and Sparrow [25]. Isothermal vertical cylinder with uniformly distributed surface mass flux were considered. The local non-similarity method was employed. The effects of the parameters characterizing the surface transverse curvature and surface mass transfer for Prandtl number ranging from 0.01 to 10 on local Nusselt numbers were studied. It was found that the local Nusselt numbers for a vertical cylinder are less sensitive to surface mass transfer in comparison with those for vertical plates. Higher Prandtl number results in higher sensitivity.

Free convection from vertical cylinders in porous media was also considered by Minkowycz and Cheng [26]. Surface temperature varies as power law variation. Analytical expressions for local surface heat flux and overall surface heat flux were obtained. Local similarity and local non-similarity solutions were obtained. Temperature and velocity profiles for several values of dimensionless streamwise variable were obtained for $\lambda = 0$, $1/2$ and 1. It was found that the local similarity solutions are sufficiently accurate compared to the local non-similarity solutions.

Nakayama et al. [27] analyzed free convection from nonisothermal curved surfaces. They applied non-Darcy law (Forchheimer) equation and neglected the normal buoyancy component. They converted the governing partial differential equations for a special case into ordinary differential equations and obtained similarity solutions. They found that similarity is obtained for Darcy flows when m and n, where m is an exponent associ-

ated with the body shape and n is an exponent associated with wall temperature, are constants. For non-Darcy flows similarity is obtained when $m = n$. Velocity and temperature profiles were obtained for Darcy and non-Darcy flows. An analytical expression for the local Nusselt number were derived. The resistance due to inertia tends to reduce the heat transfer rate.

2.2.2 Mixed convection

Mixed convection is obtained when the buoyancy affects the forced convection. Flows may occur in geothermal reservoirs due to the difference in hydrostatic heads resulting from recharge or discharge of meteoric water. Aiding or opposing flows may exist. Vertical wall configurations in porous media will first be reviewed.

Vertical surfaces

Darcy's law was applied to analyze conjugate vertical fins by Liu et al. [28]. Here, local non-similarity solutions were obtained. The parameters describing the problem was found to be Prandtl number, mixed convection (which represents a ratio of buoyancy to inertia forces) and convection-conduction parameters. The main result was that at high convection-conduction parameter, local heat transfer coefficient and local surface heat flux decreases and then increases as we move downstream.

More recently, Gill and Minkowycz [29] analyzed conjugate vertical fins. Here, a local non-similarity solution was obtained. The boundary and inertia forces were studied. It was found that neglecting boundary and inertia forces effects on heat transfer coefficient becomes more significant for higher mixed convection and convection-conduction parameters. These forces effects are less pronounced for forced convection specially downstream.

Ranganathan and Viskanta [30] applied a finite-difference scheme to solve for permeable surface bounding variable porosity media. They considered buoyancy-aided flow and took into account viscous and inertia forces. They found that these forces have significant effects on heat transfer rate and velocity profiles. It was also found that blowing at the surface affects velocity and temperature distributions while variable porosity has negligible effects.

Darcy's law was applied by Lai et al. [31] to analyze aiding and opposing flows in a vertical channel. The channel is bounded by an isothermal heated segment of finite length which is a part of a wall and an isothermally cooled wall. The free stream velocity is uniform. The governing equations were solved using a finite difference method. Rayleigh and Peclet numbers effects on the average and the overall heat transfer rates were studied. It was found that the local and overall heat transfer rates are complex functions of Rayleigh and Peclet numbers. In the free convection regime the heat transfer characteristics depend largely on the Rayleigh number.Increasing the Peclet number increases the heat transfer rate and moves the flow from free to forced convection and the average Nusselt number curve with Pe reaches a value of 0.5 in the forced convection regime .

Inclined surfaces

The works which considered mixed convection over inclined walls in porous media will be reviewed now. Only few investigations are published. Cheng [32] established the criteria for such a problem. Cheng obtained similarity solutions considering inclined wall (wedge) configuration. He assumed power law variations from leading edge of free stream velocity (i.e $u_\infty = Bx^n$) and wall temperature (i.e. $T_w = T_\infty \pm Ax^\lambda$), where u_∞ and T_∞

are the free stream velocity and temperature, respectively; T_w is the wall temperature; x is the streamwise coordinate; A and B are positive constants. The problem was solved for a special case where both free stream velocity exponent, n, and wall temperature exponent, λ, are equal (i.e. $\lambda = n$). He neglected the normal to the wall buoyancy component. His work is best applicable for vertical wall. The accuracy of his work decreases with increasing the inclination from vertical and breaks completely when only normal buoyancy to the wall exists. The parameter governing mixed convection from inclined wall in porous media was found by Cheng to be Gr/Re, where Gr is the modified Grashof number and Re is the Reynold number. Numerical results were obtained for isothermal (i.e. $\lambda = n = 0$) vertical walls and for inclined walls with an angle equals $\pi/4$ with free stream velocity and wall temperature power of 1/3 (i.e. $\lambda = n = 1/3$). Nusselt number, velocity and temperature profiles were obtained for several Gr/Re values for both aiding and opposing flows.

A similar problem to [32] was analyzed by Chandarsekhara et al. [33]. Permeability and thermal conductivity were both assumed to be functions of the normal to the wall direction. Also, a second order term accounting for boundary effects (viscous resistance) was included in the momentum equation. Similarity solutions were obtained for two special cases; uniform (i.e. $\lambda = n = 0$) and linear (i.e. $\lambda = n = 1$) variation of wall temperature. The effects of mixed convection and local porosity parameters on velocity profiles, temperature profiles, friction factor and heat transfer were studied. Velocity profiles obtained here differ from those obtained by Cheng [32] where slip was allowed. It was found that variable permeability and conductivity increases the heat transfer rate.

Horizontal surfaces

The criteria of mixed convection over horizontal plates in porous media was established by Cheng [34]. Temperature and free stream velocity vary as power law from leading edge. The mixed convection parameter was found to be $Ra/(Pe)^{3/2}$, where Ra is the Rayleigh number and Pe is the Peclet number. Similarity was found to exist when $\lambda = \frac{3n+1}{2}$. Similarity solutions, as special cases, were obtained for horizontal plate with n=0 and $\lambda = 1/2$ and stagnation point flows about horizontal flat plate with $n = 1$ and $\lambda = 2$. These values of λ and n were taken so that the governing equations are independent of the streamwise variable. The mixed convection parameter effect on velocity profiles, temperature profiles and Nusselt number were studied.

Minkowycz et al. [35] analyzed the same problem as [34] but non-similarity solutions were obtained. Velocity and temperature profiles for different values of the mixed convection parameter were obtained. Also, the variation of local Nusselt number against the mixed convection parameter was obtained.

The influence of surface mass flux (injection or withdrawal) on mixed convection over horizontal plates in porous media was analyzed among others by Lai and Kulacki [36]. Similarity solutions were obtained for mixed and free convections. It was found that heat transfer is enhanced by withdrawal of fluid from the surface and decreases by injection of fluid.

Surfaces with curvature

A different problem where conjugate mixed convection occurs over a cylindrical fin in porous media was analyzed by liu et al. [37]. Local non-similarity solutions were obtained. The convection-conduction, the mixed convection and the curvature parameters effects on fin temperature distributions, local heat transfer coefficients, local heat fluxes, total heat transfer rate and fin efficiency were reported.

2.3   Other Solutions

Integral method was used by Cheng [38] to study mixed convection over vertical and horizontal walls for such cases where similarity solutions were obtained before. Darcy law was employed and a second degree polynomial for the velocity and temperature profiles were assumed. Cheng found good agreement between the integral and the similarity solutions.

The integral method was also employed by Kaviany [39] to study the effects of the presence of a solid matrix on forced convection heat transfer rate from a flat plate. With the free stream velocity being constant, first and second order flow resistance terms due to the presence of the solid matrix are included in the momentum equation. These two terms are significant for small permeability. For high permeability, a shear stress term accounting for the presence of the boundary is also included. The flow moves through three regimes as the Reynold number and/or the permeability decrease. Regime one in which the presence of the solid matrix is not significant on the heat transfer rate. The second regime is the non-Darcian regime in which the thermal and momentum boundary layer thicknesses are of same order of magnitude. The third regime is the Darcian regime

in which the ratio of the thermal to momentum boundary layer thicknesses is larger than unity.

2.4   Experimental Works

Fand et al. [40] investigated natural convection from a horizontal cylinder in porous medium. The porous medium consists of glass spheres. Fluid was either water or silicone oil. Two subregions depending on Rayleigh number were noticed. The low Rayleigh number region corresponds to Darcy flow. The high Rayleigh number region corresponds to Forchheimer flow. In each region the Nusselt number behaves differently. Correlations for the Nusselt number for each region were presented.

Inclined porous layer in which natural convection occurs was studied experimentally by Inaba et al. [41]. The layer was bounded by four walls (cavity) and filled with fluid and spherical particles. Two walls were isothermal but at different temperatures. The other two walls were insulated. Maximum Nusselt number was observed to occur at two different inclinations depending on the Rayleigh number range. Four kinds of non-dimensional empirical correlations for the Nusselt number were derived for different ranges of inclination and Rayleigh number.

Another experimental work performed by Seki et al. [42] studied rectangular cavities packed with porous medium. The opposite vertical walls are maintained at uniform but different temperatures. Top and bottom walls are insulated. Three kinds of fluids were used: water, oil and ethyl alcohol. Wide range of Rayleigh number, Prandtl number and aspect ratio were studied and it was found that they have significant effect on heat transfer rate. A relationship was obtained for the Nusselt number which was

Chapter 3

ANALYSIS

Consider a triangular (wedge) fin placed vertically or horizontally in a saturated porous medium. The fin is of length L and subjected to combined free and forced convection. The fin is of two possible configurations (a) and (b) as shown in Figure (3-1) Configuration (a) is horizontally projecting (the porous medium is heated or cooled from below) while (b) is vertically projecting (the porous medium is heated or cooled from above). The x-axis denotes the streamwise coordinate and the y-axis denotes the transverse coordinate. The walls of the fins are inclined by ϕ degrees from the vertical.
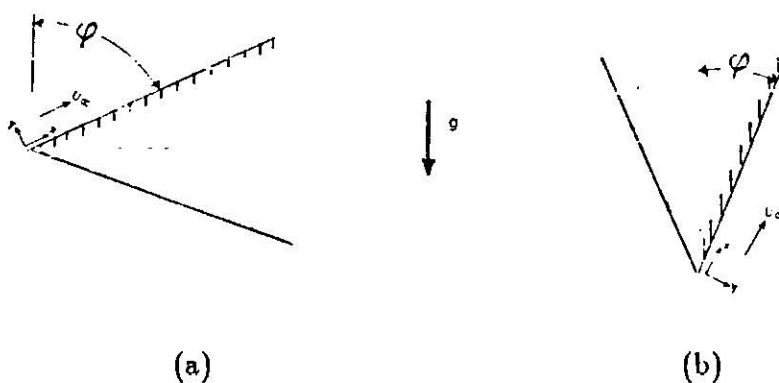

(a)   (b)

Figure (3-1) Physical model of two configurations (a) and (b).

21

The following assumptions for the mathematical formulation are assumed :

1. The flow is incompressible, steady, laminar and two-dimensional.

2. Both the convected fluid and the porous medium are everywhere in thermal equilibrium.

3. Fluid and porous medium properties are constant, except the density of the fluid in the buoyancy force terms.

4. The convected fluid temperature is everywhere below it's boiling temperature.

5. The Boussinesq approximation is invoked.

Under these assumptions the governing equations describing the problem are given by, [32]

$$\frac{\partial u}{\partial x} + \frac{\partial v}{\partial y} = 0 \qquad (3.1)$$

$$u = -\frac{K}{\mu} \left(\frac{\partial p}{\partial x} + \rho g \cos \phi \right) \qquad (3.2)$$

$$v = -\frac{K}{\mu} \left(\frac{\partial p}{\partial y} \pm \rho g \sin \phi \right) \qquad (3.3)$$

$$\frac{\partial^2 T}{\partial y^2} + \frac{\partial^2 T}{\partial x^2} = \frac{1}{\alpha} \left(u \frac{\partial T}{\partial x} + v \frac{\partial T}{\partial y} \right) \qquad (3.4)$$

$$\rho = \rho_\infty [1 - \beta(T - T_\infty)] \qquad (3.5)$$

where the '+' sign in Equation (3.3) refers to configuration (a) while the '-' sign refers to configuration (b) in Figure (3.1) u and v are Darcy's velocities in x and y directions, respectively; K is the permeability of the porous medium; ρ, μ, and β are the density, viscosity, the thermal expansion coefficient of the convected fluid; $\alpha = k_m/(\rho_\infty C)_f$ is the equivalent thermal diffusivity with $(\rho_\infty C)_f$ denoting the product of density and specific heat of the convected fluid, and k_m the thermal conductivity of the saturated porous medium which is given by $k_m = (1 - \epsilon)k_s + \epsilon k_f$ where ϵ is the porosity of the medium,

k_s and k_f are the thermal conductivity of the solid and the convicted fluid, respectively; T is the temperature; p is the pressure and g is the gravitational acceleration. The subscript "∞" refers to the condition at infinity. Equations (3.1)-(3.5) are subjected to the following boundary conditions

$$\text{at} \quad y = 0, \qquad v = 0, \qquad T_w = T_\infty \pm Ax^\lambda \qquad (3.6a,b)$$
$$\text{as} \quad y \to \infty, \quad u = u_\infty = Bx^n, \quad T = T_\infty \qquad (3.7a,b)$$

where A and B are positive constants; T_∞ is the temperature of the fluid and the porous medium far from the walls. Aiding flows are attained if the buoyancy force has a component in the free stream direction. Opposing flows are attained if the buoyancy force has a component that opposes the direction of the free-stream. Thus, aiding flows are obtained for both configurations (a) and (b) if the wall is hotter than the free stream temperature, i.e. $T_w = T_\infty + Ax^\lambda$, and opposing flows are obtained if the wall is colder than the free stream temperature, i.e. $T_w = T_\infty - Ax^\lambda$.

Now, define the stream function as

$$\frac{\partial \psi}{\partial y} = u, \qquad -\frac{\partial \psi}{\partial x} = v \qquad (3.8a,b)$$

where ψ is the stream function. Then

$$\nabla^2 \psi = \frac{\partial^2 \psi}{\partial y^2} + \frac{\partial^2 \psi}{\partial x^2} = \frac{\partial u}{\partial y} - \frac{\partial v}{\partial x} \qquad (3.9)$$

Differentiate Equation (3.2) with respect to y and Equation (3.3) with respect to x and substitute the resulting two equations into Equation (3.9) to get rid of the pressure terms and get

$$\frac{\partial^2 \psi}{\partial y^2} + \frac{\partial^2 \psi}{\partial x^2} = \pm \frac{K\rho_\infty g\beta}{\mu}[\cos\phi\frac{\partial T}{\partial y} \mp \sin\phi\frac{\partial T}{\partial x}] \qquad (3.10)$$

The $\pm$ sign on the RHS of Equation (3.10) specifies whether the flow is aiding, the '+'

sign, or the flow is opposing, the '-' sign. The $\mp$ sign is related to the two configurations considered. The '-' sign specifies configuration (a), while, the '+' sign specifies configuration (b).

Substitute Equations (3.8a,b) into Equation (3.4) to get

$$\frac{\partial^2 T}{\partial y^2} + \frac{\partial^2 T}{\partial x^2} = \frac{1}{\alpha}\left[\frac{\partial \psi}{\partial y}\frac{\partial T}{\partial x} - \frac{\partial \psi}{\partial x}\frac{\partial T}{\partial y}\right] \tag{3.11}$$

If convection takes place in a thin layer adjacent to the wall such that the gradients in the normal direction to the wall (i.e. y-direction) are much larger than those in the streamwise direction (i.e. x-direction), it follows that $\partial/\partial y \gg \partial/\partial x$. Then the first terms on the LHS of Equations (3.10) and (3.11) are larger than the second terms in them and so the second terms will be neglected and the final form of the governing equations become

$$\frac{\partial^2 \psi}{\partial y^2} = \pm \frac{K\rho_\infty g\beta}{\mu}\left[\cos\phi\frac{\partial T}{\partial y} \mp \sin\phi\frac{\partial T}{\partial x}\right] \tag{3.12}$$

$$\frac{\partial^2 T}{\partial y^2} = \frac{1}{\alpha}\left[\frac{\partial \psi}{\partial y}\frac{\partial T}{\partial x} - \frac{\partial \psi}{\partial x}\frac{\partial T}{\partial y}\right] \tag{3.13}$$

we seek to convert Equations (3.12) and (3.13) from partial differential equations into locally ordinary differential equations by introducing the following dimensionless variables

$$\eta(x,y) = \left(\frac{u_\infty x}{\alpha}\right)^{1/2}\frac{y}{x} \tag{3.14}$$

$$\xi(x) = \frac{x}{L} \tag{3.15}$$

$$\psi = (\alpha u_\infty x)^{1/2} f(\eta,\xi) \tag{3.16}$$

$$\theta(\eta,\xi) = \frac{T - T_\infty}{T_w - T_\infty} \tag{3.17}$$

By introducing these variables and upon transformation (full details of the transformation procedure is given in Appendix A) obtain the Darcian velocities

$$u = u_\infty f' \tag{3.18}$$

$$-v = \frac{1}{2}\left(\frac{\alpha u_\infty}{x}\right)^{1/2}\left[(n+1)f + 2\xi\frac{\partial f}{\partial \xi} + (n-1)\eta f'\right] \tag{3.19}$$

where $' = \partial/\partial\eta$. Also, Equations (3.12) and (3.13) become

$$f'' = \pm\left(\frac{Gr}{Re}\right)\xi^{\lambda-n}$$

$$\left[\theta'\cos\phi \mp \left(\frac{1}{Pe}\right)^{1/2}\xi^{-\left(\frac{n+1}{2}\right)}\sin\phi\left(\lambda\theta + \xi\frac{\partial\theta}{\partial\xi} + \frac{n-1}{2}\eta\theta'\right)\right] \tag{3.20}$$

In Equation (3.20) the $\pm$ sign specifies aiding , the $+$ sign, and opposing, the $-$ sign. Also, the $\mp$ sign specifies configuration (a), the $-$ sign, and configuration (b), the $+$ sign.

$$\theta'' - \lambda\theta f' + \left(\frac{1+n}{2}\right)f\theta' = \xi\left(f'\frac{\partial\theta}{\partial\xi} - \theta'\frac{\partial f}{\partial\xi}\right) \tag{3.21}$$

with boundary conditions

at $\quad \eta = 0, \quad \theta(0,\xi) = 1$ \hfill (3.22)

as $\quad \eta \to \infty, \quad \theta(\infty,\xi) = 0, \quad f'(\infty,\xi) = 1$ \hfill (3.23a, b)

also, at $\eta = 0 \implies v = 0$ and so Equation (3.19) gives

$$f(0,\xi) = \frac{-2}{1+n}\xi\frac{\partial f}{\partial\xi}\bigg|_{(0,\xi)} \tag{3.24}$$

where $Gr = \frac{g|T_w - T_\infty|_L \beta K L}{\nu^2}$ is the modified Grashof number at L, $Re = \frac{u_\infty L}{\nu}$ is the Reynold number at L and $\frac{Gr}{Re} = \frac{gA\beta K}{\nu B}L^{\lambda-n}$ is the mixed convection parameter at L. This parameter is a measure of the relative importance of free to forced convection. $Pe = \frac{(u_\infty)_L L}{\alpha} = \frac{BL^{n+1}}{\alpha}$ is the Peclet number at L; ϕ is the inclination from vertical; λ is the exponent in Equation (3.6b); n is the exponent in Equation (3.7a); f is the dimensionless stream function and θ is the dimensionless temperature.

The presence of ξ and it's derivatives shows that the problem is non-similar and similarity was not attained. However, similarity may be achieved as a special case when $\lambda = n = -1$. Similarity does exist, as a special case, in the case of vertical wall when the normal buoyancy force (the second term on the RHS of Equation(3.20)) does not exist. This is also the case for inclined walls when the normal buoyancy is neglected. This was the case considered by Cheng [32], whereby $\lambda = n$. If $Gr/Re = 0$, which is the case of forced convection, similarity is also obtained.

Inspection of the governing Equations (3.20) and (3.21) reveales that the non-similarity is caused by the power law variation of the wall temperature, the free stream velocity and the normal buoyancy component. The non-similarity is more explicit in the velocity field. The value of the Peclet number specifies the effect of both the stream-wise and the normal to the wall buoyancy force components on the convected fluid. The higher the Peclet number, the less the buoyancy effects, the closer the flow to the forced convection.

The boundary layer approximation used here is valid if (i) $\partial/\partial y \gg \partial/\partial x$ and (ii) $u \gg v$. From Equation (3.14) the ratio y/x is of the order of $(Pe)^{-1/2}$. From Equations (3.18) and (3.19) the ratio v/u is of the order of $(Pe)^{-1/2}$ also. So, conditions (i) and (ii) above are valid for large (Pe) values. At $x = 0$ and close to the tip of the fin (the leading edge) the boundary layer approximation is not expected to be valid.

Chapter 4

LOCAL NON-SIMILARITY SOLUTION

4.1 Introduction

The local non-similarity method to obtain solutions of Equations (3.20)-(3.24) will now be introduced. The method is well documented in the literature and a full description of the numerical scheme is given by Minkowycz and Sparrow [44]. The method is approximate and based on the weak dependence of f and θ on ξ. So, derivatives with respect to ξ are selectively deleted for three levels of truncation discussed below. The method provides no restrictions on n and λ values. For the three levels, ξ is regarded as a constant prescribed parameter. Then, upon solving for a specific streamwise location, ξ became a constant number and the governing equations became ordinary differential equations. This means that the solution at a specific streamwise location is independent of the the solution anywhere else. The local non-similarity method retains all the non-similar terms in the governing equations and only in the subsidiary equations these terms are selectively deleted. The major disadvantage of this method is that the validity of neglection of the non-similar terms is uncertain. However, this neglection is based on the assumption that either ξ values are small or the dependence of f and θ on ξ is weak, hence, the derivative of f and θ with respect to ξ are small. By proceeding from first to second to third level of truncation, the non-similar terms that are deleted become more

27

and more remote. So, higher accuracy is expected for higher levels. This was confirmed by researchers who observed that results become closer by moving to higher levels [6,7,28] . By comparing the local non-similarity results with finite difference method results, good agreement was observed [24,35]. The results of the first level (local similarity) are considered to be accurate for most practical cases [5,6,26].

Now, let

$$G = \partial f / \partial \xi \tag{4.1}$$

and

$$\Phi = \partial \theta / \partial \xi \tag{4.2}$$

then Equations (3.20) and (3.21) become

$$f'' = \pm \Omega \xi^{\lambda-n}$$

$$\left[\theta' \cos \phi \mp \left(\frac{1}{Pe} \right)^{1/2} \xi^{-\left(\frac{n+1}{2}\right)} \sin \phi \right.$$

$$\left. \left(\lambda\theta + \xi\Phi + \frac{n-1}{2}\eta\theta' \right) \right] \tag{4.3}$$

$$\theta'' - \lambda\theta f' + \left(\frac{1+n}{2} \right) f\theta' = \xi \left(f'\phi - \theta' G \right) \tag{4.4}$$

and the boundary conditions are

at $\eta = 0$, $\theta(0,\xi) = 1$, $f(0,\xi) = \frac{-2}{1+n}\xi G$ $\qquad (4.5a,b)$

as $\eta \to \infty$, $\theta(\infty,\xi) = 0$, $f'(\infty,\xi) = 1$ $\qquad (4.6a,b)$

where Ω in Equation (4.3) is Gr/Re.

4.2 First Level of Truncation (Local-Similarity)

At this level the variables G and Φ in Equations (4.3), (4.4) and (4.5b) are deleted. Then, the governing equations for this level are

$$f'' = \pm\Omega\xi^{\lambda-n}$$

$$\left[\theta'\cos\phi \mp \left(\frac{1}{Pe}\right)^{1/2}\xi^{-\left(\frac{n+1}{2}\right)}\sin\phi \right.$$

$$\left. \left(\lambda\theta + \frac{n-1}{2}\eta\theta'\right)\right] \tag{4.7}$$

$$\theta'' - \lambda\theta f' + \left(\frac{1+n}{2}\right)f\theta' = 0 \tag{4.8}$$

Another way to put these two equations is

$$f'' + P_{1f}f' = Q_{1f} \tag{4.9}$$

$$\theta'' + P_{1\theta}\theta' = Q_{1\theta} \tag{4.10}$$

where

$$P_{1f} = 0 \tag{4.11}$$

$$Q_{1f} = \pm\Omega\xi^{\lambda-n}$$

$$\left[\theta'\cos\phi \mp \left(\frac{1}{Pe}\right)^{1/2}\xi^{-\left(\frac{n+1}{2}\right)}\sin\phi\left(\lambda\theta + \frac{n-1}{2}\eta\theta'\right)\right] \tag{4.12}$$

$$P_{1\theta} = \frac{1+n}{2}f \tag{4.13}$$

$$Q_{1\theta} = \lambda\theta f' \tag{4.14}$$

and the boundary conditions are

$$at \quad \eta = 0, \quad \theta(0,\xi) = 1, \quad f(0,\xi) = 0 \tag{4.15a, b}$$

$$as \quad \eta \to \infty, \quad \theta(\infty,\xi) = 0, \quad f'(\infty,\xi) = 1 \tag{4.16a, b}$$

$$\Phi'' + P_{2\Phi} = Q_{2\Phi} \qquad (4.22)$$

where

$$P_{2f} = 0.0 \qquad (4.23)$$

$$Q_{2f} = \pm \Omega \xi^{\lambda-n} \left[\theta' \cos \phi \mp \left(\frac{1}{Pe} \right)^{1/2} \right.$$
$$\left. \xi^{-\left(\frac{n+1}{2}\right)} \sin \phi \left(\lambda\theta + \xi\Phi + \frac{n-1}{2}\eta\theta' \right) \right] \qquad (4.24)$$

$$P_{2\theta} = P_{1\theta} + \xi G \qquad (4.25)$$

$$Q_{2\theta} = Q_{1\theta} + \xi\Phi f' \qquad (4.26)$$

and

$$P_{2G} = 0.0 \qquad (4.27)$$

$$Q_{2G} = D\Omega(\lambda - n)\xi^{\lambda-n-1}\theta' \cos \phi + D\Omega\xi^{\lambda-n}$$
$$\Phi' \cos \phi - D\Omega(1/Pe)^{1/2} E \sin \phi$$
$$\left[\lambda cc \xi^{cc-1}\theta + \xi^{cc}\lambda\Phi + (cc+1)\xi^{cc}\Phi \right.$$
$$\left. + \left(\frac{n-1}{2} \right) cc\xi^{cc-1}\eta\theta' + \left(\frac{n-1}{2} \right) \xi^{cc}n\Phi' \right] \qquad (4.28)$$

$$P_{2\Phi} = P_{2\theta} \qquad (4.29)$$

$$Q_{2\Phi} = \lambda\theta G' + (\lambda+1)f'\Phi - \left(\frac{n+3}{2} \right) \theta'G + \xi\Phi G' \qquad (4.30)$$

where $cc = (2\lambda - 3n - 1)/2$; $E = 1$ for configuration (a) and -1 for configuration (b) and $D = 1$ for aiding flows and -1 for opposing flows.

The value of f at $\eta = 0$ is obtained by differentiating Equation (4.5 b) with respect to ξ and deleting the H term obtained. Then, we get $G(0, \xi) = 0$ and substitute back in

Equation (4.5 b) and get $f(0,\xi) = 0$.

Equations (4.19)-(4.30) are subjected to boundary conditions

$$\theta(0,\xi) = 1, \quad f(0,\xi) = 0 \tag{4.31}$$

$$\Phi(0,\xi) = 0, \quad G(0,\xi) = 0 \tag{4.32}$$

and

$$\theta(\infty,\xi) = 0, \quad f'(\infty,\xi) = 1 \tag{4.33}$$

$$\Phi(\infty,\xi) = 0, \quad G'(\infty,\xi) = 0 \tag{4.34}$$

The set of equations of this level are coupled and simultaneous solution is required. These equations are ordinary differential equations if ξ is regarded as a parameter. In this level note that the two basic equations (i.e. Equations (4.3) and (4.4) or (4.19) and (4.20)) are retained without approximation. The neglected terms (i.e. H and χ) are in the two subsidiary equations (i.e. Equations (4.21) and (4.22)). Thus , higher accuracy than the first level is expected.

4.4 Third Level of Truncation

A set of six equations is required for this level. The first two equations are the first two equations of the first level (i.e. Equations (4.3) and (4.4)), which are the basic equations without approximation. Two more equations are the two equations obtained in the second level by deriving the basic governing equations (i.e. Equations (4.3) and (4.4)) with respect to ξ but no approximation is required and the variables H and χ are retained. The last two equations are obtained by deriving the second two equations of this level with respect to ξ. In the obtained two equations the $\partial H/\partial\xi$ and $\partial\chi/\partial\xi$ terms are deleted and the H and χ variables are retained. The set of equations governing the third level of truncation are

$$f'' + P_{3f}\,f' = Q_{3f} \tag{4.35}$$

الصفحة غير موجودة من أصل المصدر

the value of $(Gr/Re)_x$ and so the buoyancy force decreases as ξ increases. On the other hand, for $\lambda = 1$, $(Gr/Re)_x$ value increases with ξ. Also, note that the free stream velocity is increasing with downstream direction.

Figure (5-9) shows that increasing λ decreases the velocity. Opposite behavior is observed for OF. Higher λ values mean lower $(T_w - T_\infty)$ values and as a result lower buoyancy forces.

5.2 Temperature Profiles

Figures (5-10)-(5-18) present the temperature fields. Figures (5-10) and (5-11) show that higher Gr/Re values results in higher temperature- gradients (higher heat transfer values). This is caused by the buoyancy effects. For OF higher Gr/Re values lessen the temperature-gradients since the free stream dominates the buoyancy.

Figures (5-12) and (5-13) show that higher inclinations from vertical decrease the temperature-gradients. As ϕ increases the normal buoyancy component develops. For OF the higher the normal buoyancy component (higher ϕ) the higher the temperature-gradients. The free stream is facing less resistance from the tangential buoyancy force component. The effect of ϕ is more pronounced in the case of $\lambda = 0$ than in the case of $\lambda = 1$. In the case of $\lambda = 0$, higher buoyancy forces are involved. The effect of ϕ is also more pronounced for configuration (a) where the normal buoyancy force has higher effect.

Figures (5-14) and (5-15) show that increasing the Pe number decreases the dimensionless temperature-gradients. It was found that increasing the Peclet number decreases the dimensionless velocity and lower dimensionless temperature is expected. Also, in-

creasing Pe means lower thermal diffusivity and lower heat transfer rate.

Figures (5-16) and (5-17) show that for IW, moving downstream decreases the temperature-gradients, while opposite behavior is observed for LW. This is caused by the decreasing f' in the case of IW and the enhancing f' in the case of LW.

Figure (5-18) shows that increasing λ decreases the temperature-gradients caused by the decreased temperature difference, $T_w - T_\infty$.

5.3 Heat Transfer Characteristics

In this section analytical expressions for local surface heat flux, local Nusselt number, local thermal boundary layer thickness, total heat transfer rate and average Nusselt number will be obtained.

5.3.1 Local surface heat flux

Firstly, obtain an expression for local surface heat flux along the fin using

$$q = -k_m \left(\frac{\partial T}{\partial y} \right)_{y=0} \tag{5.1}$$

and using Equation (A.22) for the expression for $\partial T / \partial y$ this becomes

$$q = -k_m A \left(\frac{B}{\alpha} \right)^{1/2} x^{\frac{2\lambda+n-1}{2}} \theta'(0, \xi) \tag{5.2}$$

arranging

$$q^* = \frac{qL}{k_m \Delta T_L} = \xi^{\frac{2\lambda+n-1}{2}} (Pe)^{1/2} [-\theta'(0, \xi)] \tag{5.3}$$

where q^* is the dimensionless local surface heat flux. Equation (5. 2) indicates that to attain constant heat flux the boundary layer should be similar and the exponent $\frac{2\lambda+n-1}{2} = 0$. Thus, constant heat flux is only obtained for vertical surface with $\lambda = n = 1/3$.

Representative distributions for $\lambda = 0$ and 1 and $n = 1/3$ for selective values of Gr/Re, Ra, ϕ and Pe are presented in Figures (5-19)-(5-26). Figures (5-19)-(5-23) represent the case of $\lambda = 0$ and $n = 1/3$. In Figure (5-19) increasing Gr/Re increases the value of q^* as expected. Figure (5-20) shows that increasing the ϕ decreases q^*. The effect of Rayleigh number, Ra, is similar to the effect of the mixed convection parameter, $Gr/Re = Ra/Pe$, as shown in Figure (5-21). With the dimensionless heat flux is proportional to the Peclet number as shown in Equation (5.3), Figure (5-22) shows that increasing Peclet number increases the heat flux which is caused by the enhanced free stream velocity.

For $\lambda = 1$ in Figures (5-23)-(5-26), similar argument to that for $\lambda = 0$ may be said. However, we can notice the following. The distributions for both configurations are almost identical indicating that the normal buoyancy force component is very small compared to the streamwise component for the selected parameters range. For $\lambda = 0$ maximum heat flux occurs near the tip of the wedge and decreases as moving downstream [18,28,29,37]. Opposite to this occurs when $\lambda = 1$ where the temperature difference between the free stream and the wall increases as moving downstream. This enhance the buoyancy and accelerates the flow.

5.3.2 Local Nusselt number

An analytical expression will now be obtained for the local heat transfer coefficient at every ξ position noting that

$$q = h(T_w - T_\infty) \tag{5.4}$$

equating Equations (5.2) and (5.4) get

$$h = -k_m \left(\frac{B}{\alpha}\right)^{1/2} x^{\frac{n-1}{2}} \theta'(0, \xi) \tag{5.5}$$

upon arranging, get the expression for dimensionless h

$$h^* = Nu = \frac{hL}{k_m} = \xi^{\frac{n-1}{2}}(Pe)^{1/2}[-\theta'(0,\xi)] \qquad (5.6)$$

where h^* is the dimensionless local heat transfer coefficient. which is the Nusselt number based on L. From Equations (5-3) and (5-6), note that at $\lambda = 0$; $q^* = h^*$.

Representative distributions of Nusselt number for selective values of Gr/Re, ϕ, Ra and Pe are presented in Figures (5-19)-(5-22) for $\lambda = 0$ and in Figures (5-27)-(5-30) for $\lambda = 1$ where $n = 1/3$ for both cases. The Nusselt number for $\lambda = 0$ decreases with increasing ξ due to the decrease in buoyancy effects along the surface. For $\lambda = 1$ The buoyancy effects increase with increasing ξ, hence the Nusselt number increases as ξ increases.

An expression will now be derived for the local Nusselt number in which x is the characteristic length, with

$$Nu_x = \frac{hx}{k_m} \qquad (5.7)$$

Using Equation (5.5)

$$\frac{Nu_x}{(Pe)_x^{1/2}} = -\theta'(0,\xi) \qquad (5.8)$$

using Equation (5.6) and arranging obtain

$$Nu_x = \xi^{\frac{n+1}{2}}(Pe)^{1/2}[-\theta'(0,\xi)] \qquad (5.9)$$

Expressions can now be obtained to compare the three dimensionless values h^*, q^* and Nu_x. By comparing Equations (5-3),(5-6) and (5-9), get

$$h^* = \frac{Nu_x}{\xi} \qquad (5.10)$$

$$h^* = \frac{q^*}{\xi^\lambda} \qquad (5.11)$$

equating Equation (5.10) with Equation (5.11)

$$q^* = \xi^{\lambda-1} Nu_x \qquad (5.12)$$

It should be noted that at and near the tip the solutions are not applicable as a result of the boundary layer approximations. A finite value of h^* at $\xi = 0$ is expected.

5.3.3 Thermal boundary layer thickness

An expression for the thermal boundary layer thickness will now be obtained. From Equation (3.14) get

$$\eta_T = (Pe)_x^{1/2} \frac{\delta_T}{x} \qquad (5.13)$$

where η_T is the value of η at which θ equals 0.01, and δ_T is the thermal boundary layer thickness.

Now, obtain the following analytical expression from Equation (5.13)

$$\delta_T^* = \frac{\delta_T}{L} = \xi^{-\left(\frac{n-1}{2}\right)}(Pe)^{-1/2}\eta_T \qquad (5.14)$$

where δ_T^* is the dimensionless thermal boundary layer thickness . Representative distribution Figures of the dimensionless thermal boundary layer thickness for selective values of Gr/Re, ϕ, Ra and Pe are shown in Figures (5-31)-(5-38). Higher heat fluxes indicate lower thermal boundary layer thicknesses. With the local $(T_w - T_\infty)$ values being constant, higher temperature-gradients decrease the thermal boundary layer thickness.

5.3.4 Total heat transfer rate

Total heat transfer from one face of the fin and for unit width could be obtained by integrating Equation (5.2) from 0 to L

$$Q = \int_0^L -k_m A \left(\frac{B}{\alpha}\right)^{1/2} x^{\frac{2\lambda+n-1}{2}} \theta'(0,\xi)dx \qquad (5.15)$$

or using Equation (5.3)

$$Q^* = \frac{Q}{k_m \Delta T_L} = \int_0^1 \xi^{\frac{2\lambda+n-1}{2}} (Pe)^{1/2}[-\theta'(0,\xi)]d\xi \tag{5.16}$$

Where Q^* is the dimensionless total heat transfer rate. Values for Q^* for selective values of Gr/Re, ϕ, Ra' and Pe are shown in Tables [5.1]-[5.4]. Simpson 1/3 rule is used to perform the integrations .

5.3.5 Average Nusselt number

An expression for the average heat transfer coefficient can be obtained by integrating the local heat transfer coefficient, Equation (5.6), and dividing by the fin length, in dimensional form

$$\overline{h} = \frac{1}{L} \int_0^L h(x)dx \tag{5.17}$$

substituting Equation (5.5) for h

$$\overline{h} = \frac{-k_m}{L} \int_0^1 \left(\frac{B}{\alpha}\right)^{1/2} x^{\frac{n-1}{2}} \theta' dx \tag{5.18}$$

or, upon using Equation (5.6), in dimensionless form

$$\overline{Nu} = \overline{h}^* = \frac{\overline{h}L}{k_m} = \int_0^1 \xi^{\frac{n-1}{2}} (Pe)^{1/2}[-\theta'(0,\xi)]d\xi \tag{5.19}$$

Values for $\overline{Nu}$ for selective values of Gr/Re, ϕ, Ra and Pe are shown in Tables [5.1]-[5.4]. Simpson 1/3 rule is used to perform the integrations.

In the case of similarity the value of $\overline{Nu}$ from Equation (5.19) becomes

$$\overline{Nu} = \frac{2}{n+1}(Pe)^{1/2}[-\theta'(0)] \tag{5.20}$$

One such case is the case of vertical isothermal surface over which uniform free stream velocity occurs, Equation (5.20) is then reduced to

$$\overline{Nu} = 2(Pe)^{1/2}[-\theta'(0)] \tag{5.21}$$

Table [5.1]. Effect of Gr/Re on the average Nusselt number and total heat transfer rate for $Pe = 70$ and $\phi = 45$.

| $\frac{Gr}{Re}$ | $\lambda = 0$ and $n = 1/3$ | | | | $\lambda = 1$ and $n = 1/3$ | | | |
| | configuration (a) | | configuration (b) | | configuration (a) | | configuration (b) | |
	$\overline{Nu}$	Q^*	$\overline{Nu}$	Q^*	$\overline{Nu}$	Q^*	$\overline{Nu}$	Q^*
1	8.948	8.948	8.668	8.668	14.845	7.076	14.337	6.858
3	11.793	11.793	11.178	11.178	18.052	8.846	17.023	8.441
5	14.026	14.026	13.250	13.250	20.673	10.277	19.367	9.786

Table [5.2]. Effect of ϕ on the average Nusselt number and total heat transfer rate for $Gr/Re = 3$ and $Pe = 100$.

| ϕ | $\lambda = 0$ and $n = 1/3$ | | | | $\lambda = 1$ and $n = 1/3$ | | | |
| | configuration (a) | | configuration (b) | | configuration (a) | | configuration (b) | |
	$\overline{Nu}$	Q^*	$\overline{Nu}$	Q^*	$\overline{Nu}$	Q^*	$\overline{Nu}$	Q^*
30	14.808	14.808	14.410	14.410	22.352	11.050	21.696	10.796
45	14.024	14.024	13.412	13.412	21.481	10.535	20.452	10.129
60	12.890	12.890	12.240	12.240	20.223	9.800	18.755	9.204

Table [5.3]. Effect of Ra on the average Nusselt number and total heat transfer rate for $Pe = 70$ and $\phi = 45$.

| Ra | $\lambda = 0$ and $n = 1/3$ | | | | $\lambda = 1$ and $n = 1/3$ | | | |
| | configuration (a) | | configuration (b) | | configuration (a) | | configuration (b) | |
	$\overline{Nu}$	Q^*	$\overline{Nu}$	Q^*	$\overline{Nu}$	Q^*	$\overline{Nu}$	Q^*
50	8.458	8.458	8.258	8.258	14.305	6.775	13.915	6.604
70	8.948	8.948	8.668	8.668	14.843	7.075	14.337	6.858
100	9.636	9.636	9.256	9.256	15.604	7.498	14.950	7.223

Table [5.4]. Effect of Pe on the average Nusselt number and total heat transfer rate for $Ra = 70$ and $\phi - 45$.

| | $\lambda = 0$ and $n = 1/3$ | | | | $\lambda = 1$ and $n = 1/3$ | | | |
| | configuration (a) | | configuration (b) | | configuration (a) | | configuration (b) | |
Pe	$\overline{Nu}$	Q^*	$\overline{Nu}$	Q^*	$\overline{Nu}$	Q^*	$\overline{Nu}$	Q^*
50	8.143	8.413	7.755	7.755	13.195	6.334	12.548	6.063
70	8.948	8.948	8.668	8.668	14.843	7.076	14.337	6.858
100	10.054	10.054	9.861	9.861	17.029	8.063	16.644	7.895

It should be noted that the values of $\overline{Nu}$ and Q^* in this work and in similar works [18,28,29,37], are underpredicted since non-similar solutions, in this work and in the other works [18,28,29, 37], were not been obtained for $\xi < 0.05$ due to numerical system difficulties. The values of $\overline{Nu}$ and Q^* in these Tables cover only the ξ range from 0.05 to 1. A difference of about 21% was found between $\overline{Nu}$ values in this work and the works that use similarity solution for vertical [32] and horizontal surfaces [34]. Several cases were compared and the difference was found to range between $21.2 - 21.7\%$. Tables [5.1]-[5.4] show that higher values of selected Gr/Re, Ra and Pe give higher $\overline{Nu}$ and Q^- values. Higher ϕ values in the selected range give lower $\overline{Nu}$ and Q^* values. All these results can now be easily explained. Configuration (a) gives higher $\overline{Nu}$ and Q^* values than configuration (b) for the selected parameters tested. Note that the difference between the two configurations in the $\overline{Nu}$ and Q^* values increases with the increased Gr/Re, ϕ and Ra values. The opposite is observed for higher Pe values. This all related to the buoyancy forces. Higher Pe values decrease the effect of buoyancy.

5.4 Comparison with Previous Works

To the author's knowledge, no literature data is available for mixed or forced convection from inclined non-similar boundary layers in porous medium. The available works cover only similar boundary layers from vertical, inclined or horizontal surfaces [32,34]. However, it should be stated here that Cheng [1] mentioned an experimental work performed by Combarnous and Bories [45] in which they investigated mixed convection in a sloping porous layer which is not the case here.

To perform the comparison, solutions using the present work's numerical method will be obtained for the cases which admit similarity and was solved in previous works.

5.4.1 Vertical surfaces

Table [5.5] gives comparison between the present work and the works of Cheng [32,38], Lai et al. [31] and Lui et al. [28] for aiding flows and Table [5.6] for opposing flows. The surfaces are under isothermal conditions and the free stream velocity is uniform (i.e. $\lambda = n = 0$). Cheng [32] obtained similarity solutions, Cheng [38] obtained integral solutions, Lai et al. [31] obtained finite-difference solutions and Liu et al. [28] obtained non-similar solutions. The value that will be tested is the value of $\theta'(0)$.

Table [5.5]. Comparison of $-\theta'(0)$ values for mixed convection about isothermal vertical surfaces. $\lambda = n = 0$. Aiding flows.

Gr/Re	Cheng [32]	Cheng [38]	Lai et al.[31]	Lui et al[28]	present work
.5	0.6471	0.6582	0.6475	0.5959	0.6474
1	0.7205	-	0.7205	0.6633	0.7205
2	-	-	0.8202	0.7801	0.8474
3	0.9574	0.9666	-	-	0.9573
10	1.516	1.527	1.5163	-	1.5159
20	2.066	2.081	2.0661	-	2.0658
0	0.5641	0.5773	0.564	0.5191	0.5646

The value for $-\theta'(0)$ was given in [39] to be 0.53 for forced convection. This value is compared with the last row in Table [5.5].

Table [5.6]. Comparison of $-\theta'(0)$ values for mixed convection about isothermal vertical surfaces. $\lambda = n = 0$. Opposing flows

Gr/Re	Cheng [32]	Cheng [38]	Lai et al.[36]	present work
0.1	-	-	0.5450	0.5460
0.2	0.5269	0.5416	0.5268	0.5274
0.4	0.4865	0.5033	-	0.4873
0.6	0.4420	0.4618	-	0.4432
0.8	0.3916	0.4163	-	0.3937
1	0.3320	0.3651	0.3320	0.3363

5.4.2 Inclined Surfaces

The only work that it is possible to compare with is the work of Cheng [32]. The wall is of $45°$ inclination with $\lambda - n = 1/3$. $\overline{Nu}$ values are compared in Tables [5.7] and [5.8] for aiding flows and opposing flows,respectively. It should be noted that Cheng obtained similarity solutions through the neglection of the normal buoyancy component. In the present work similarity is not possible for this case. However, for the sake of comparison, the normal buoyancy component will be deleted in the results of the present work.

Table [5.7]. Comparison of $-\theta'(0)$ values for mixed convection about inclined surfaces for $\lambda = n = 1/3$. Aiding flows.

$\frac{Gr}{Re} \cos \phi$	Aiding flows	
	Cheng [32]	present work
0 (forced convection)	0.8540	0.8541
0.5	0.9816	0.9816
1	1.093	1.094
3	1.456	1.457
10	2.311	2.312
20	3.152	3.153

Table [5.8]. Comparison of $-\theta'(0)$ values for mixed convection about inclined surfaces for $\lambda = n = 1/3$. Opposing flows.

$\frac{Gr}{Re} \cos \phi$	Opposing flows	
	Cheng [32]	present work
0.2	0.7970	0.7970
0.4	0.7351	0.7352
0.6	0.6671	0.6672
0.8	0.5903	0.5904
1	0.4999	0.5002

5.4.3   Horizontal surfaces

Three works are available. The works of Cheng [34,38] who obtained similarity solutions in [34] and integral solutions in [38], and the work of Minkowycz et al. [35] who obtained non-similar solutions. Comparison with the last work will be for $\xi = 1$. Table [5.9] shows the comparison.
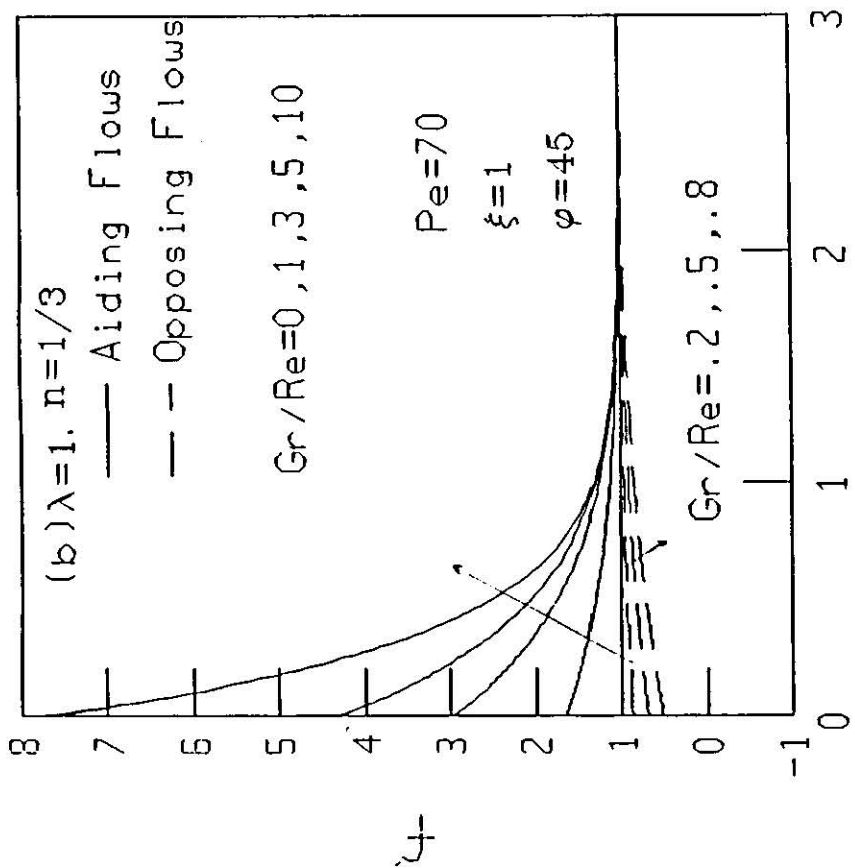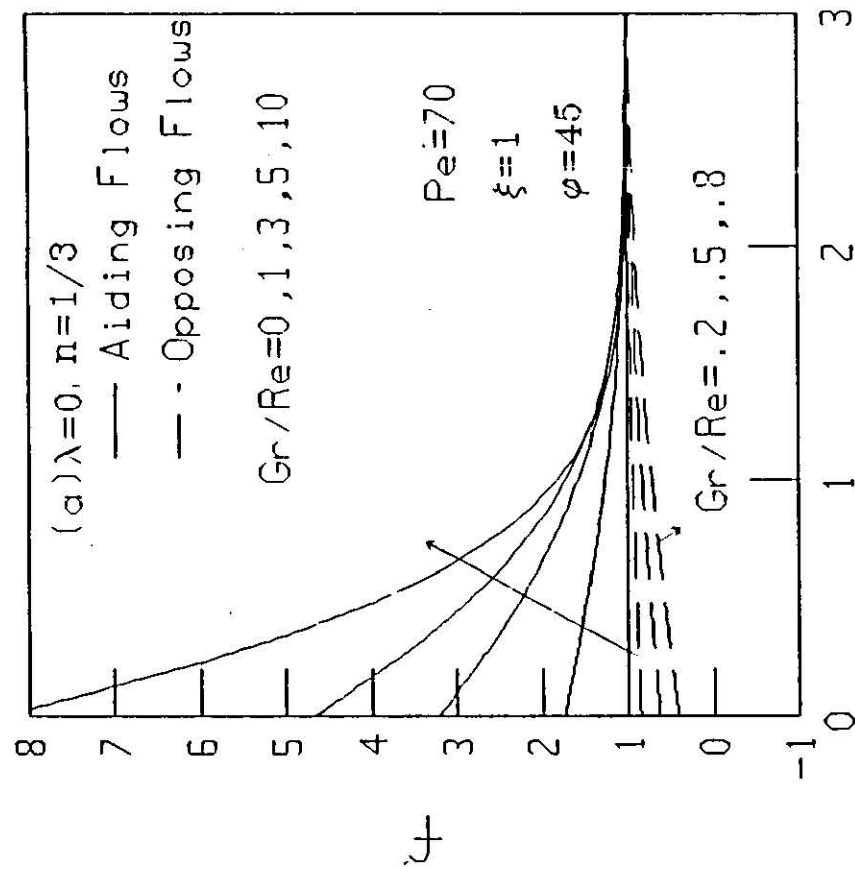
Fig.(5.2) Configuration (b) Velocity Profiles For Aiding
And Opposing Flows For Selected Values Of Gr/Re.
(a)Isothermal Plate (b)Linear Temperature Variation
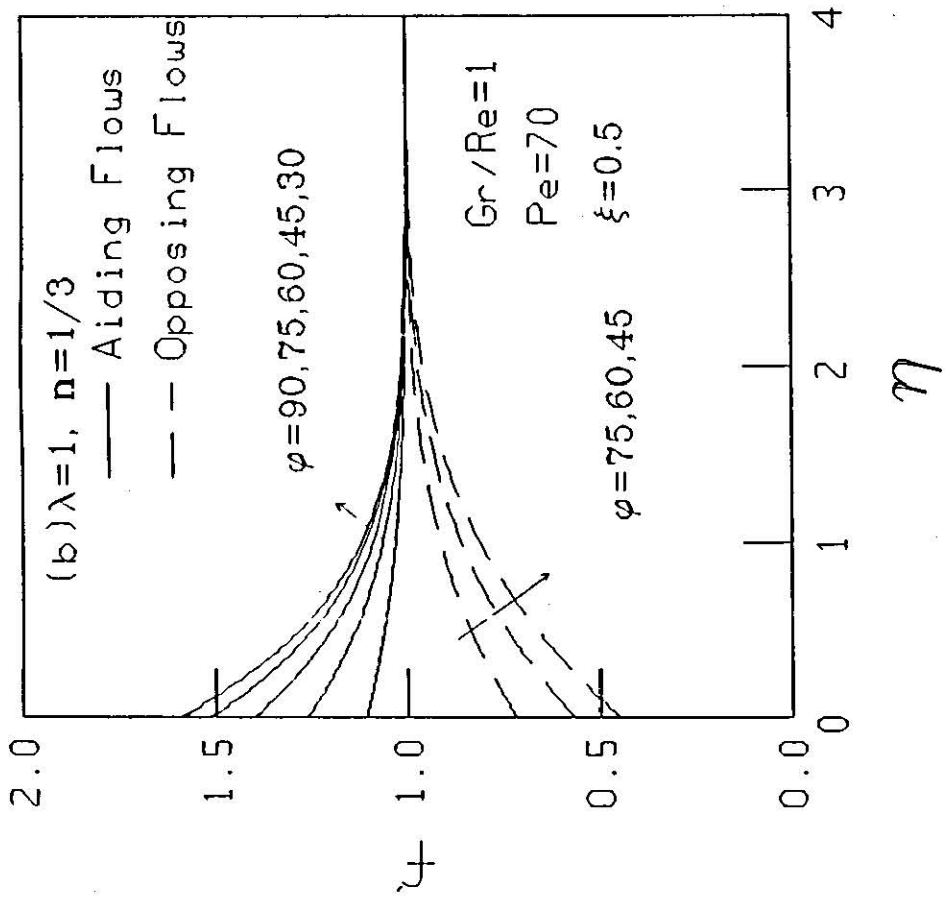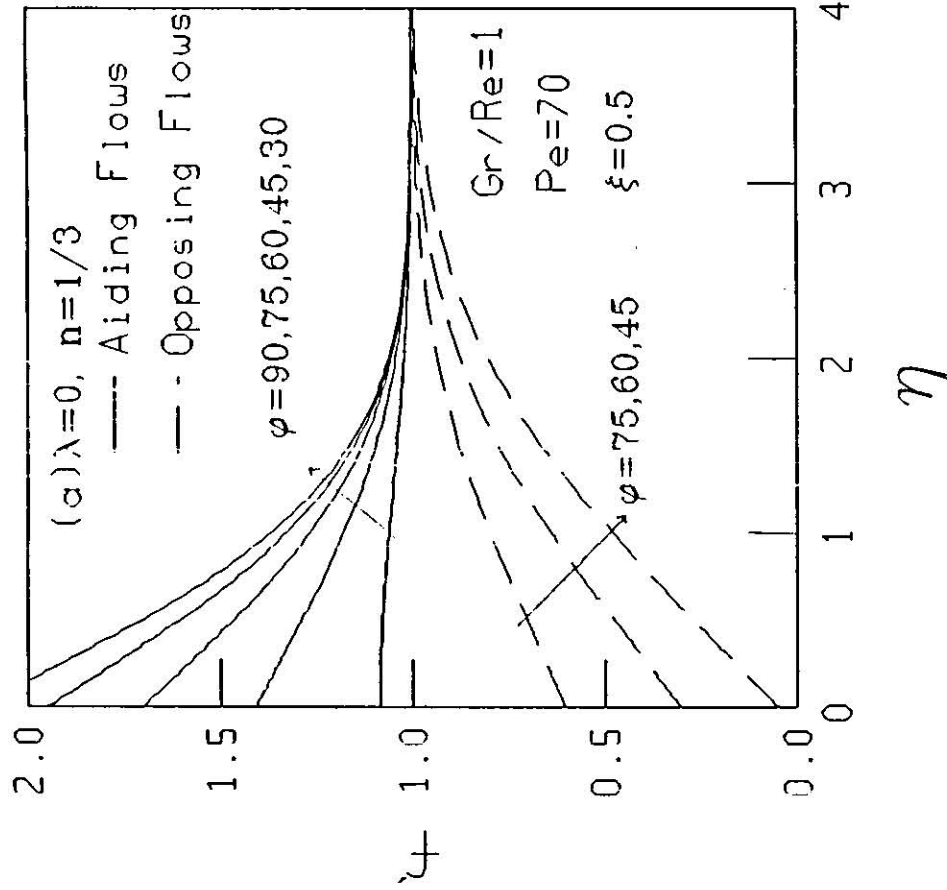
Fig.(5.3) Configuration (a) Velocity Profiles For Aiding
And Opposing Flows For Selected Values Of φ
(a)Isothermal Wall (b)Linear Wall Temperature Variation.
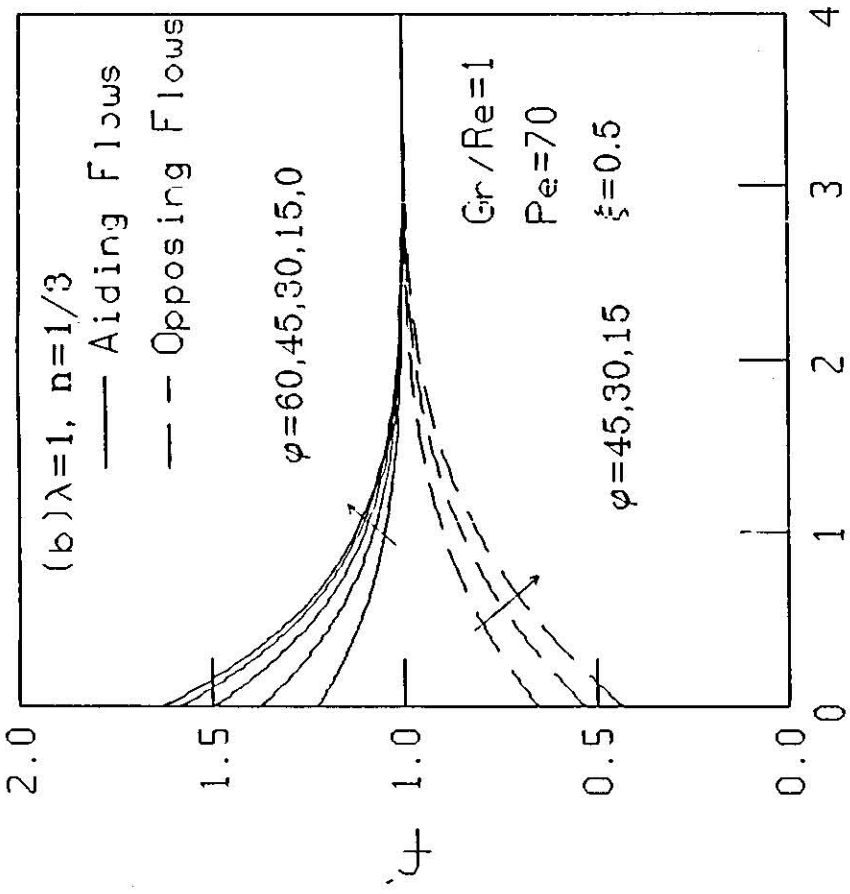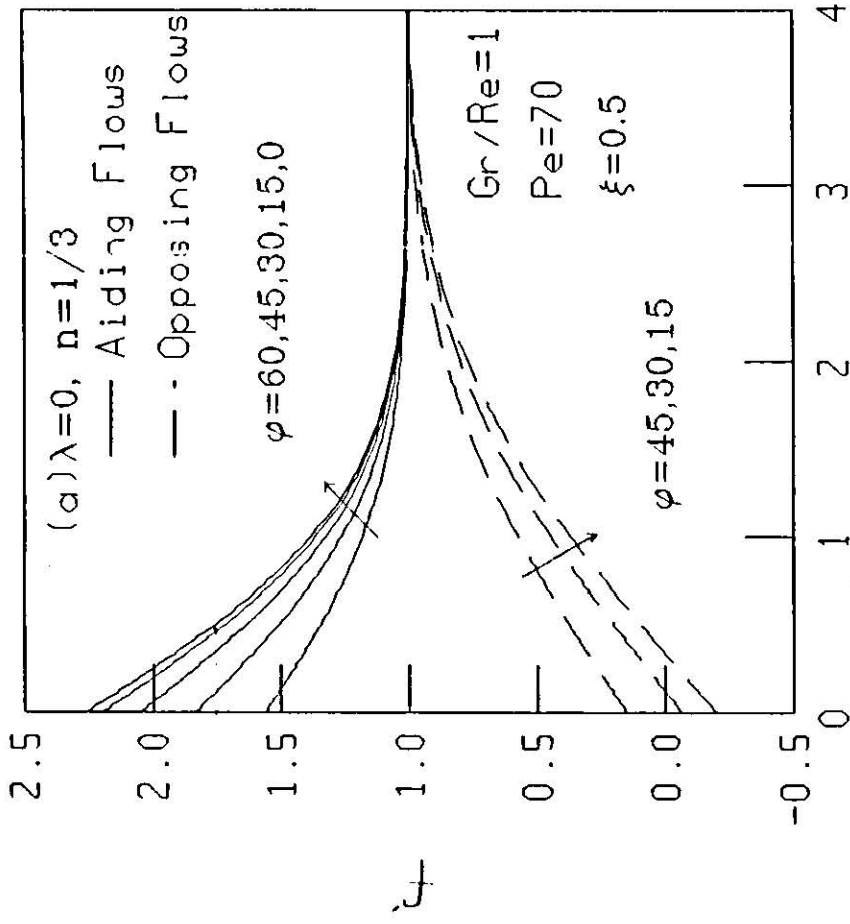
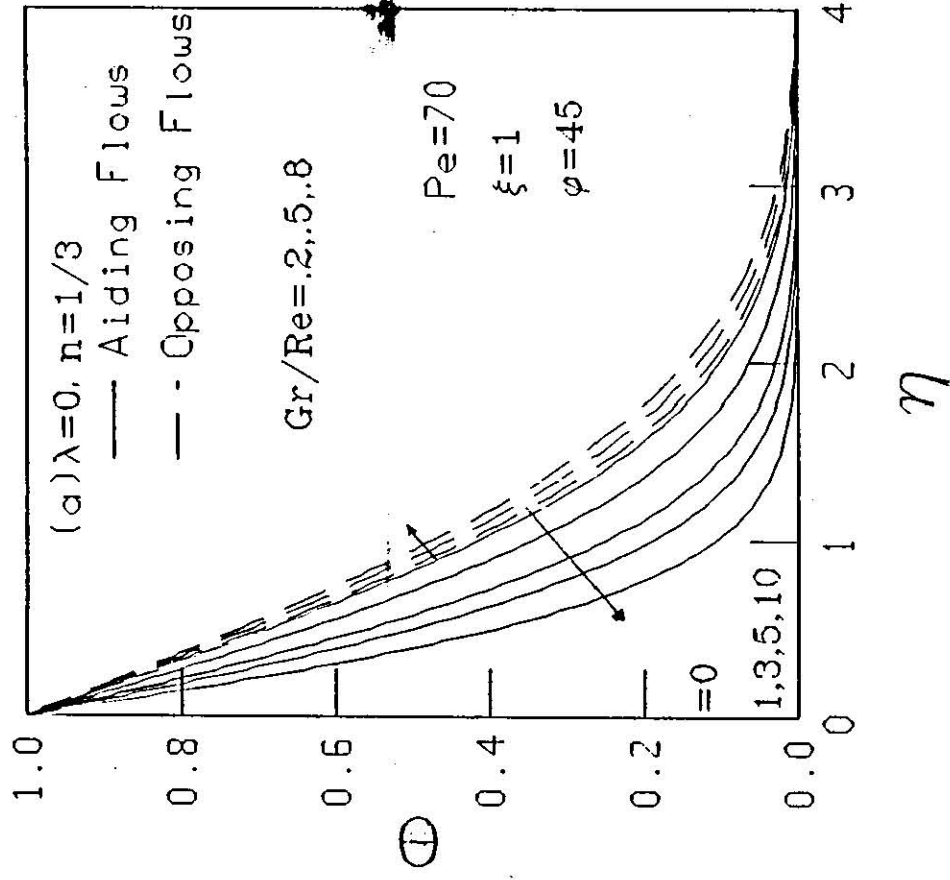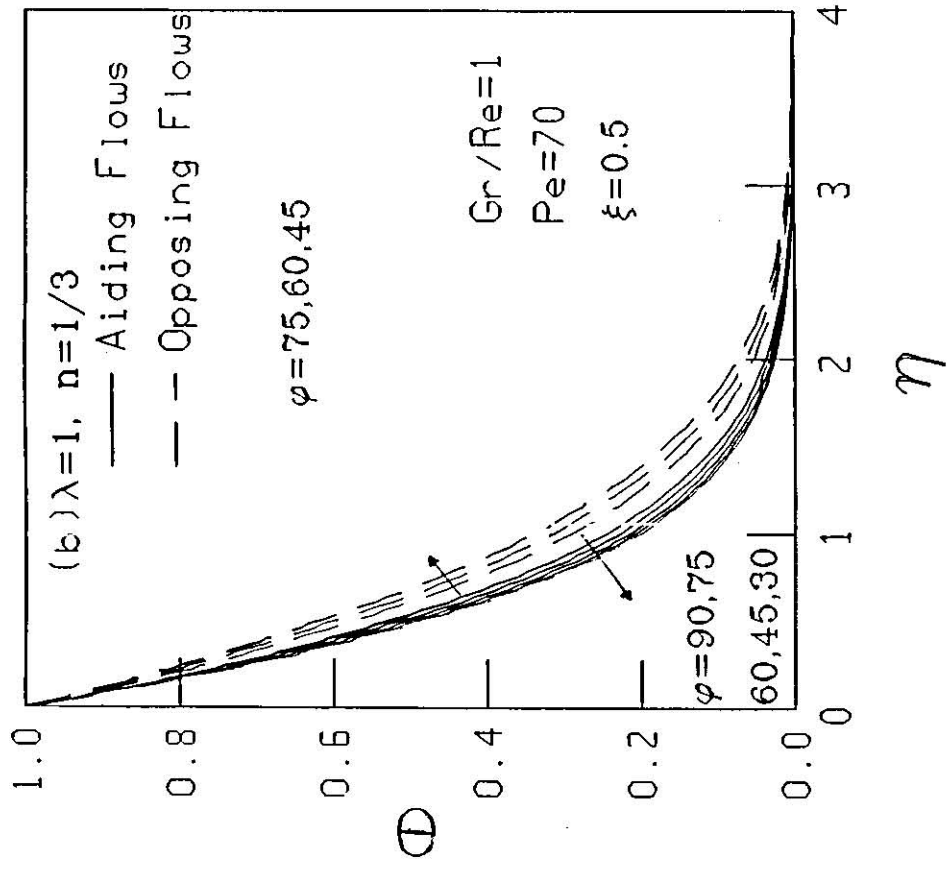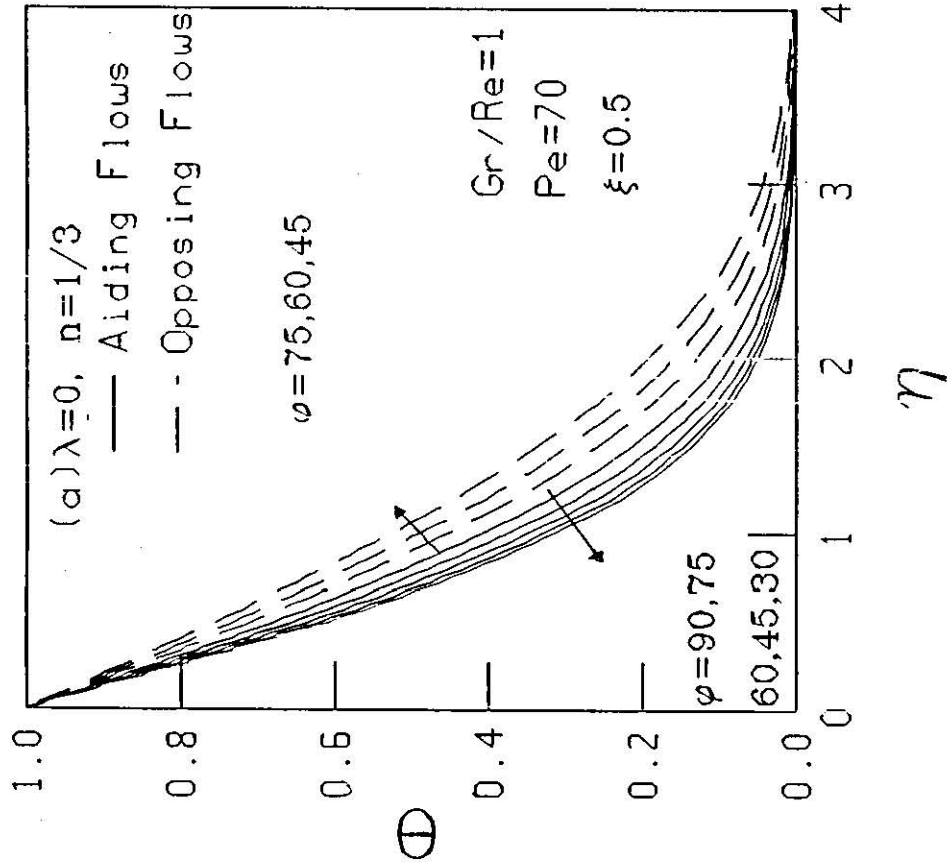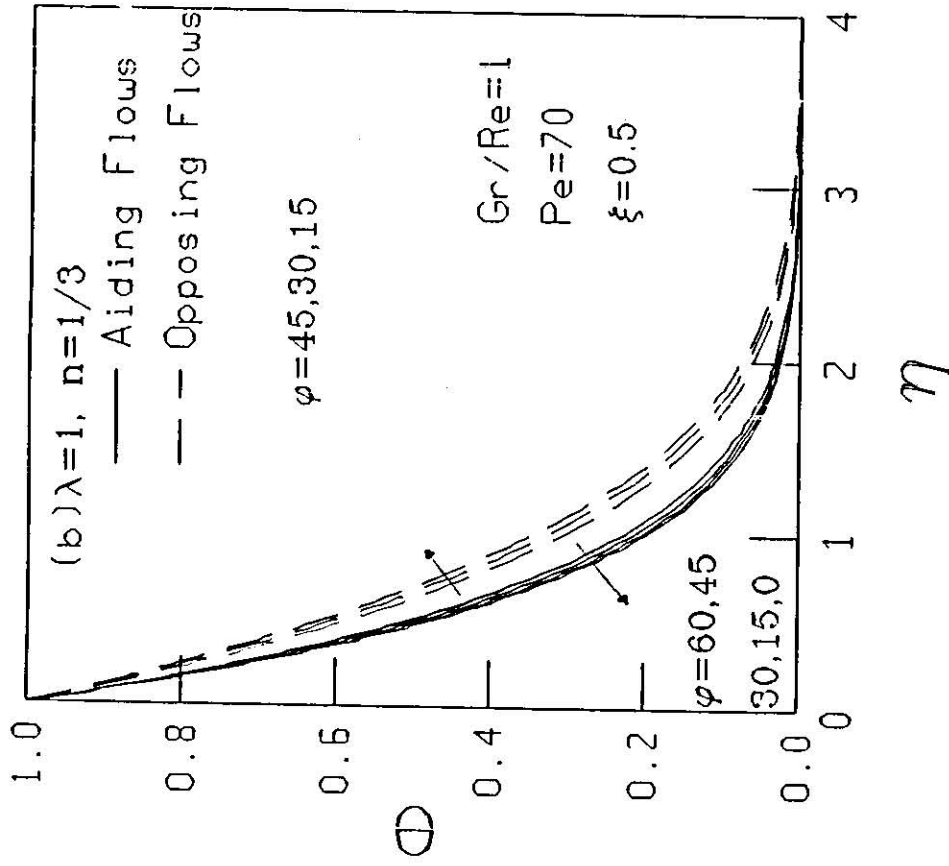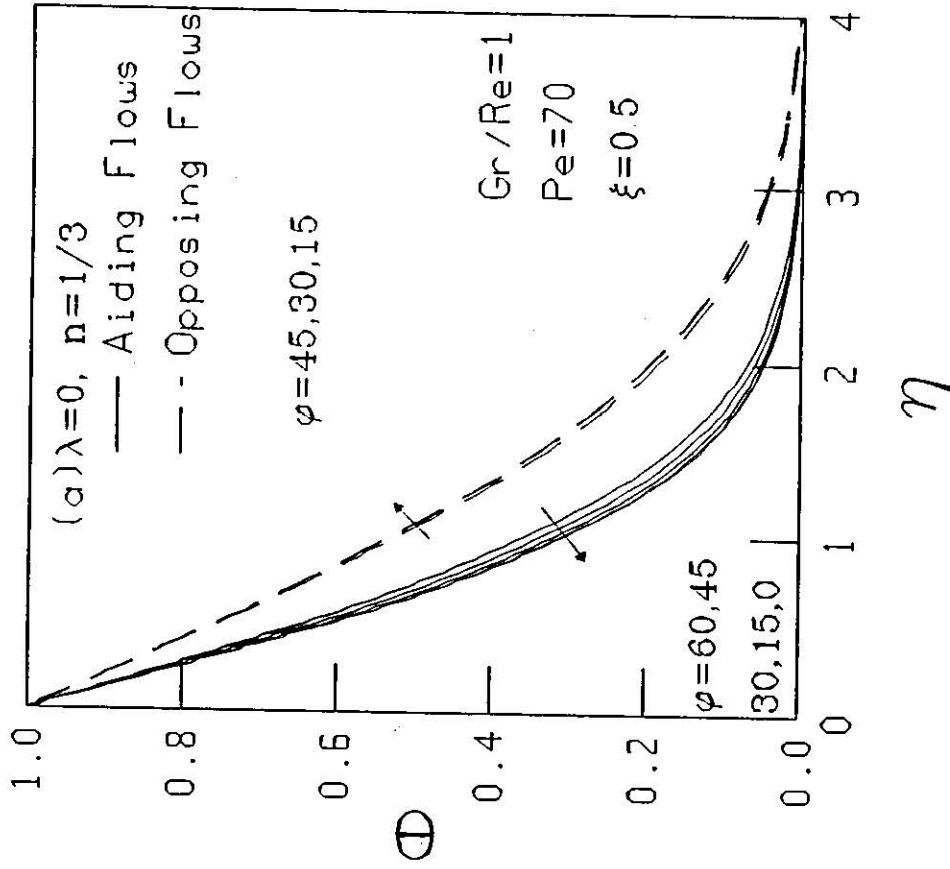Fig.(5.4) Configuration (b) Velocity Profiles For Aiding
And Opposing Flows For Selected Values Of φ
(a)Isothermal Wall (b)Linear Wall Temperature Variation.
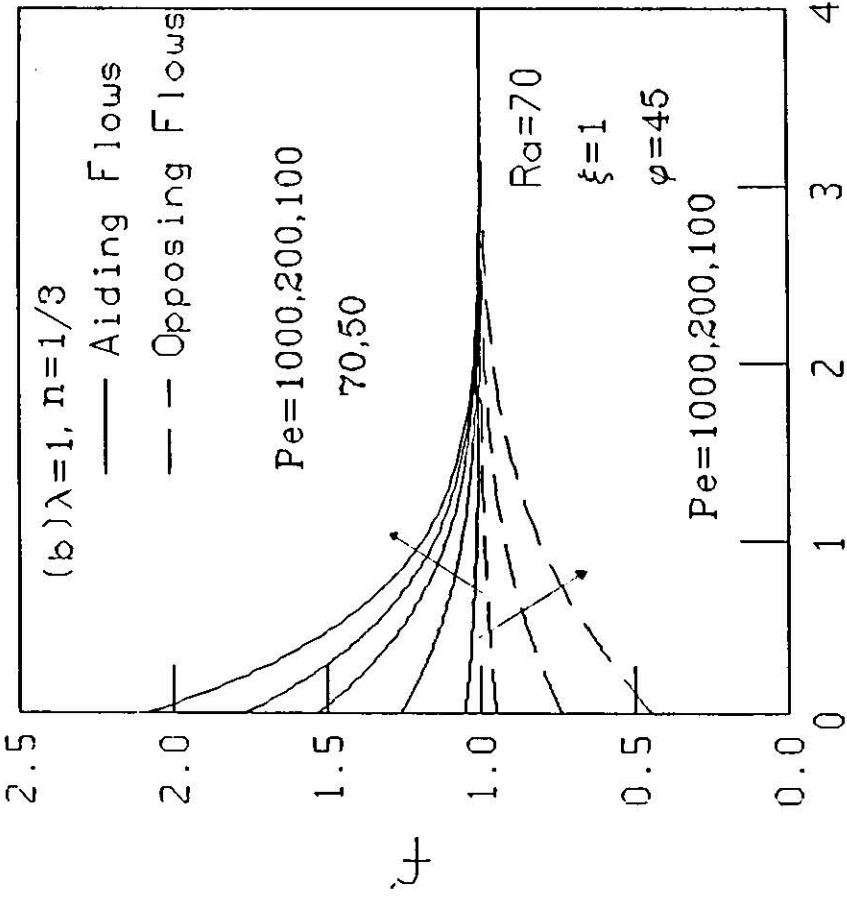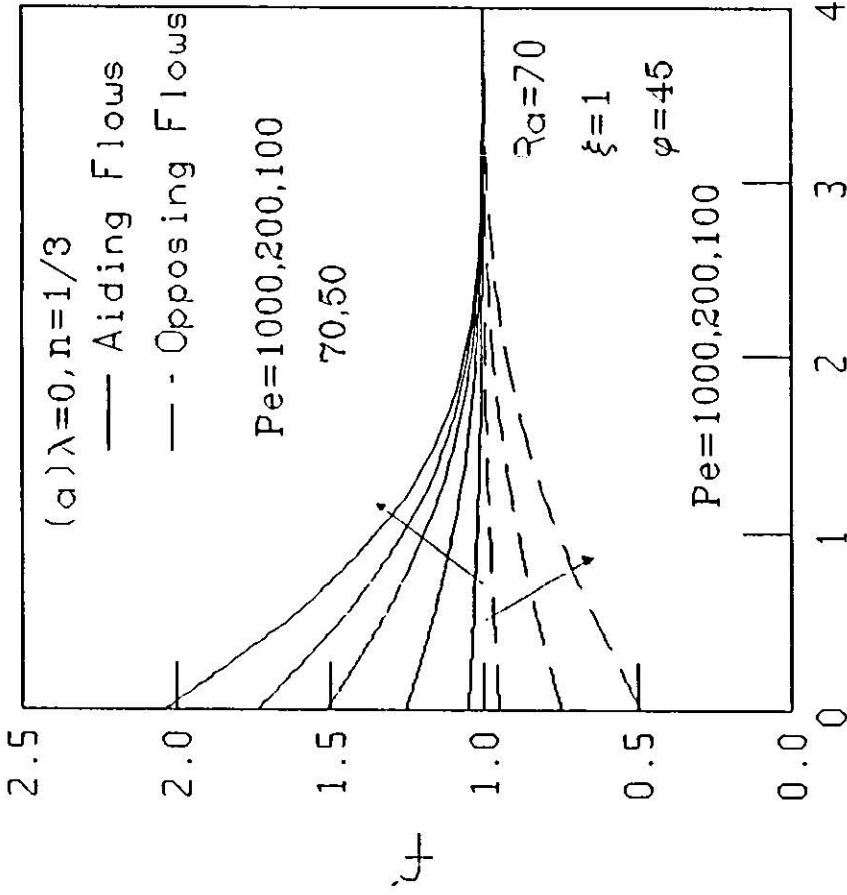
Fig.(5.5) Configuration (a) Velocity Profiles For Aiding And Opposing Flows For Selected Values Of Pe. (a)Isothermal Wall (b)Linear Wall Temperature Variation.
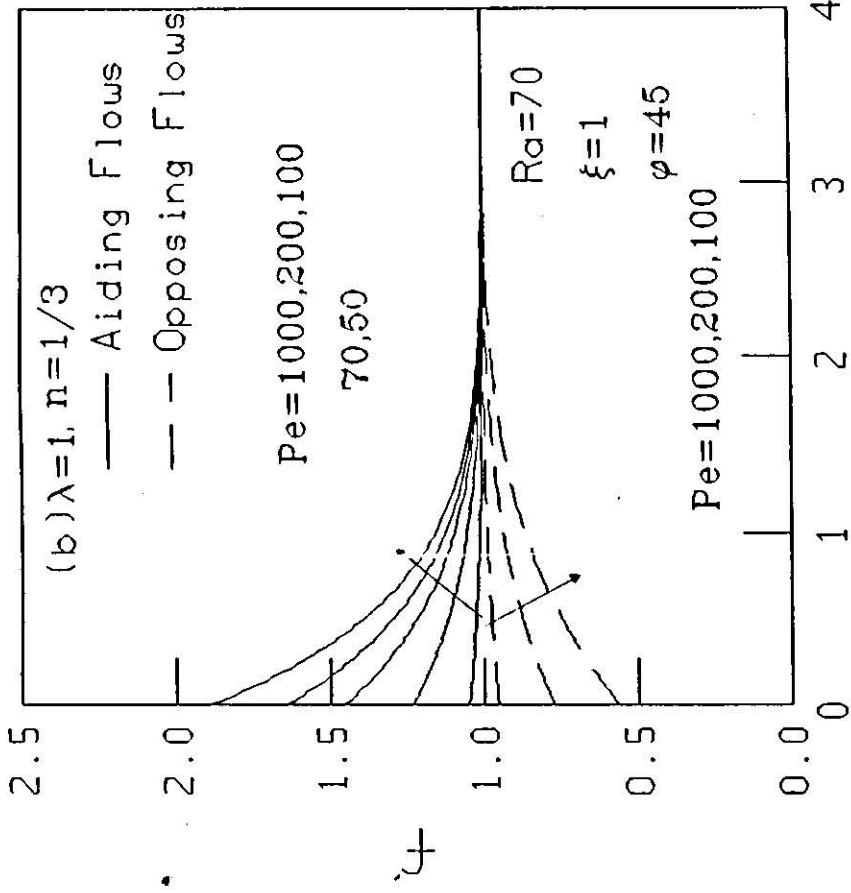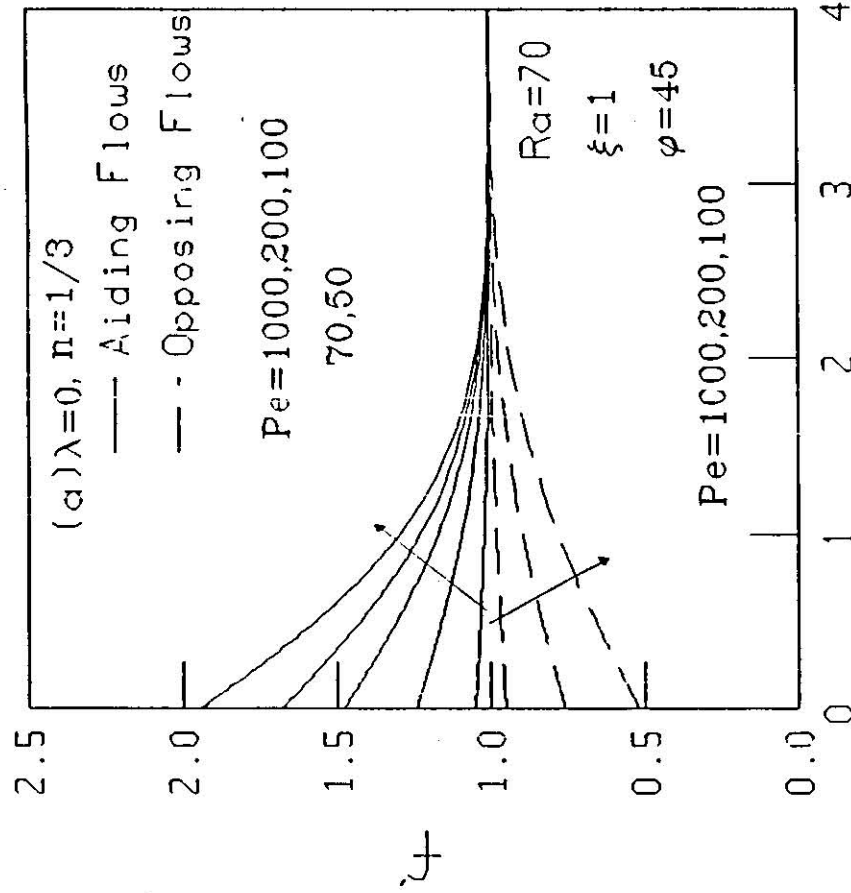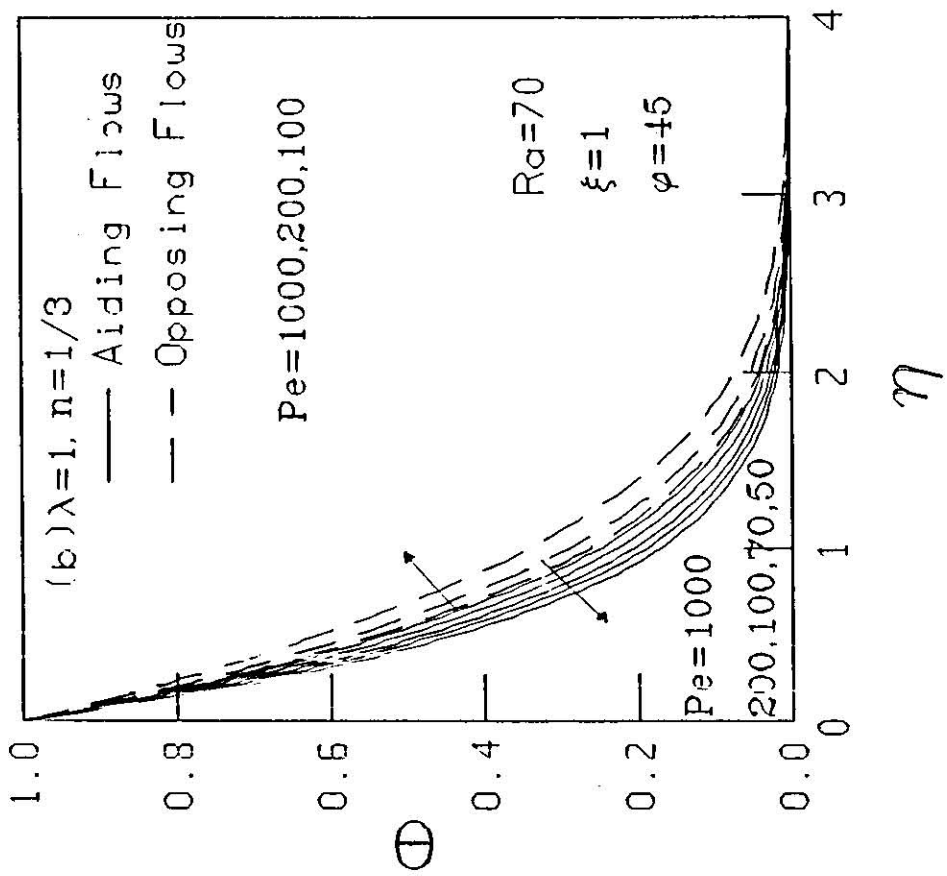
Fig.(5.6) Configuration (b) Velocity Profiles For Aiding
And Opposing Flows For Selected Values Of Pe.
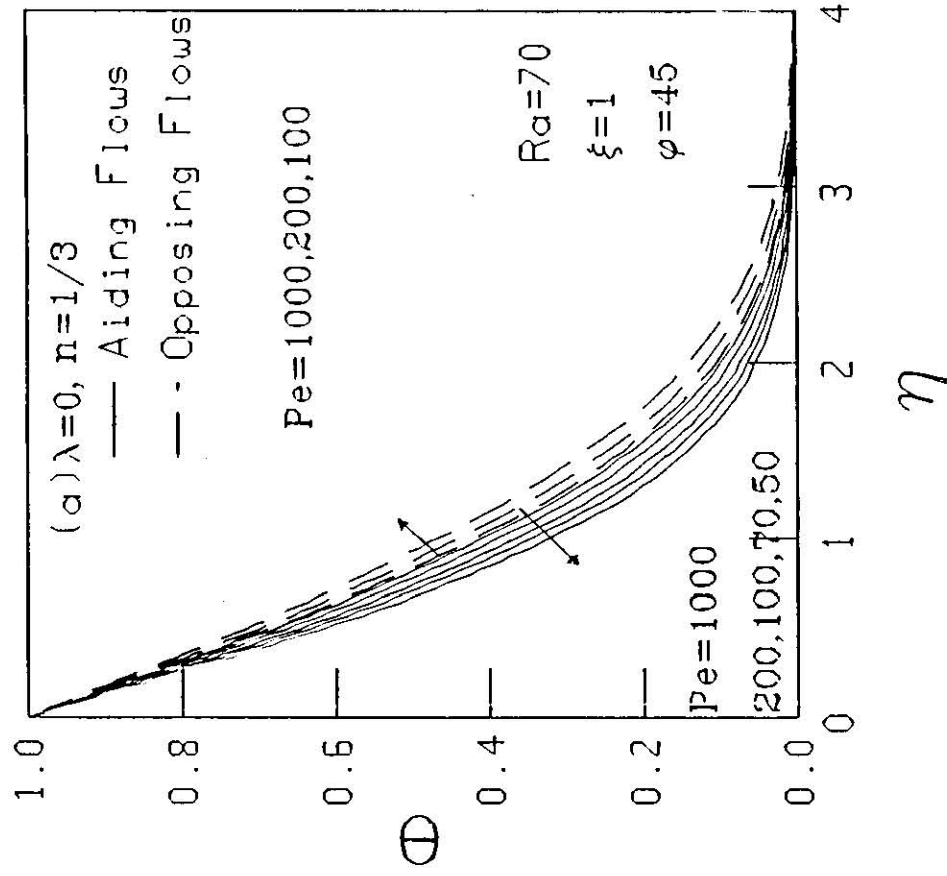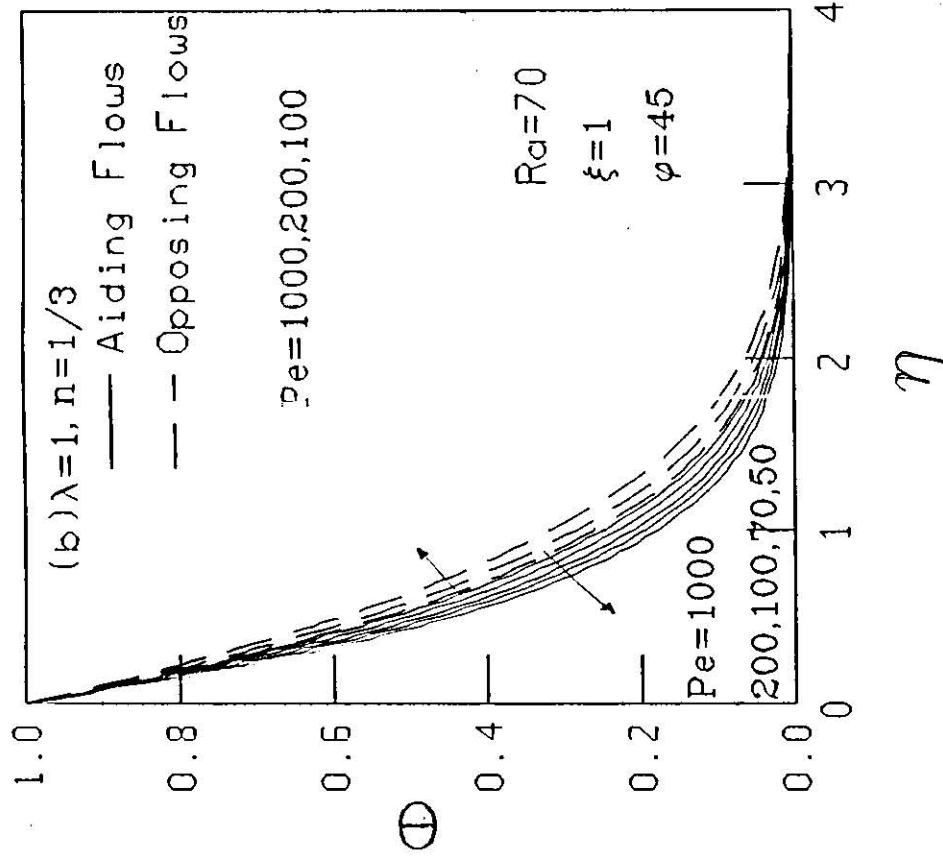
(a)Isothermal Wall (b)Linear Wall Temperature Variation.
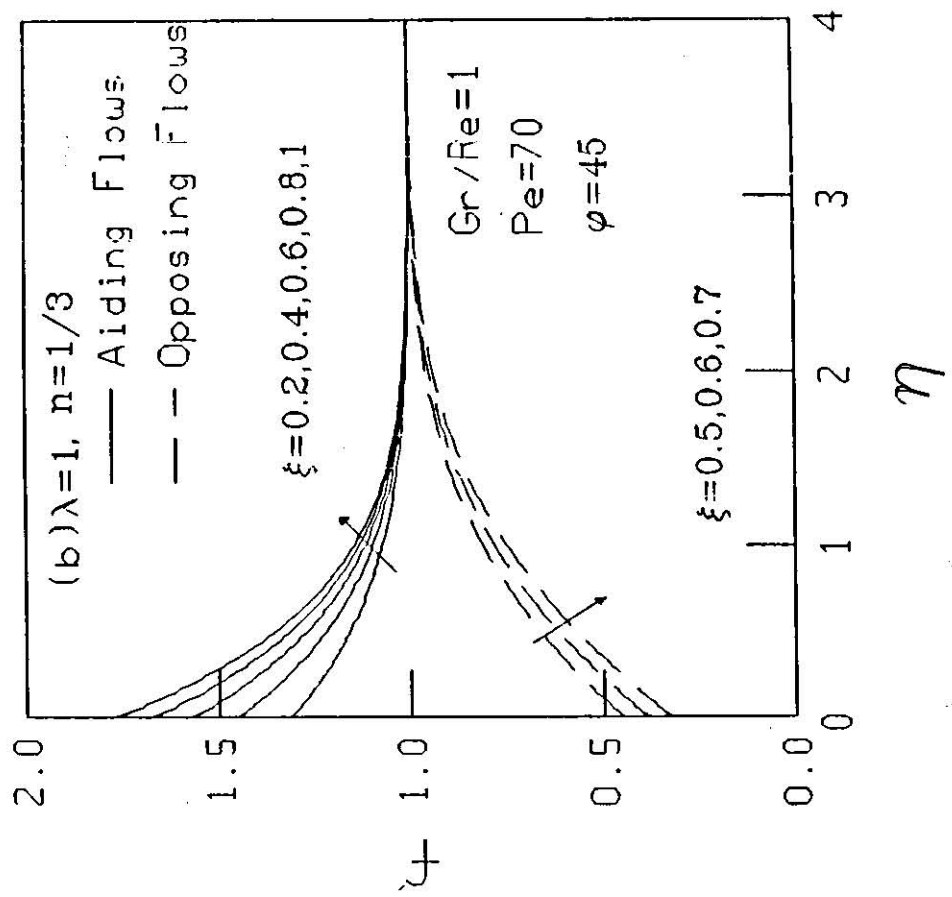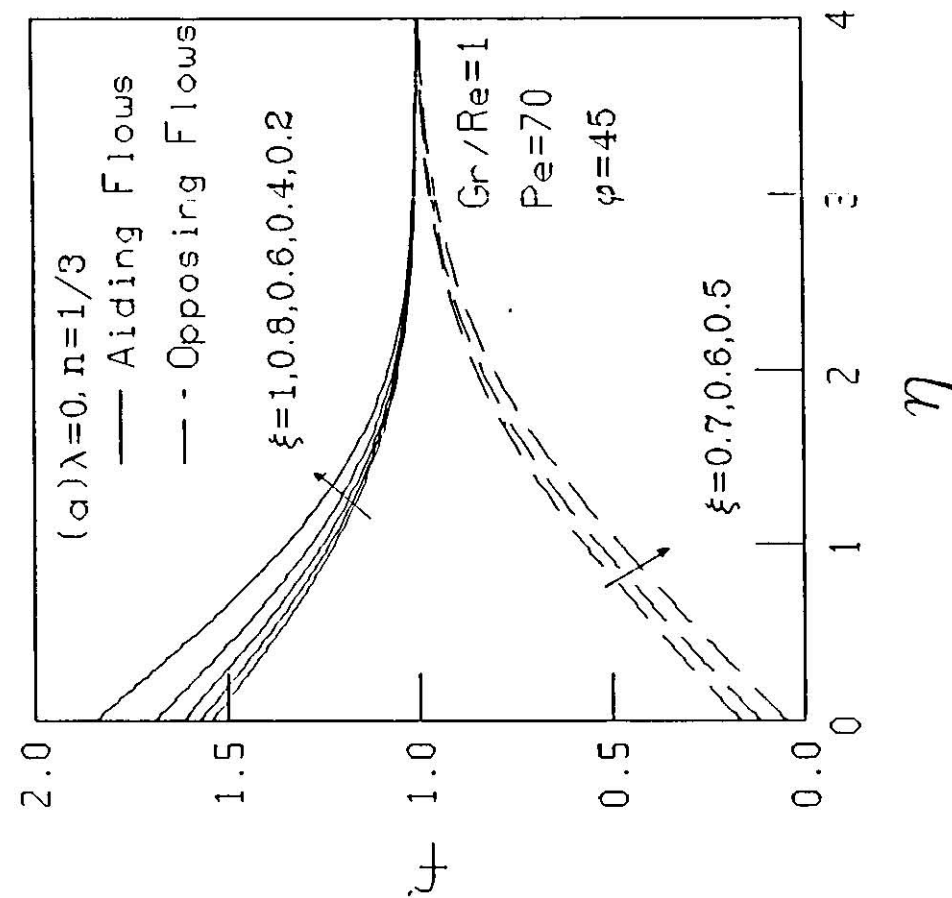
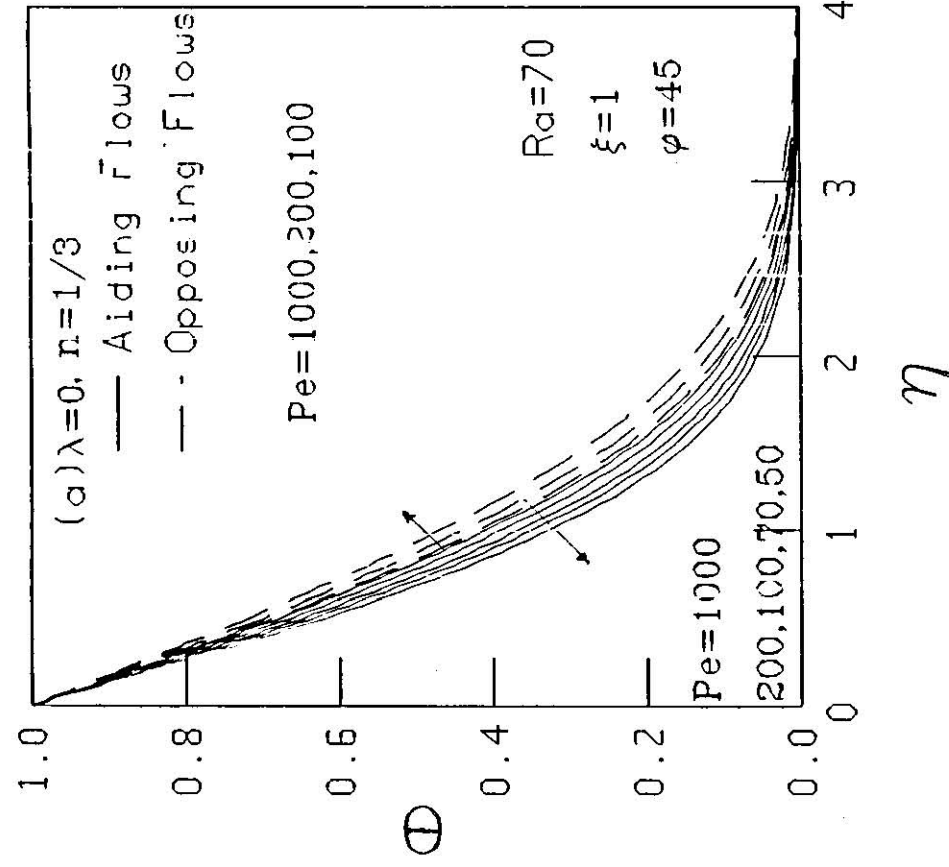Fig.(5.7) Configuration (a) Velocity Profiles For Aiding
And Opposing Flows For Selected Values Of ξ
(a)Isothermal Wall (b)Linear Wall Temperature Variation.
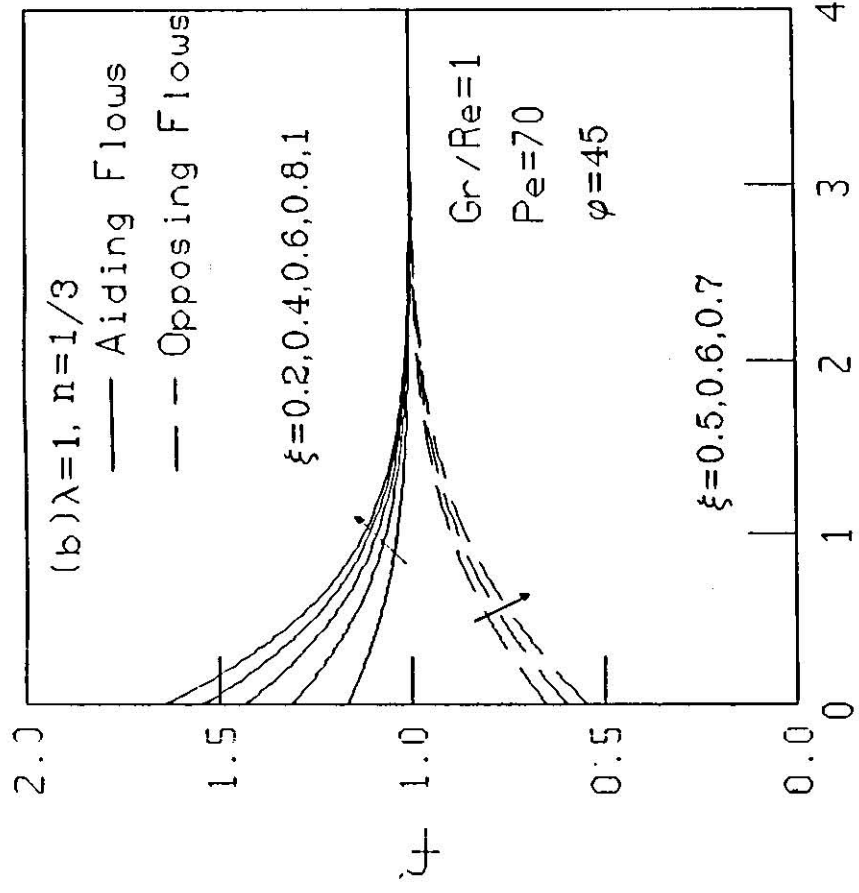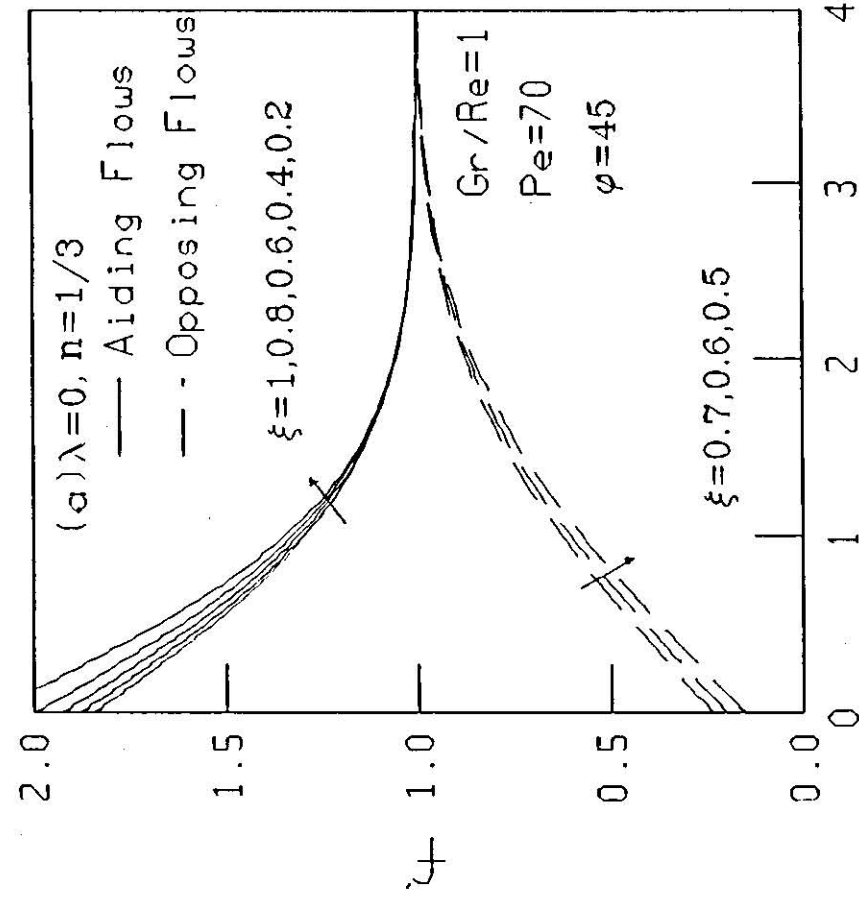
Fig.(5.8) Configuration (b) Velocity Profiles For Aiding
And Opposing Flows For Selected Values Of ξ
(a)Isothermal Wall (b)Linear Wall Temperature Variation.
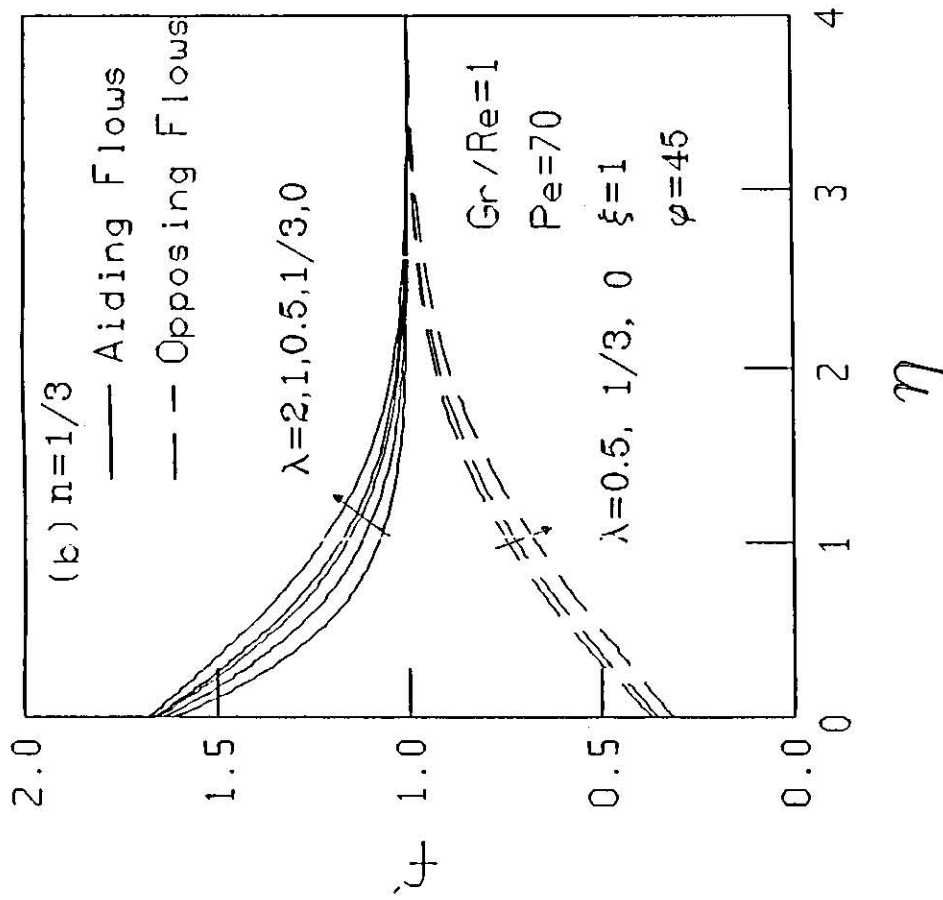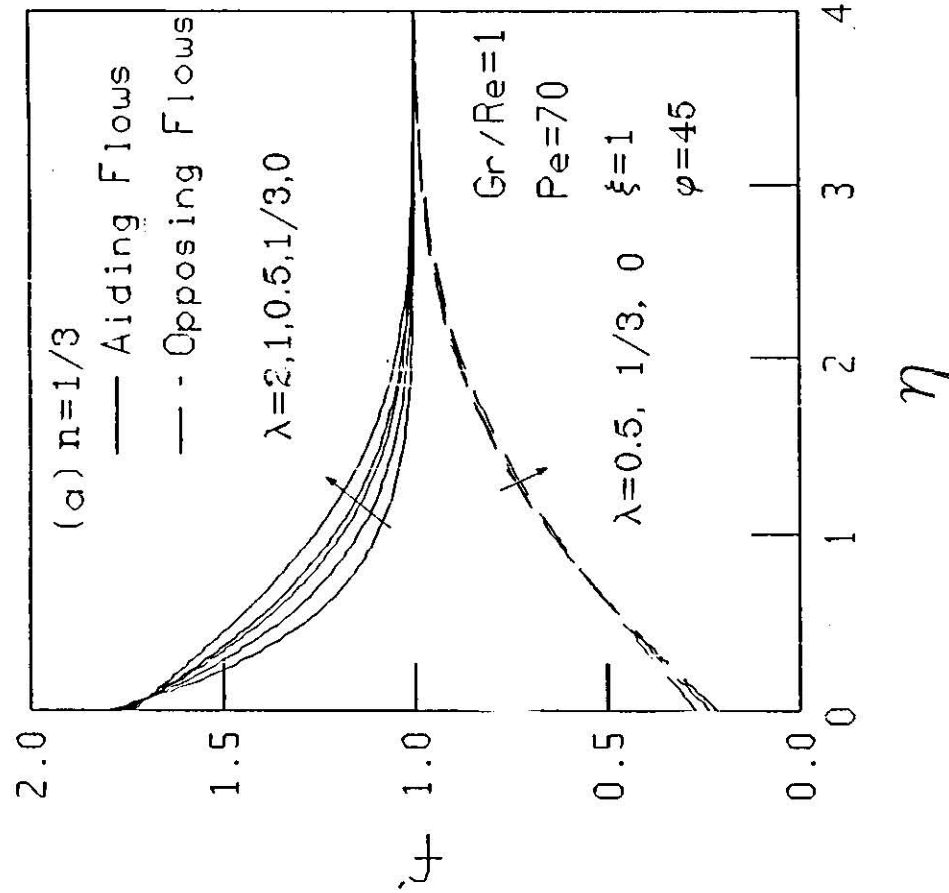
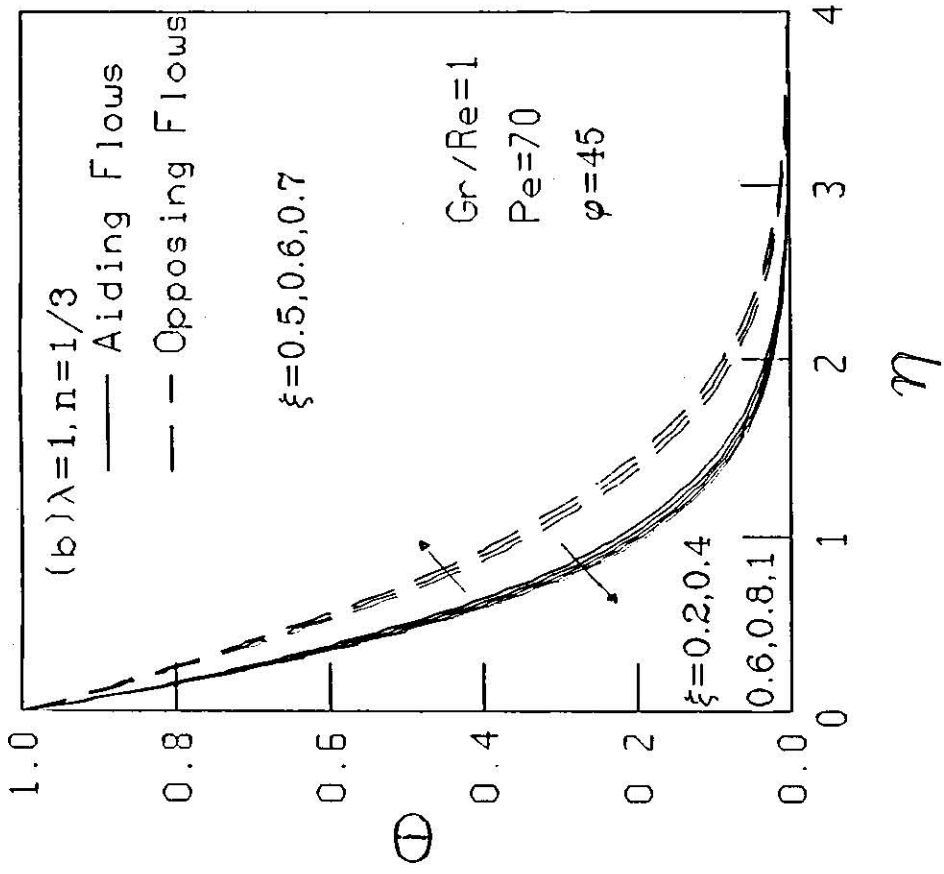Fig.(5.9) Velocity Profiles For Aiding And Opposing
Flows For Selected Values Of λ

(a)Configuration (a)   (b)Configuration (b)
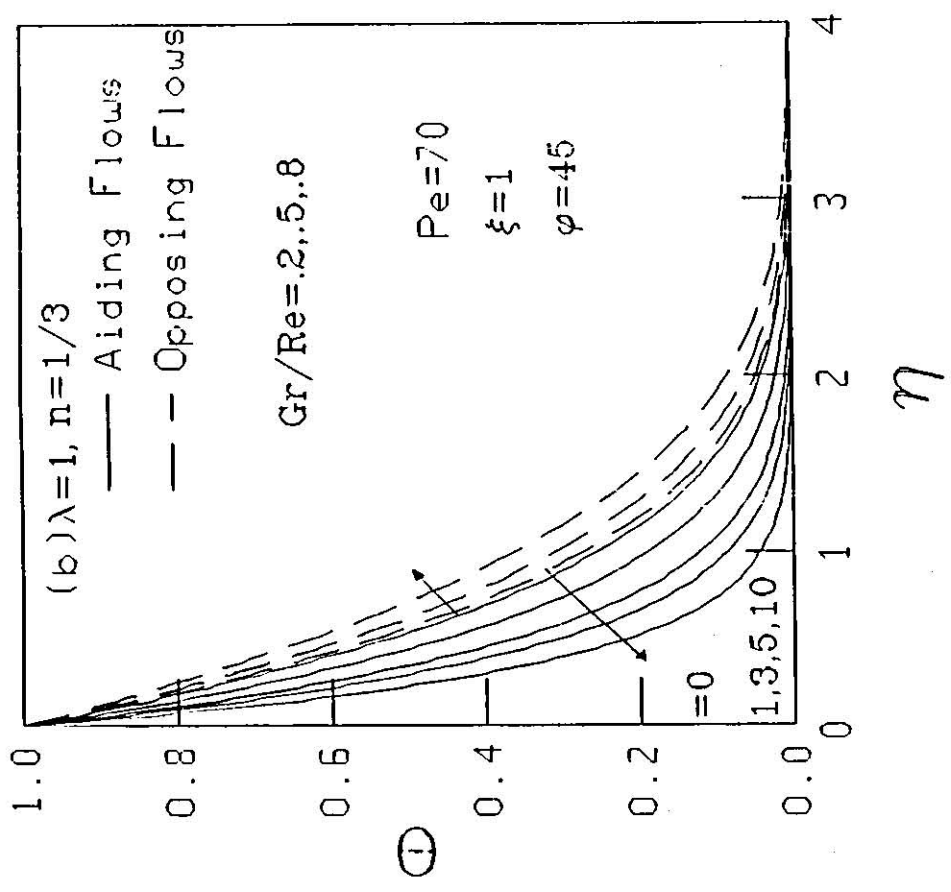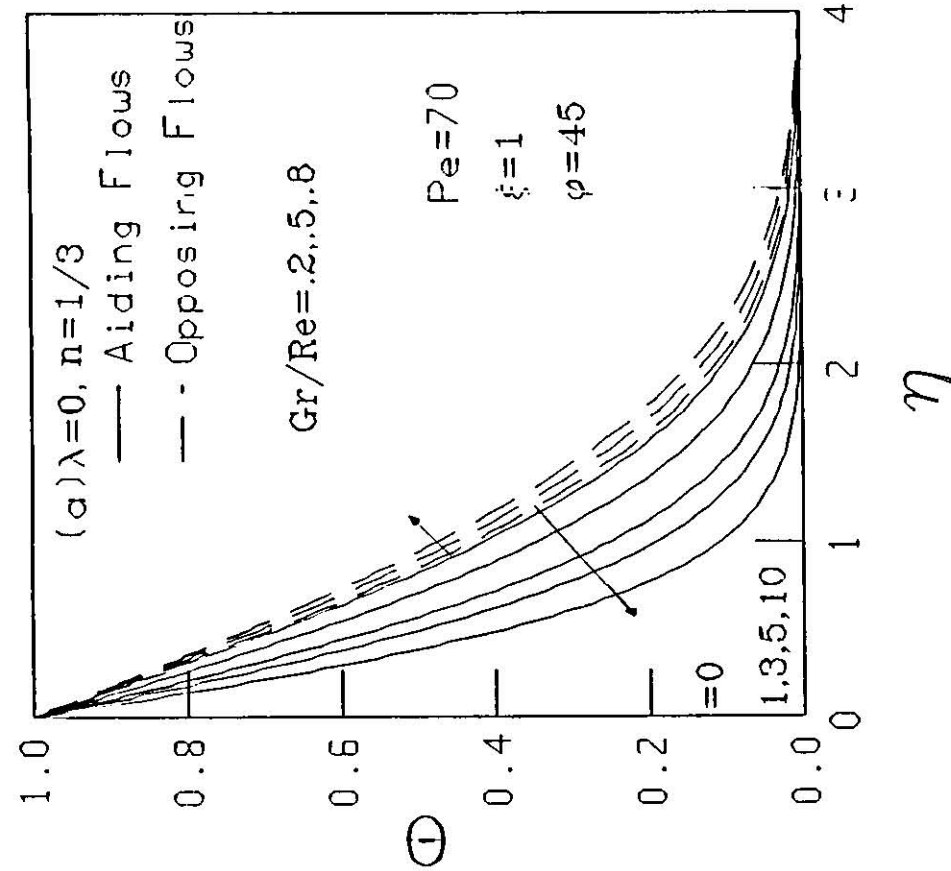
Fig.(5.10) Configuration (a) Temperature Profiles For Aiding
And Opposing Flows For Selected Values Of Gr/Re.
(b)Linear Wall Temperature Variation.
(a)Isothermal Wall
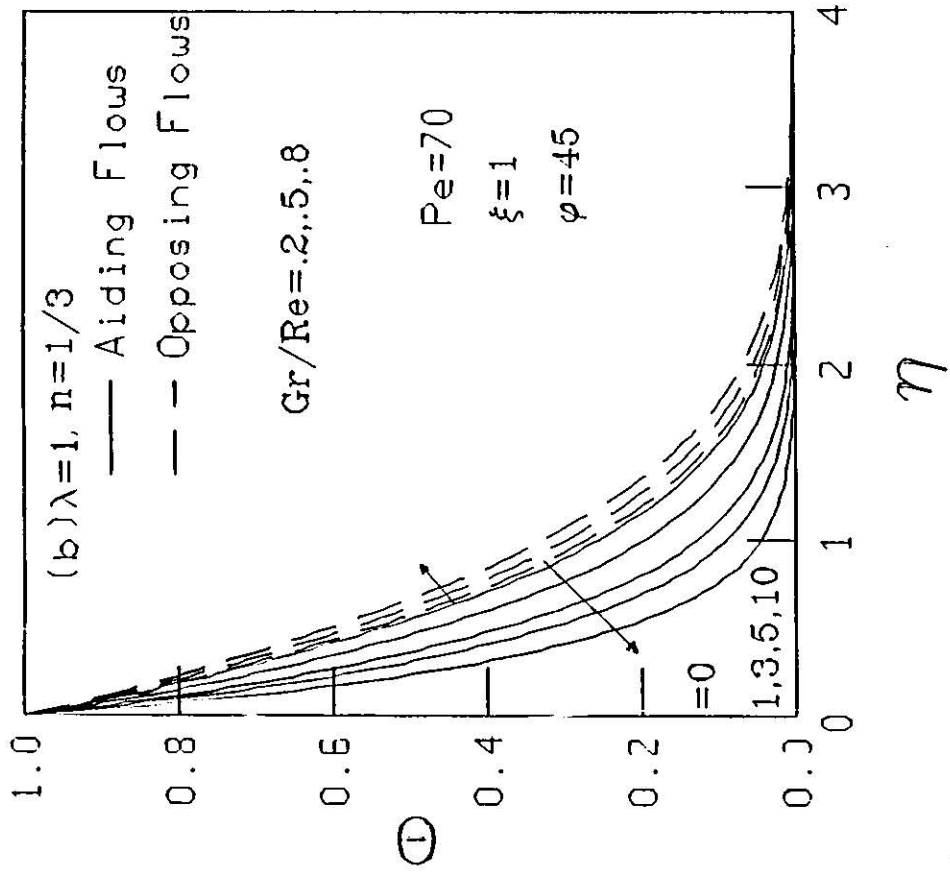
Fig.(5.11) Configuration (b) Temperature Profiles For Aiding
And Opposing Flows For Selected Values Of Gr/Re.
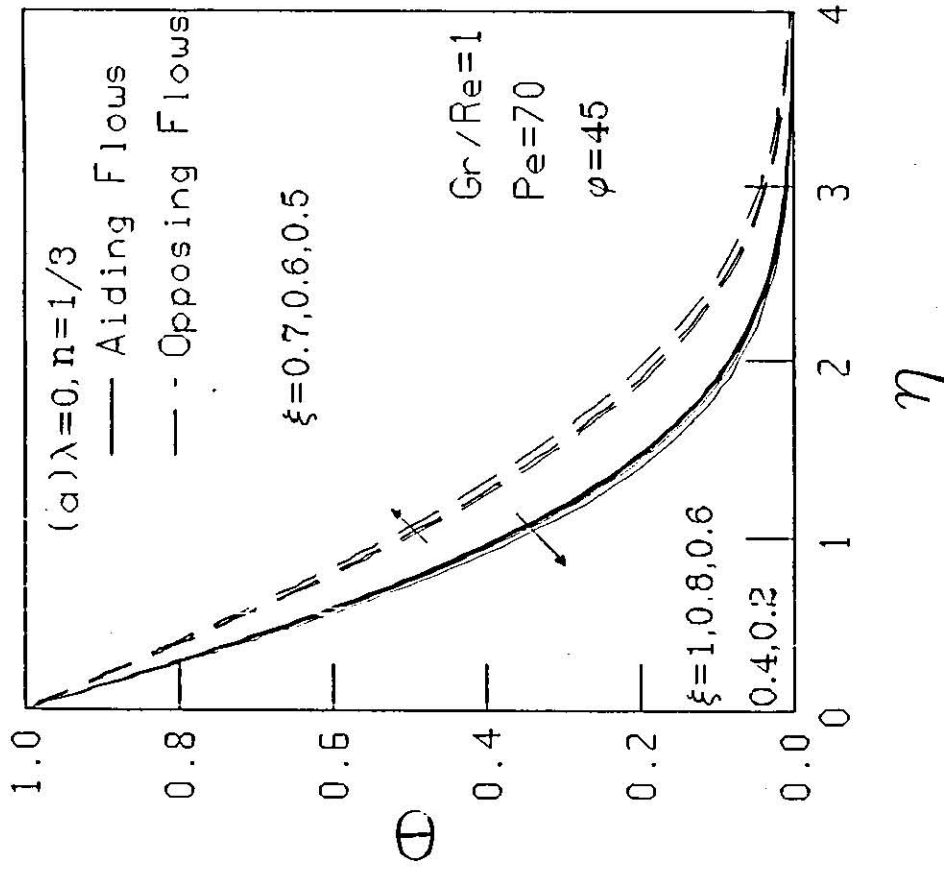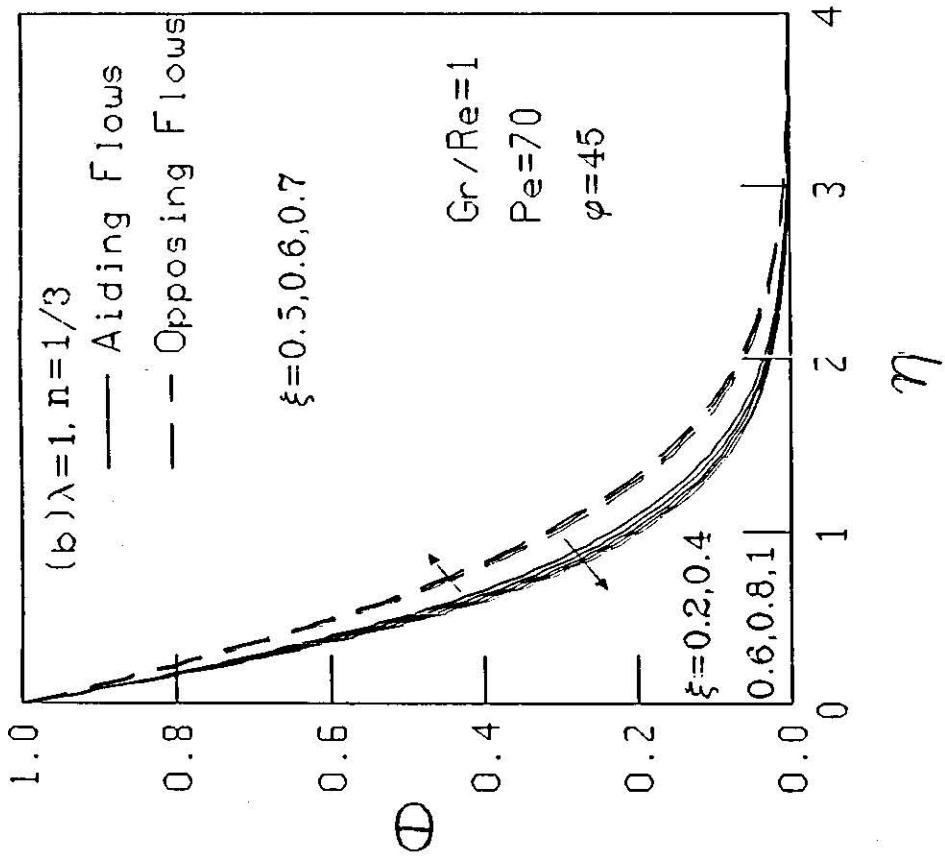(a)Isothermal Wall (b)Linear Wall Temperature Variation.

Fig.(5.12) Configuration (a) Temperature Profiles For Aiding
And Opposing Flows For Selected Values Of φ
(a)Isothermal Wall (b)Linear Wall Temperature Variation.

Fig.(5.13) Configuration (b) Temperature Profiles For Aiding
And Opposing Flows For Selected Values Of φ
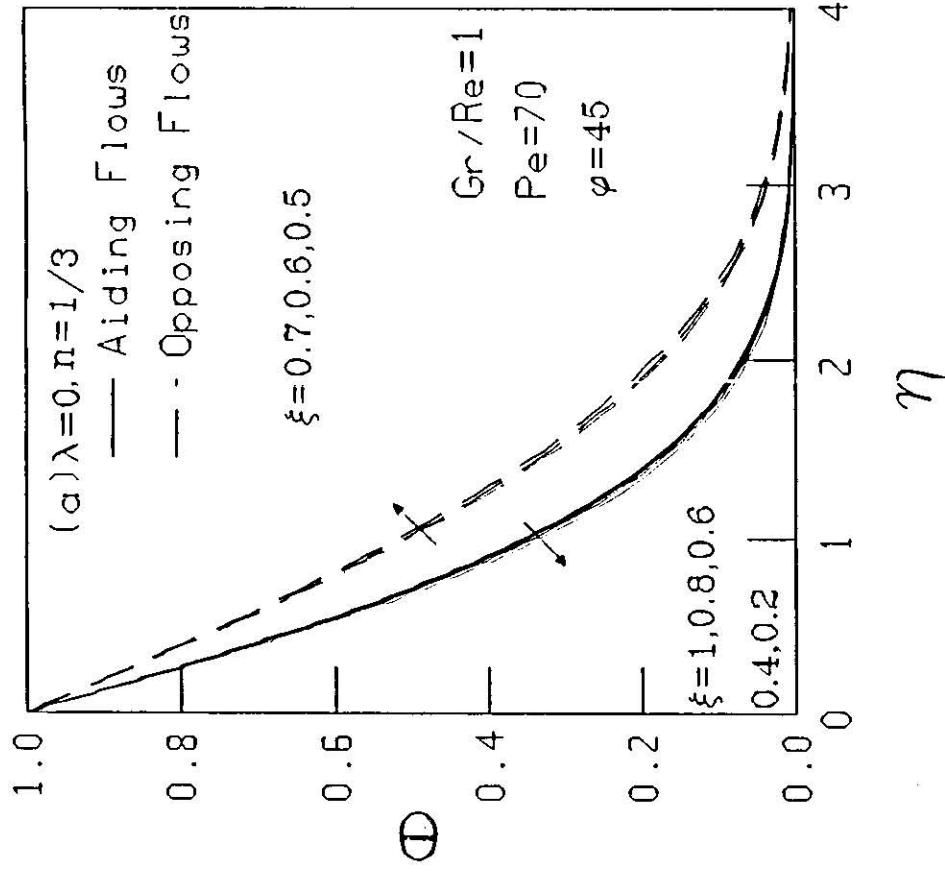(a)Isothermal Wall (b)Linear Wall Temperature Variation.

Fig.(5.14) Configuration (a) Temperature Profiles For Aiding
And Opposing Flows For Selected Values Of Pe.
(a)Isothermal Wall (b)Linear Wall Temperature Variation.

Fig.(5.15) Configuration (b) Temperature Profiles For Aiding
And Opposing Flows For Selected Values Of Pe.
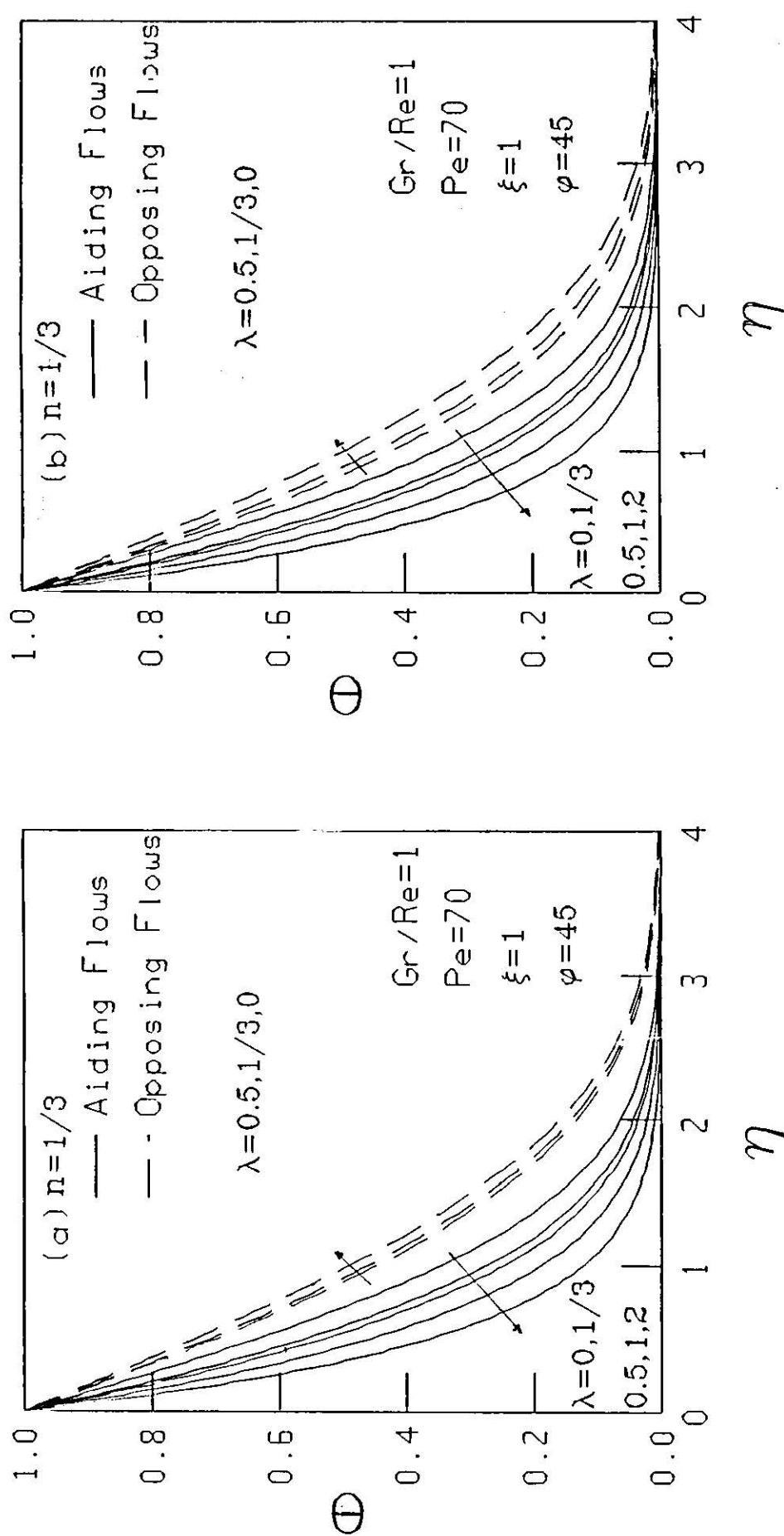(a)Isothermal Wall (b)Linear Wall Temperature Variation.

Fig.(5.15) Configuration (a) Temperature Profiles For Aiding
And Opposing Flows For Selected Values Of ξ
(a)Isothermal Wall (b)Linear Wall Temperature Variation.

Plot (b):

(b)λ=1,n=1/3
—— Aiding Flows
— — Opposing Flows

ξ=0.5,0.6,0.7

Gr/Re=1
Pe=70
φ=45

ξ=0.2,0.4
0.6,0.8,1

Plot (a):

(a)λ=0,n=1/3
—— Aiding Flows
— —Opposing Flows

ξ=0.7,0.6,0.5

Gr/Re=1
Pe=70
φ=45

ξ=1,0.8,0.6
0.4,0.2

Fig.(5.17) Configuration (b) Temperature Profiles For Aiding
And Opposing Flows For Selected Values Of ξ
(a)Isothermal Wall (b)Linear Wall Temperature Variation.

Fig.(5.18) Temperature Profiles For Aiding And Opposing
Flows For Selected Values Of λ
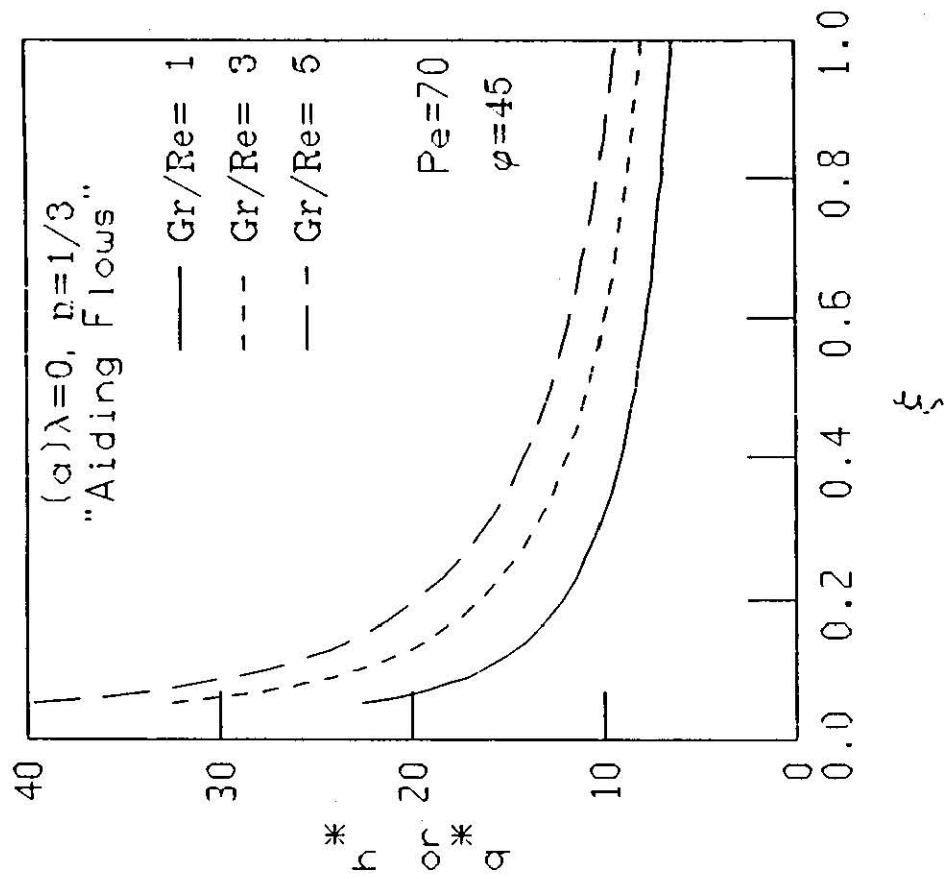
(a)Configuration (a)   (b)Configuration (b)
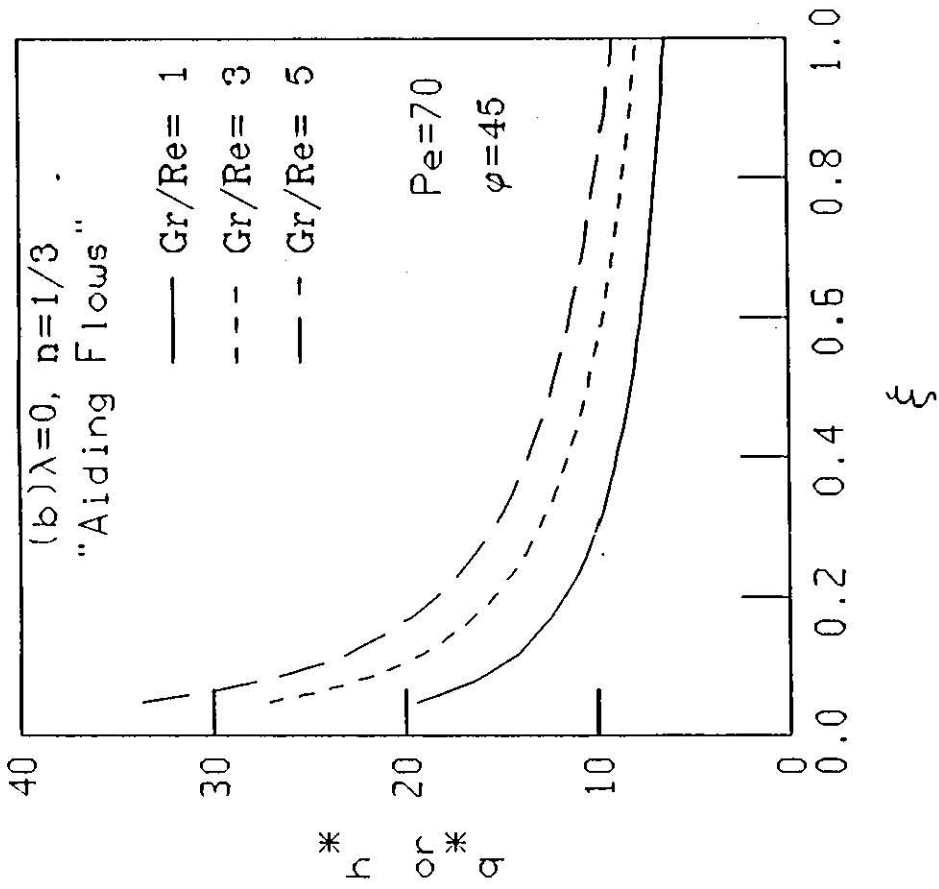
Fig.(5 – 19) Local Heat Transfer Coefficients And local Heat Fluxes
For Selected Values Of Gr/Re. Isothermal Walls.
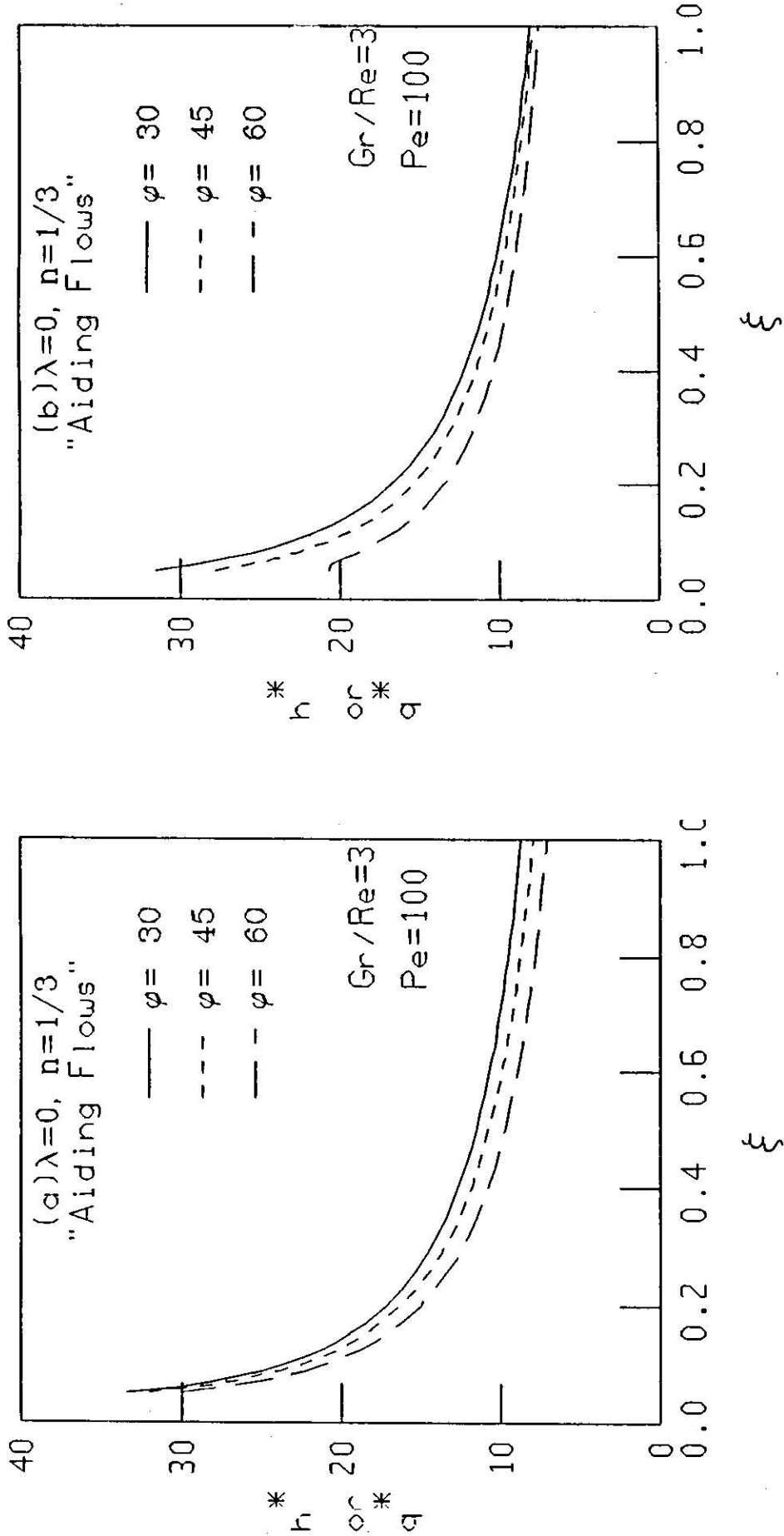
(a) Configuration (a)   (b) Configuration (b)

Fig.(5 – 20) Local Heat Transfer Coefficients And local Heat Fluxes
For Selected Values Of φ . Isothermal Walls.
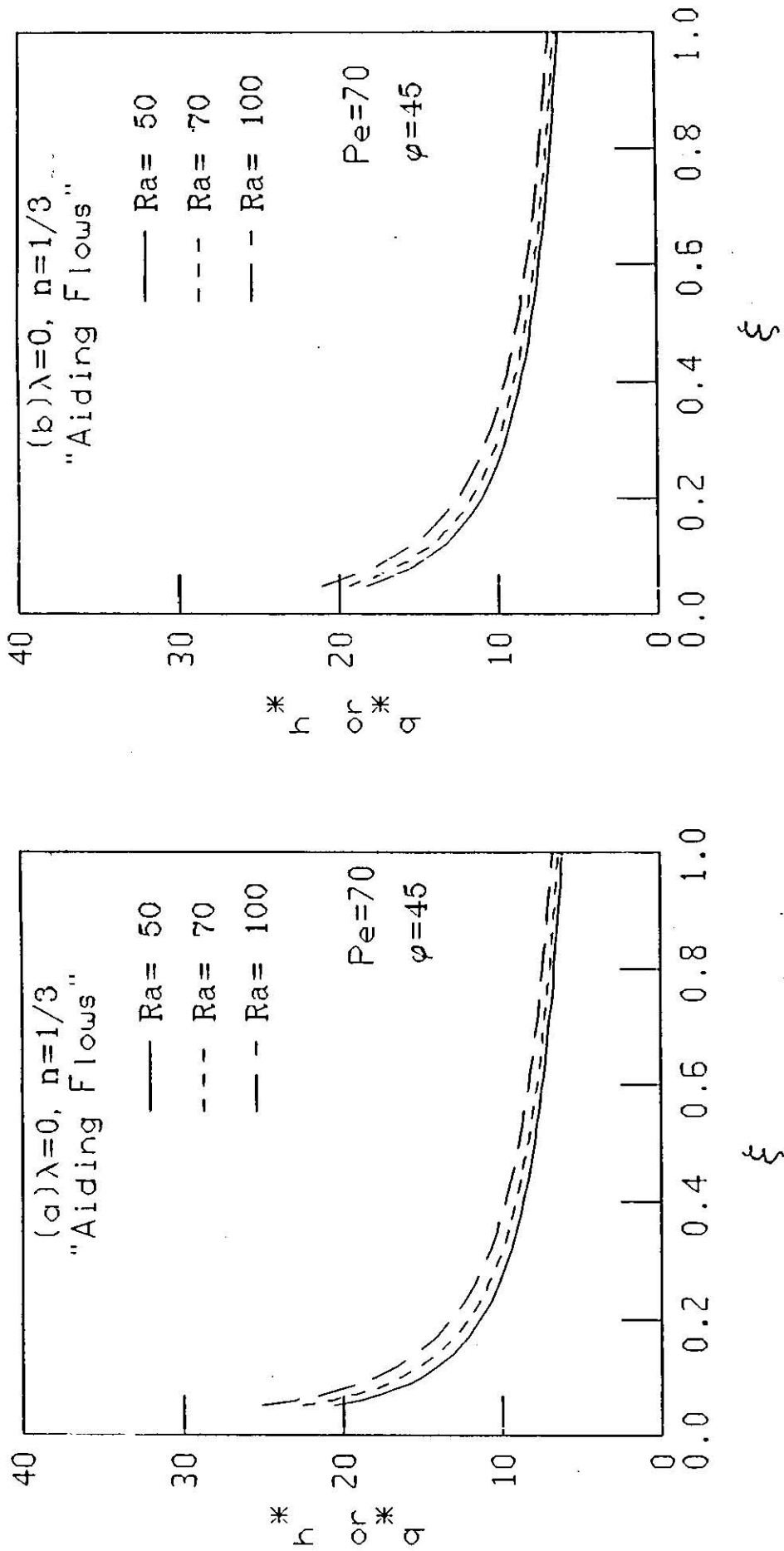(a) Configuration (a)   (b) Configuration (b)

Fig.(5 – 21) Local Heat Transfer Coefficients And local Heat Fluxes
For Selected Values Of Ra . Isothermal Walls.
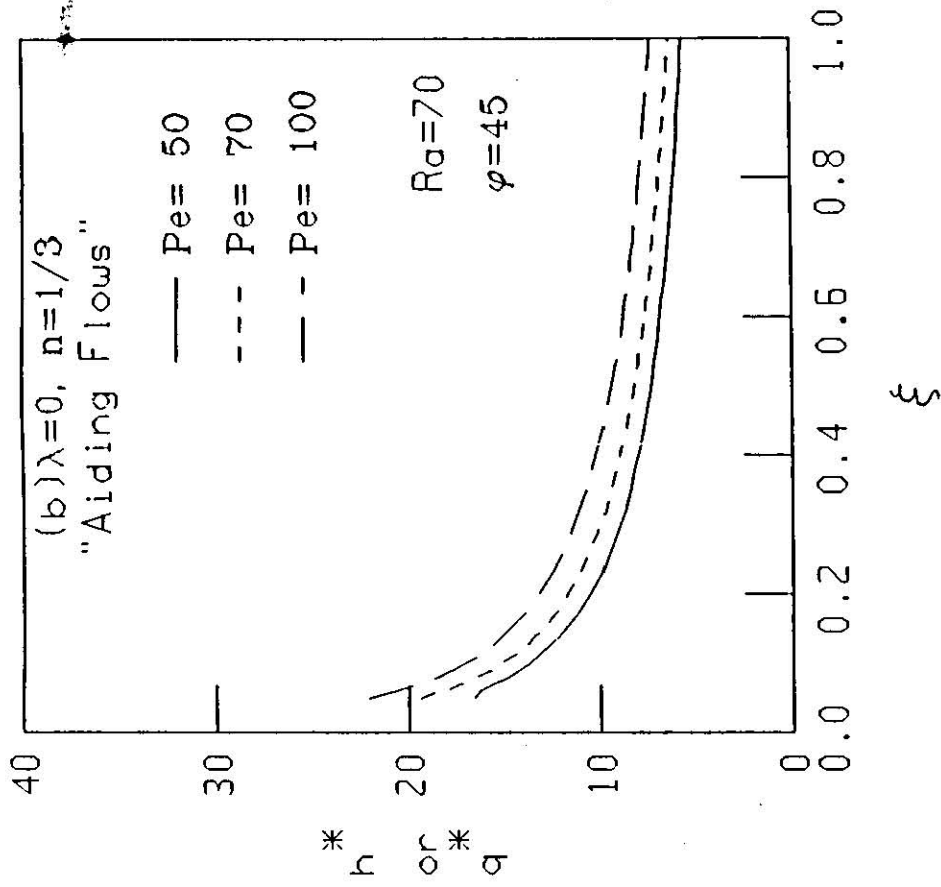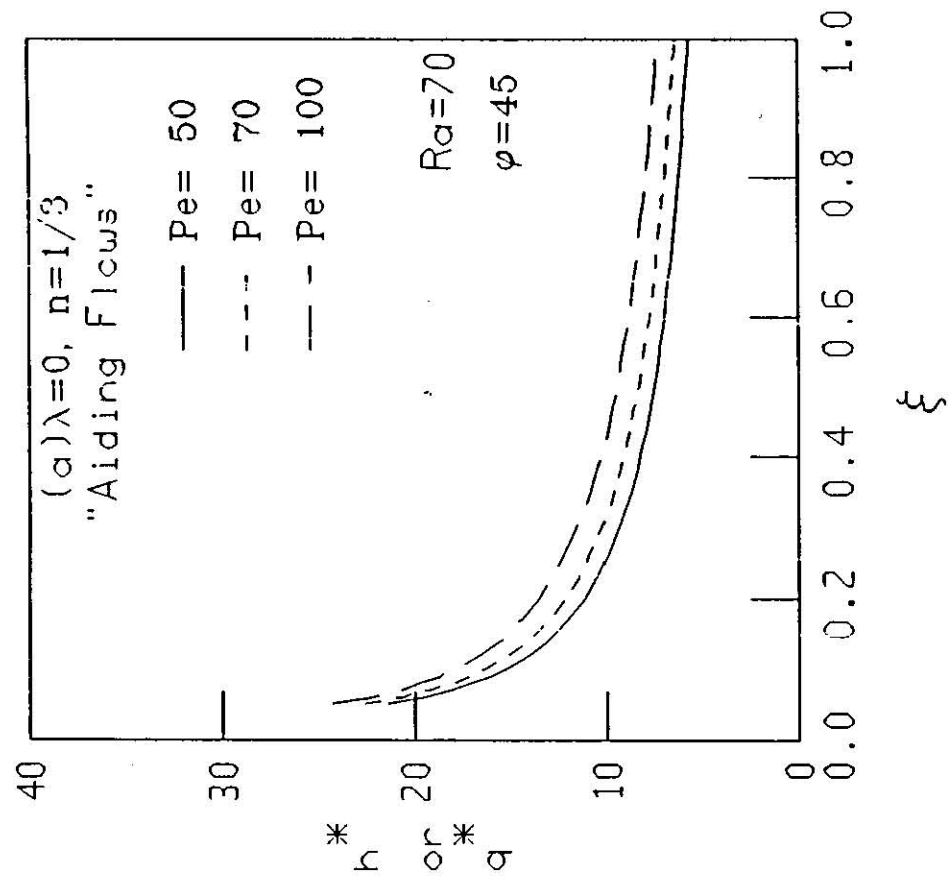(a) Configuration (a)   (b) Configuration (b)

Fig.(5 - 22) Local Heat Transfer Coefficients And local Heat Fluxes
For Selected Values Of Pe . Isothermal Walls.
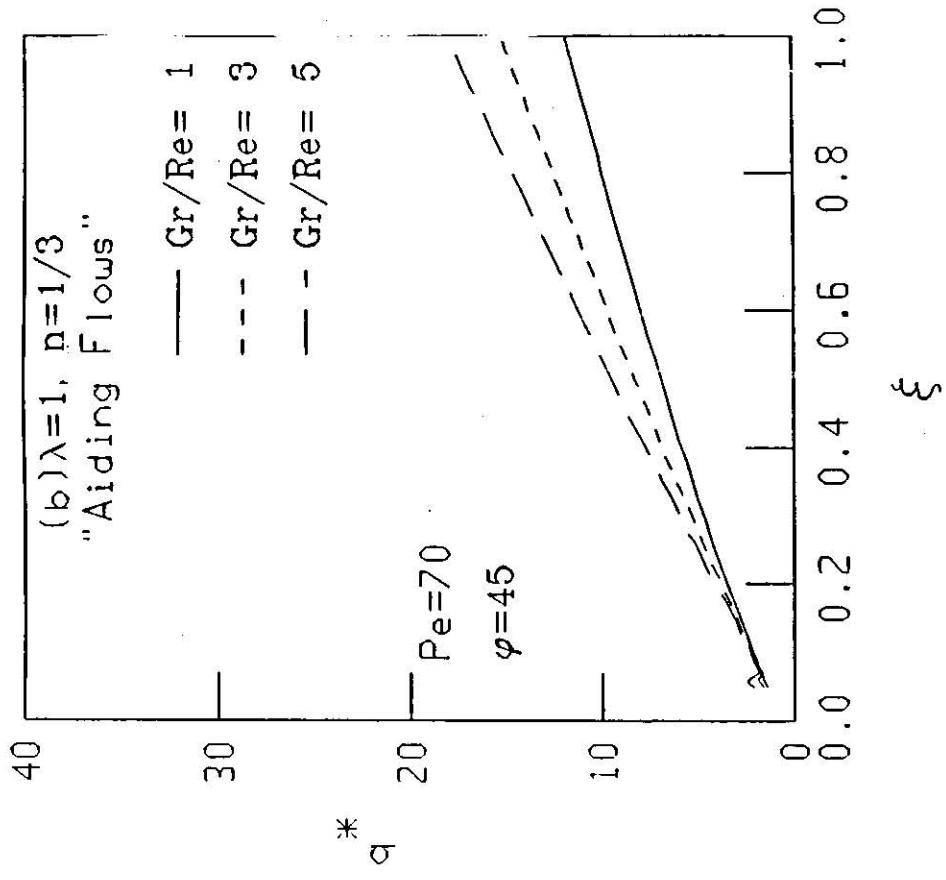
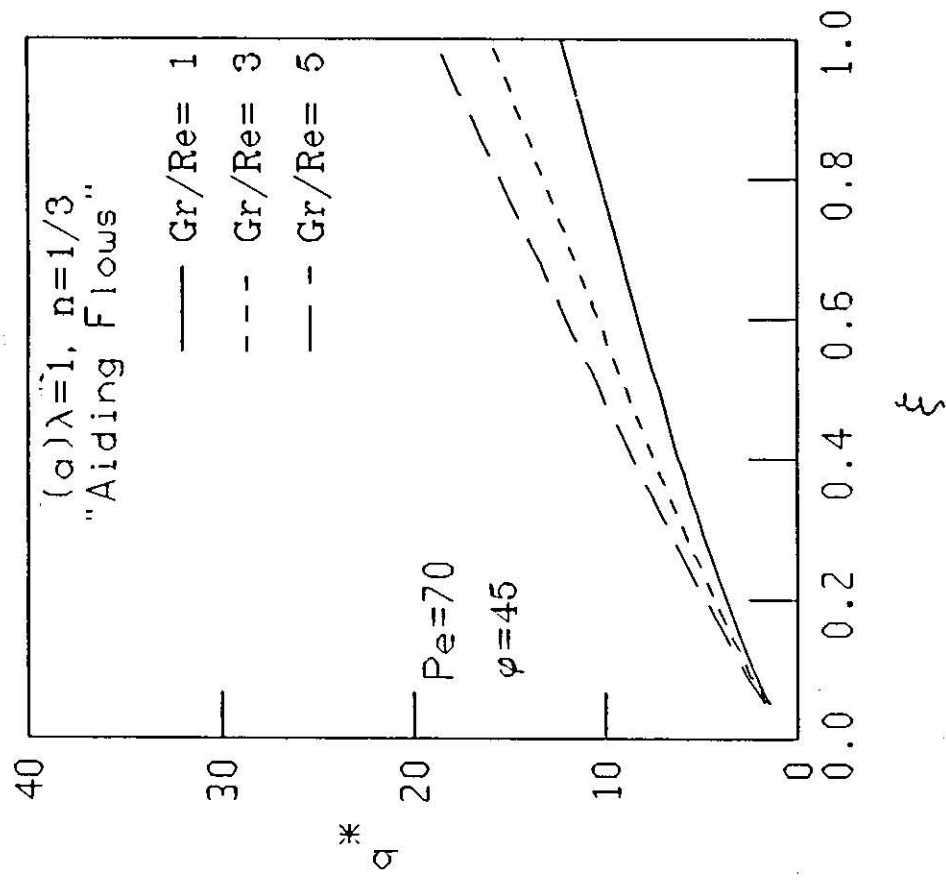(a) Configuration (a)   (b) Configuration (b)

Fig.(5 - 23) Local Heat Fluxes For Selected Values Of Gr/Re.

Linear Wall Temperature Variation

(a) Configuration (a) (b) Configuration (b)

Fig.(5 - 24) Local Heat Fluxes For Selected Values Of φ .

Linear Wall Temperature Variation

(a) Configuration (a) , (b) Configuration (b)

Fig.(5 - 25) Local Heat Fluxes For Selected Values Of Ra .

Linear Wall Temperature Variation
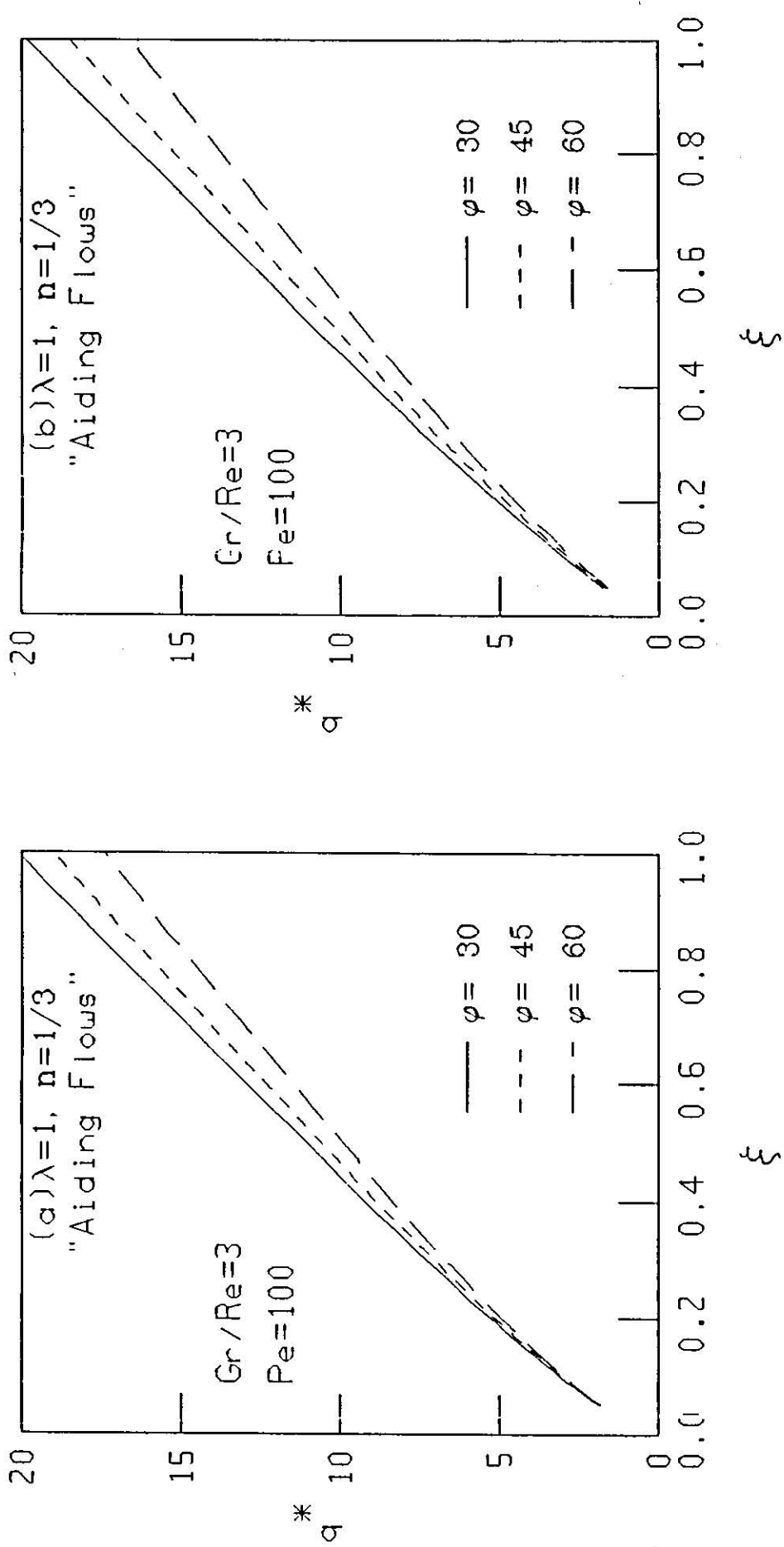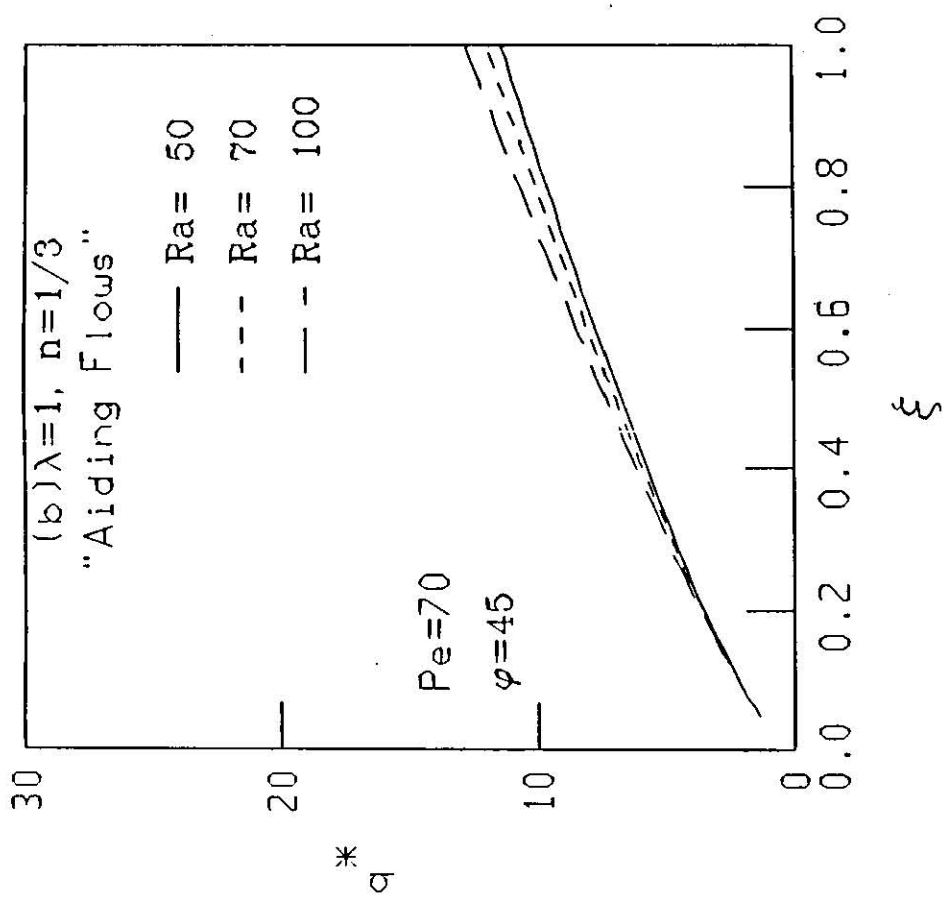
(a) Configuration (a) (b) Configuration (b)

Fig.(5 - 26) Local Heat Fluxes For Selected Values Of Pe .

Linear Wall Temperature Variation
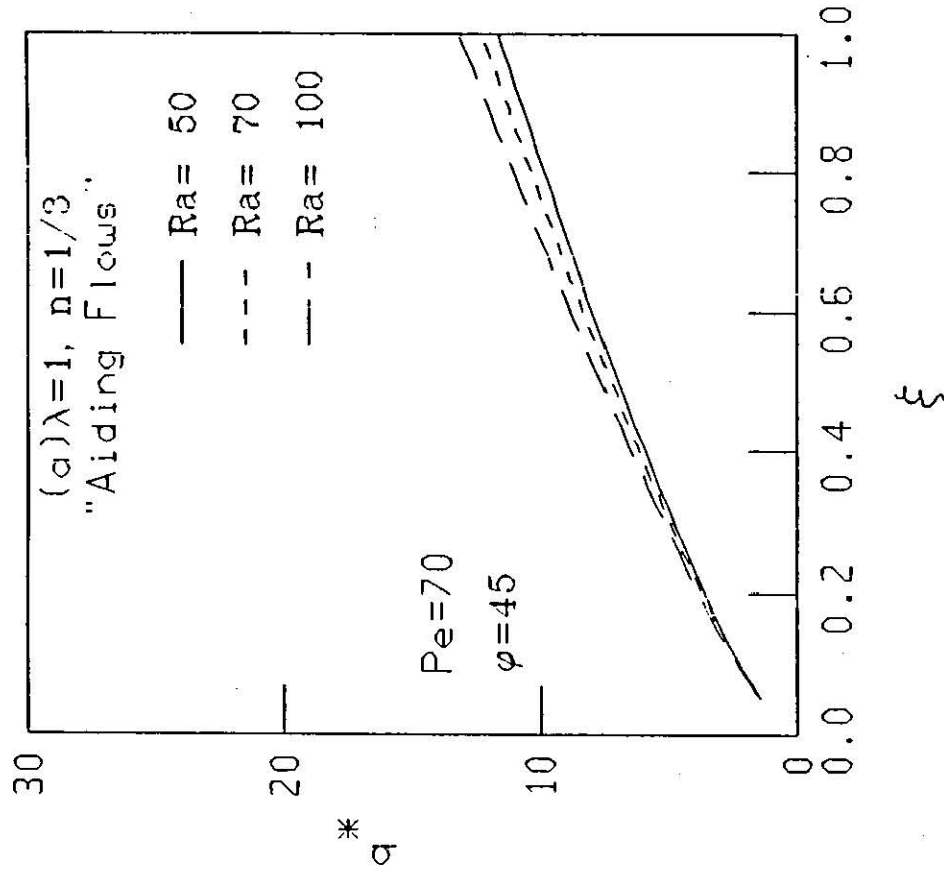
(a) Configuration (a) (b) Configuration (b)

Fig.(5 - 27) Local Heat Transfer Coefficient For Selected Values
of Gr/Re . Linear Wall Temperature Variation.

(a) Configuration (a) , (b) Configuration (b)

Fig.(5 – 28) Local Heat Transfer Coefficient For Selected Values

of φ · Linear Wall Temperature Variation.

(a) Configuration (a) , (b) Configuration (b)
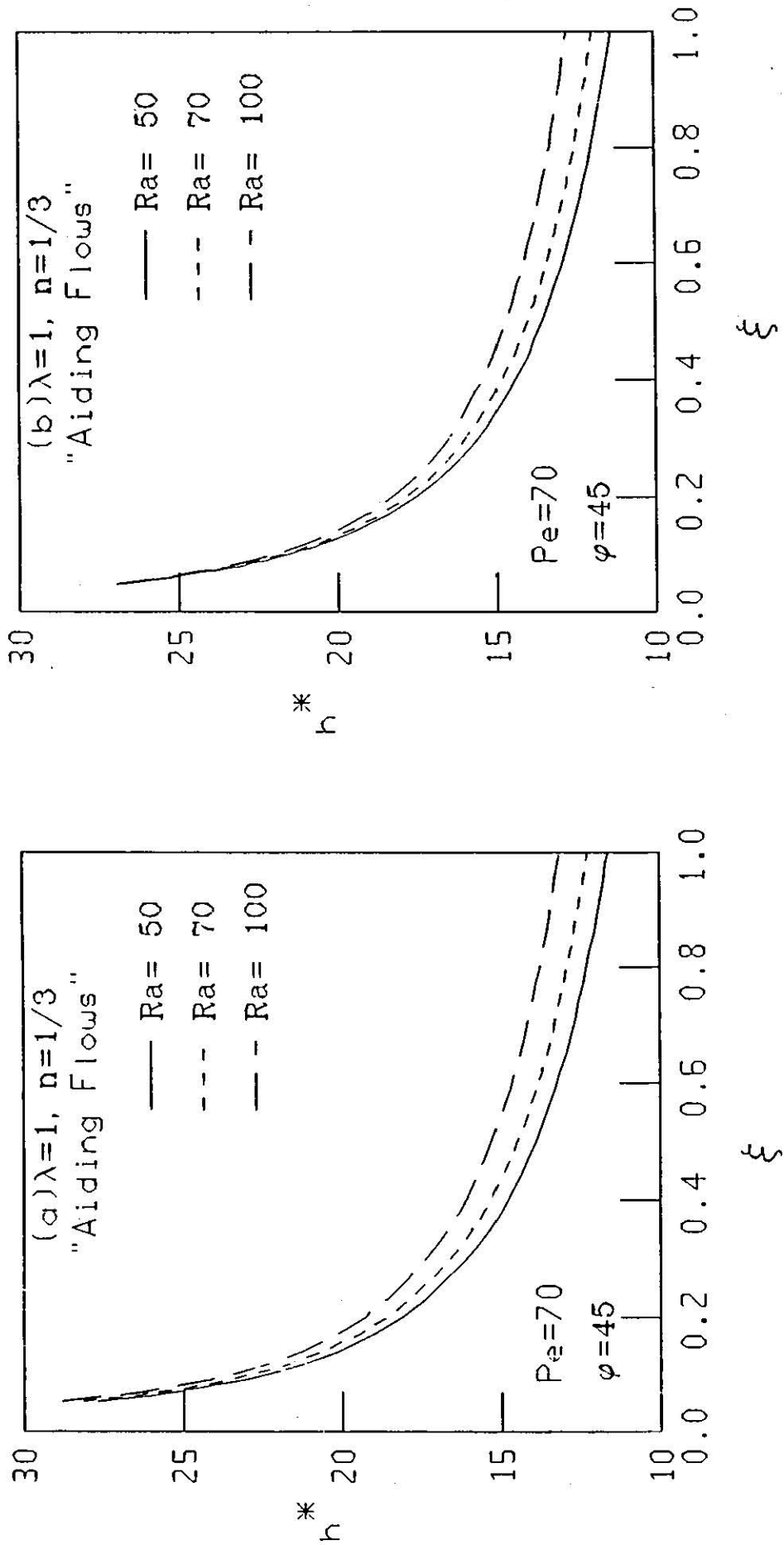
Fig.(5 – 29) Local Heat Transfer Coefficient For Selected Values
of Ra . Linear Wall Temperature Variation.
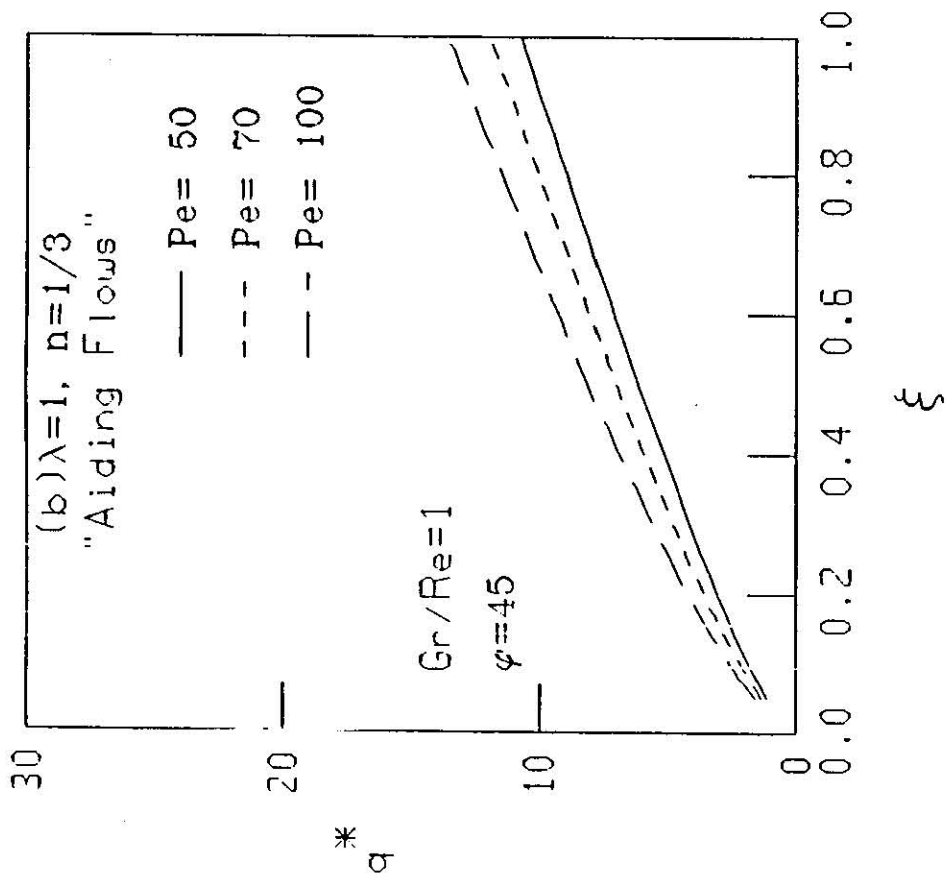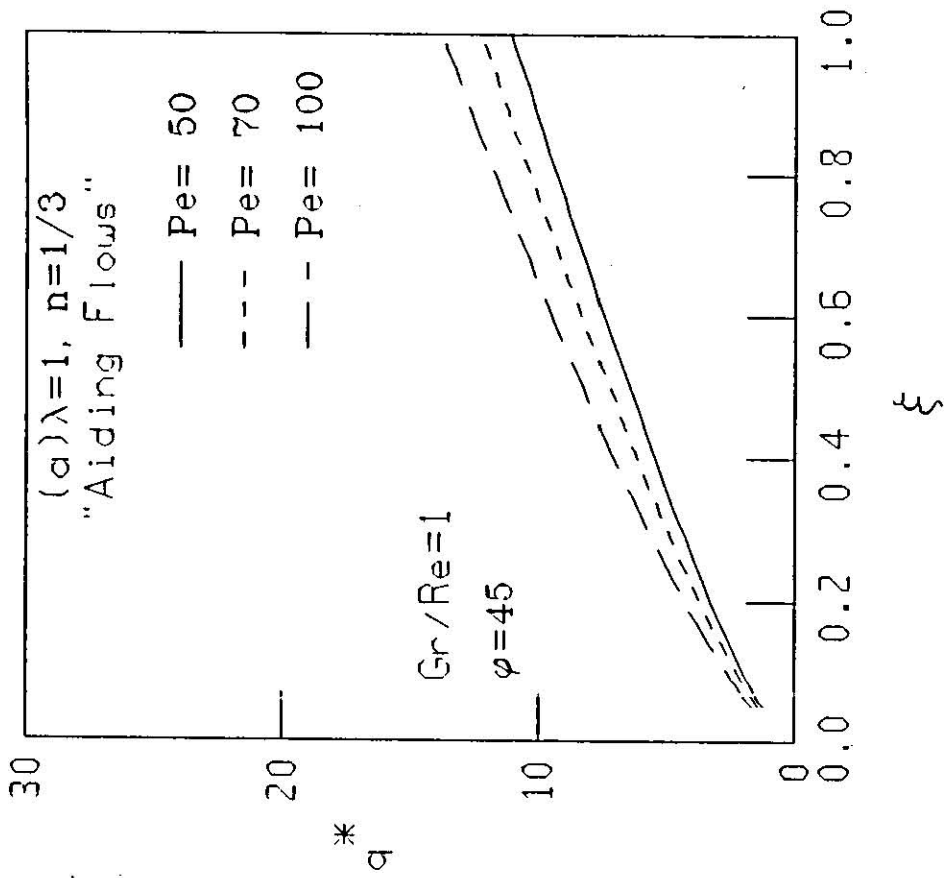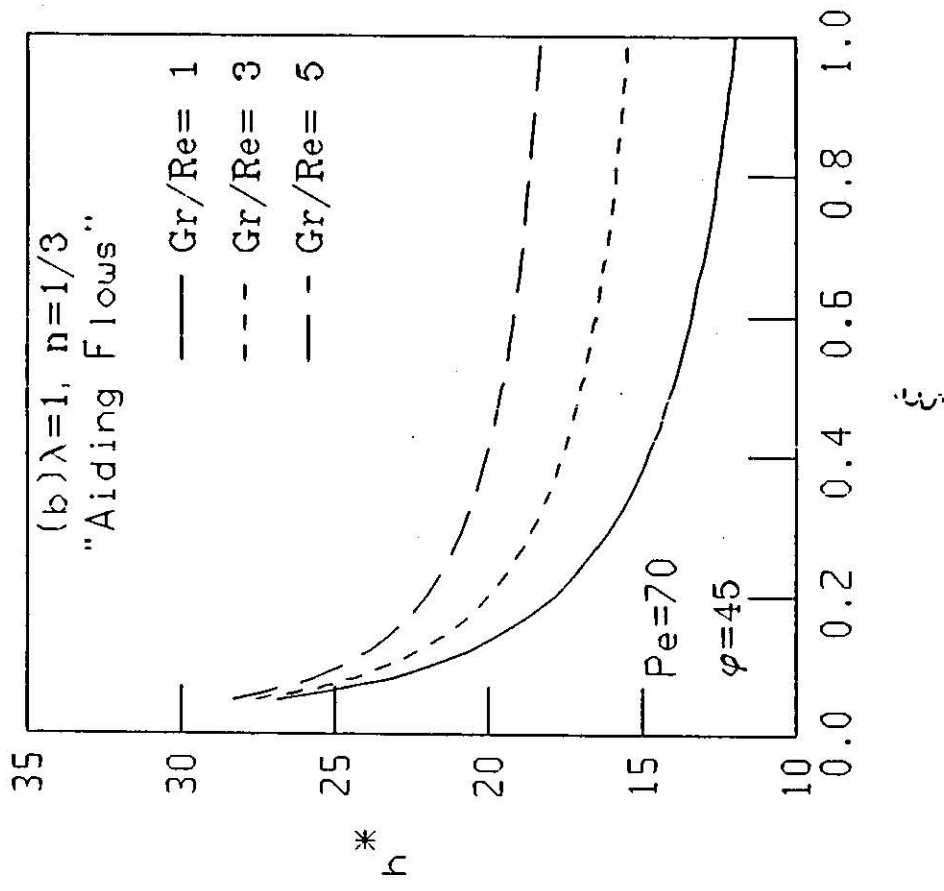(a) Configuration (a) , (b) Configuration (b)
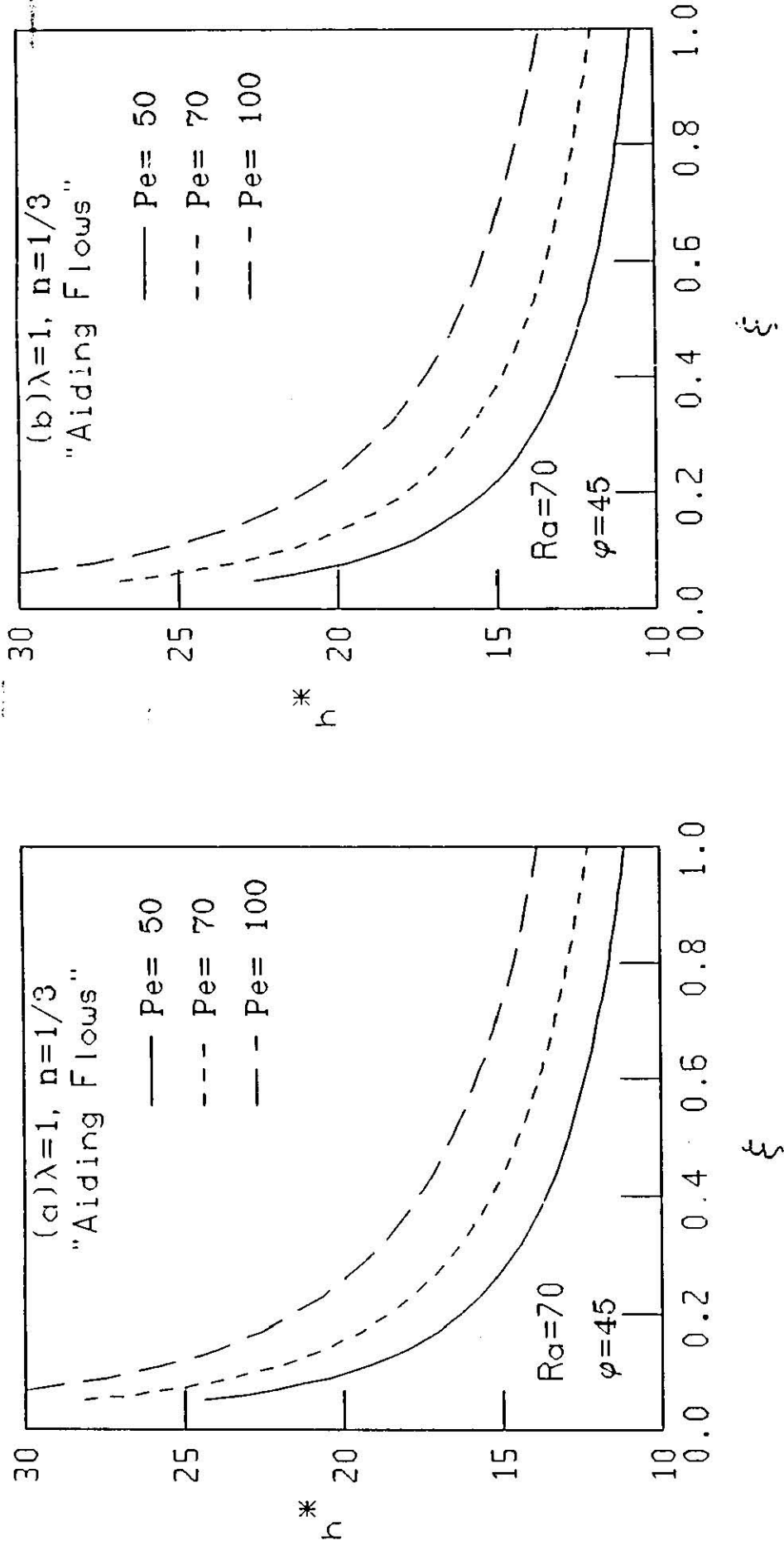
Fig.(5 – 30) Local Heat Transfer Coefficient For Selected Values
of Pe. Linear Wall Temperature Variation.
(a) Configuration (a) , (b) Configuration (b)
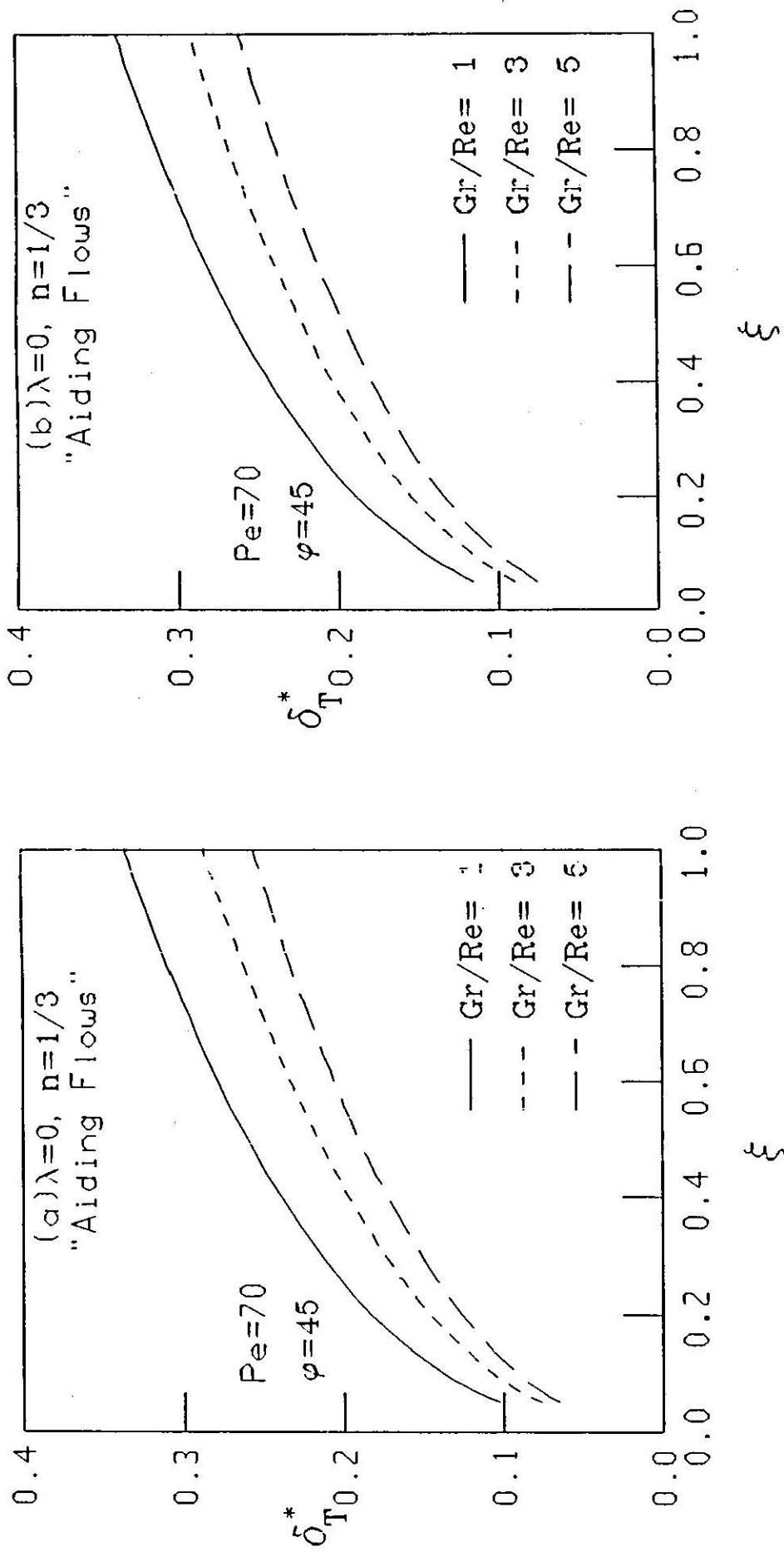
Fig.(5 – 31) Local Thermal Boundary Layer Thickness For Selected

Values of Gr/Re. Isothermal Walls.

(a) Configuration (a) , (b) Configuration (b)
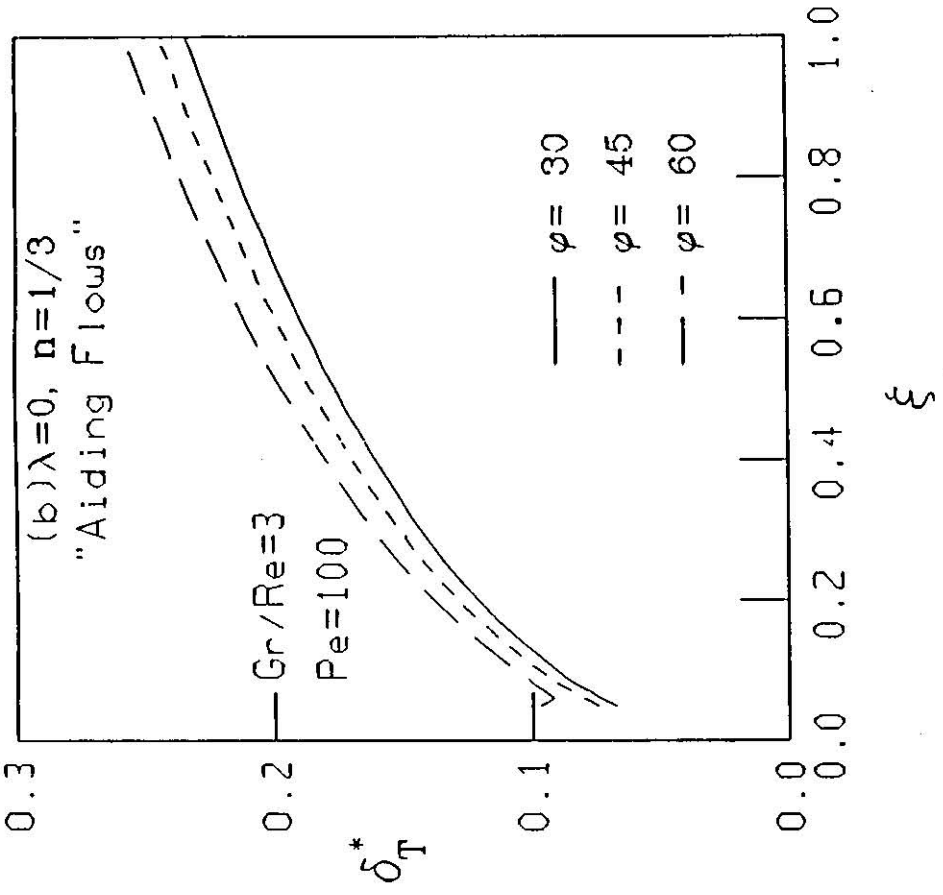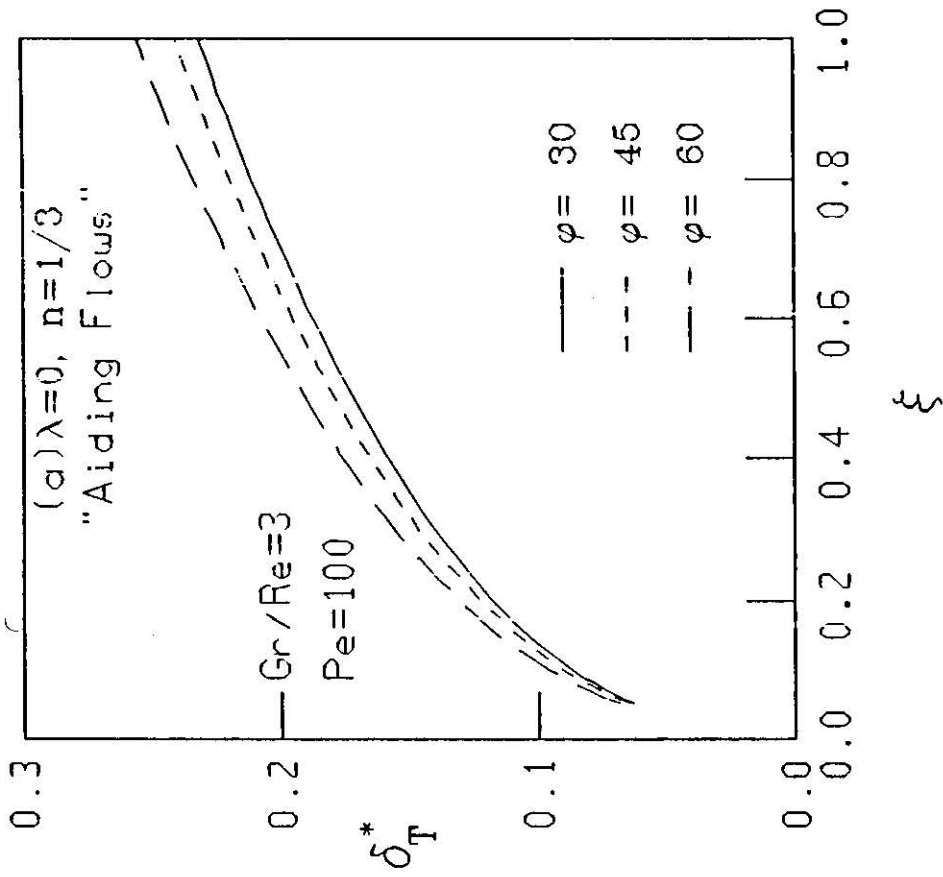
Fig.(5 – 32) Local Thermal Boundary Layer Thickness For Selected

Values of φ . Isothermal Walls.

(a) Configuration (a) , (b) Configuration (b)
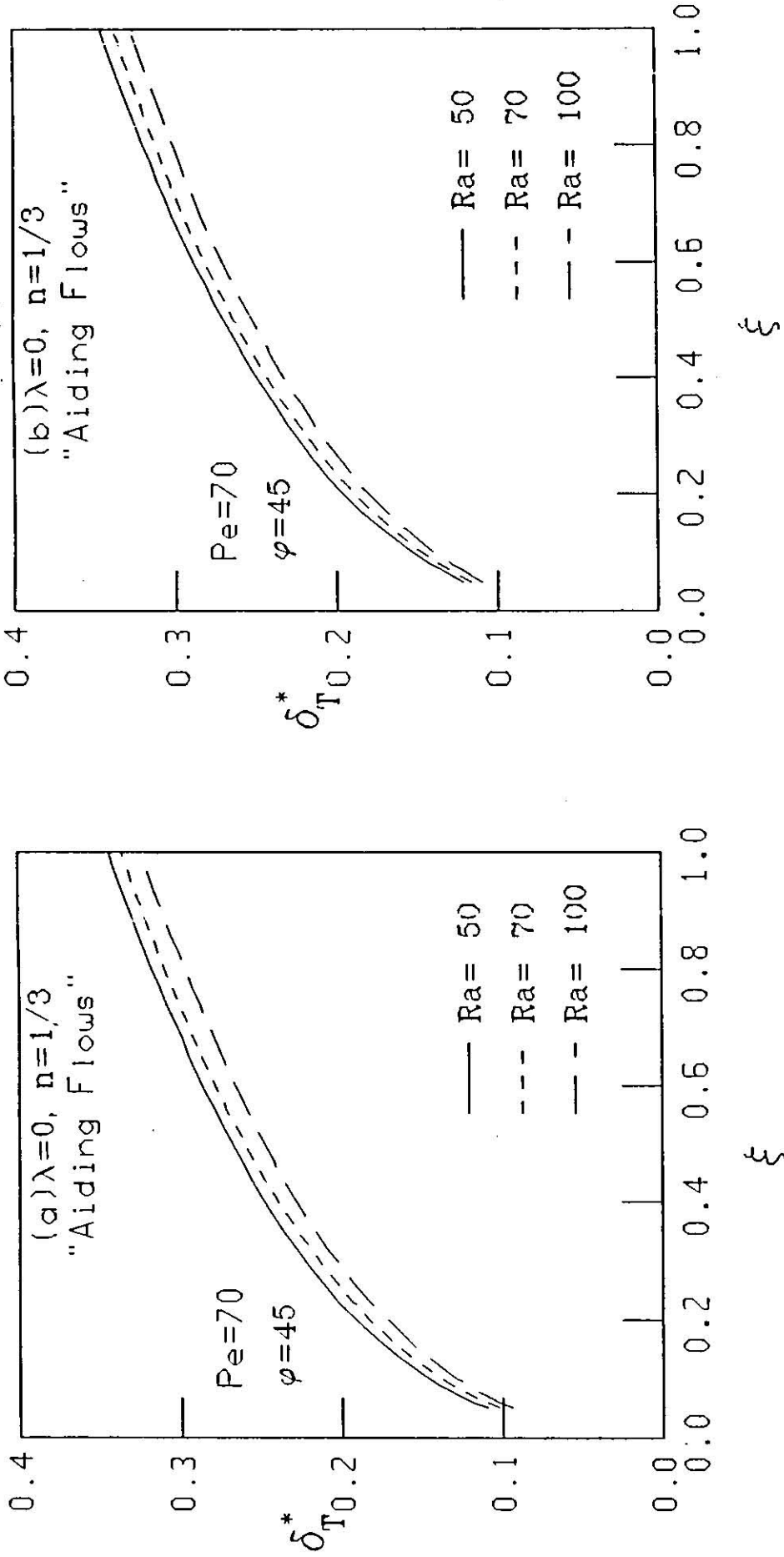
Fig.(5 – 33) Local Thermal Boundary Layer Thickness For Selected
Values of Ra. Isothermal Walls.

(a) Configuration (a) , (b) Configuration (b)
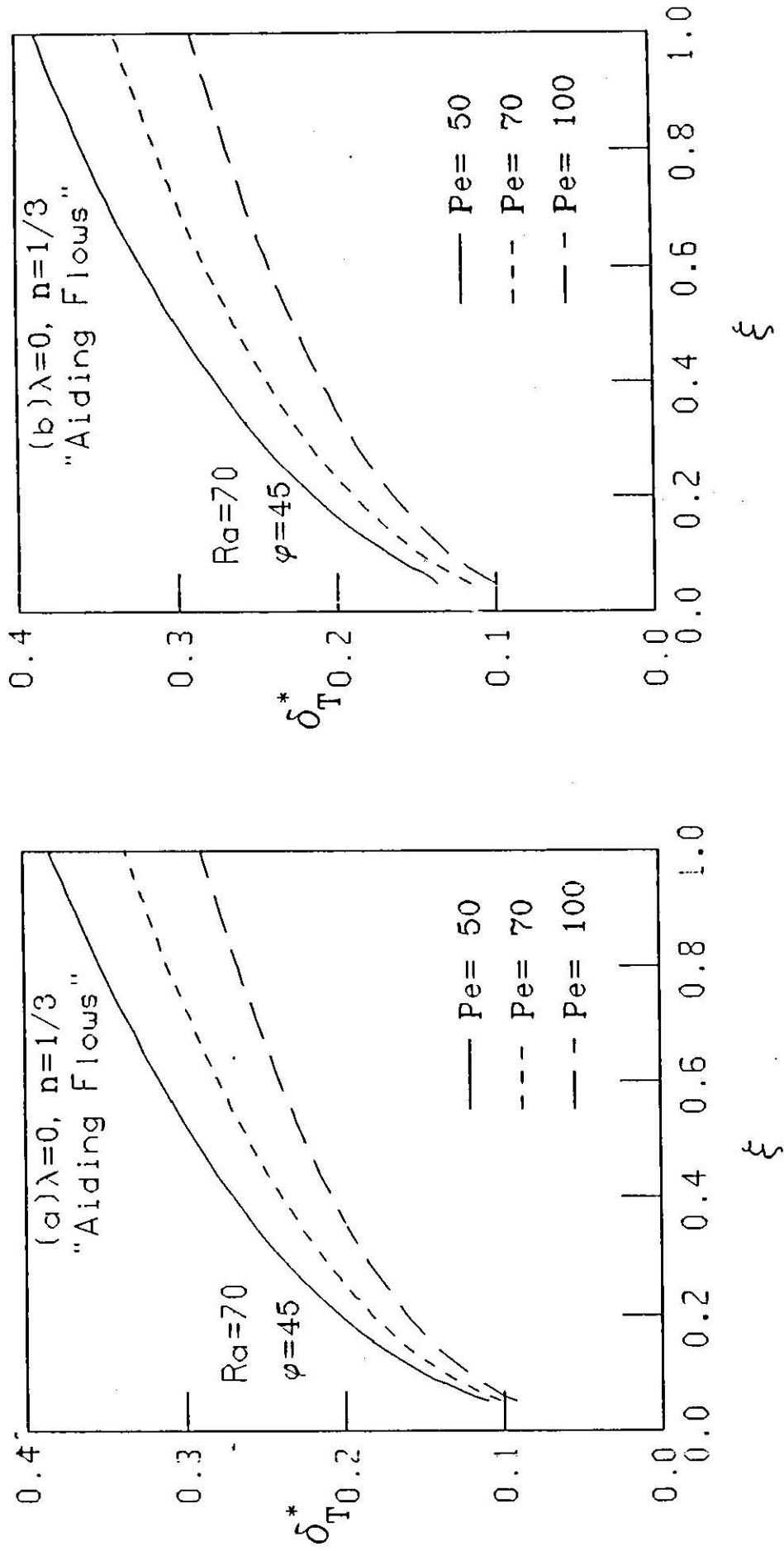
Fig.(5 - 34) Local Thermal Boundary Layer Thickness For Selected

Values of Pe. Isothermal Walls.
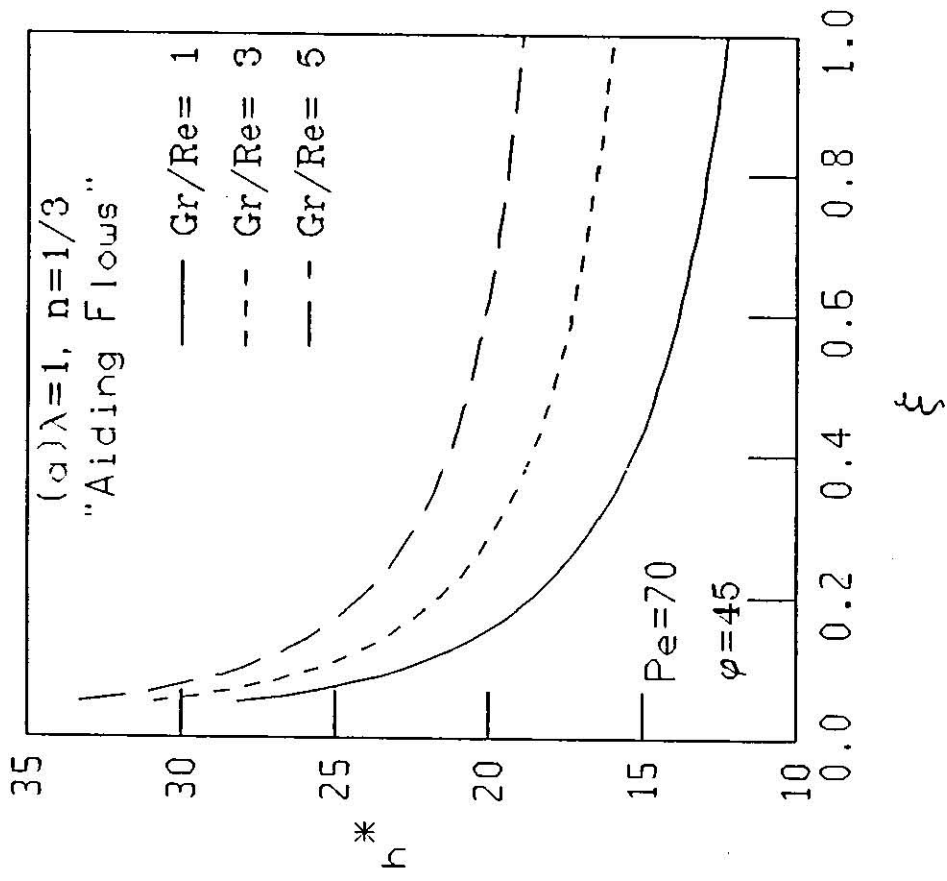
(a) Configuration (a) , (b) Configuration (b)
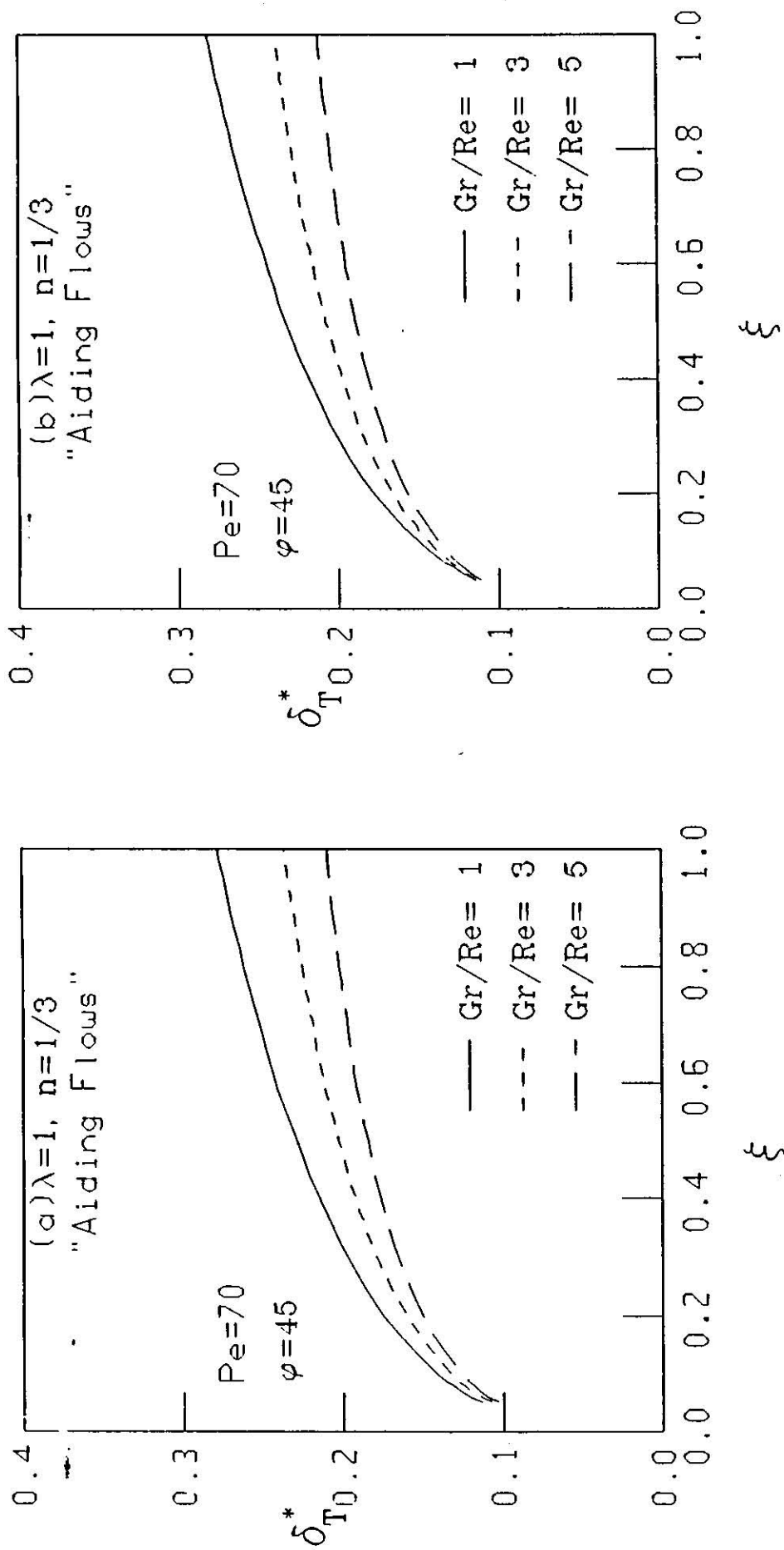
Fig.(5 - 35) Local Thermal Boundary Layer Thickness For Selected
Values of Gr/Re. Linear Wall Temperature Variation.
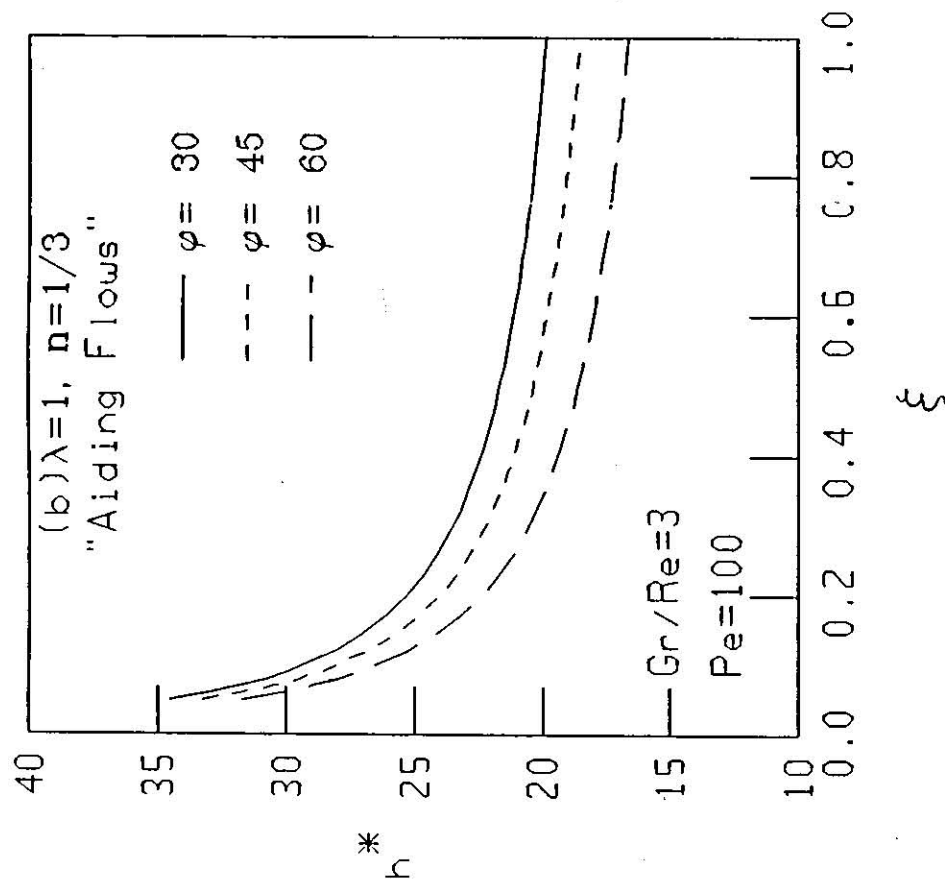(a) Configuration (a) , (b) Configuration (b)
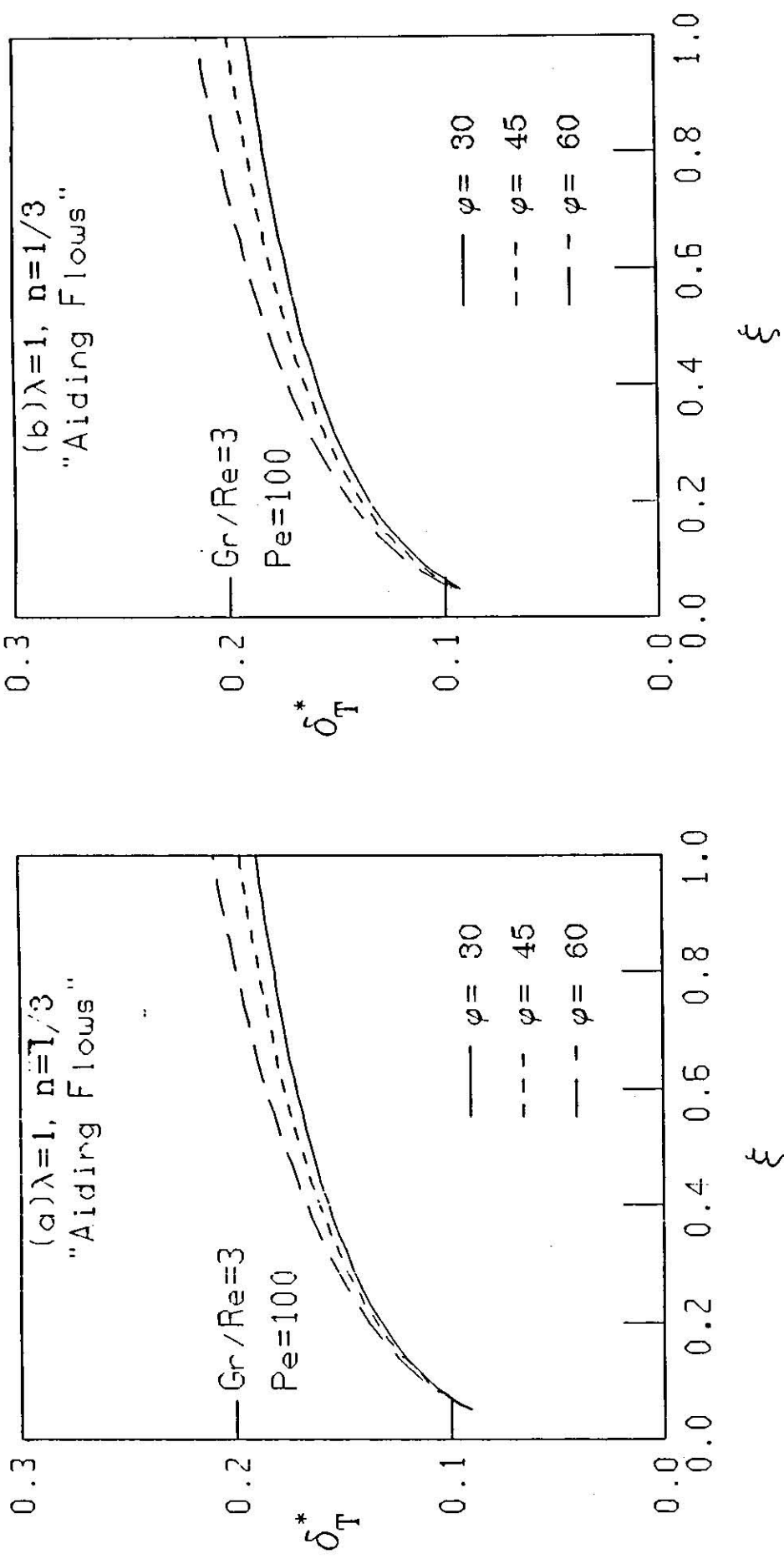
Fig.(5 – 36) Local Thermal Boundary Layer Thickness For Selected
Values of φ · Linear Wall Temperature Variation.
(a) Configuration (a) , (b) Configuration (b)
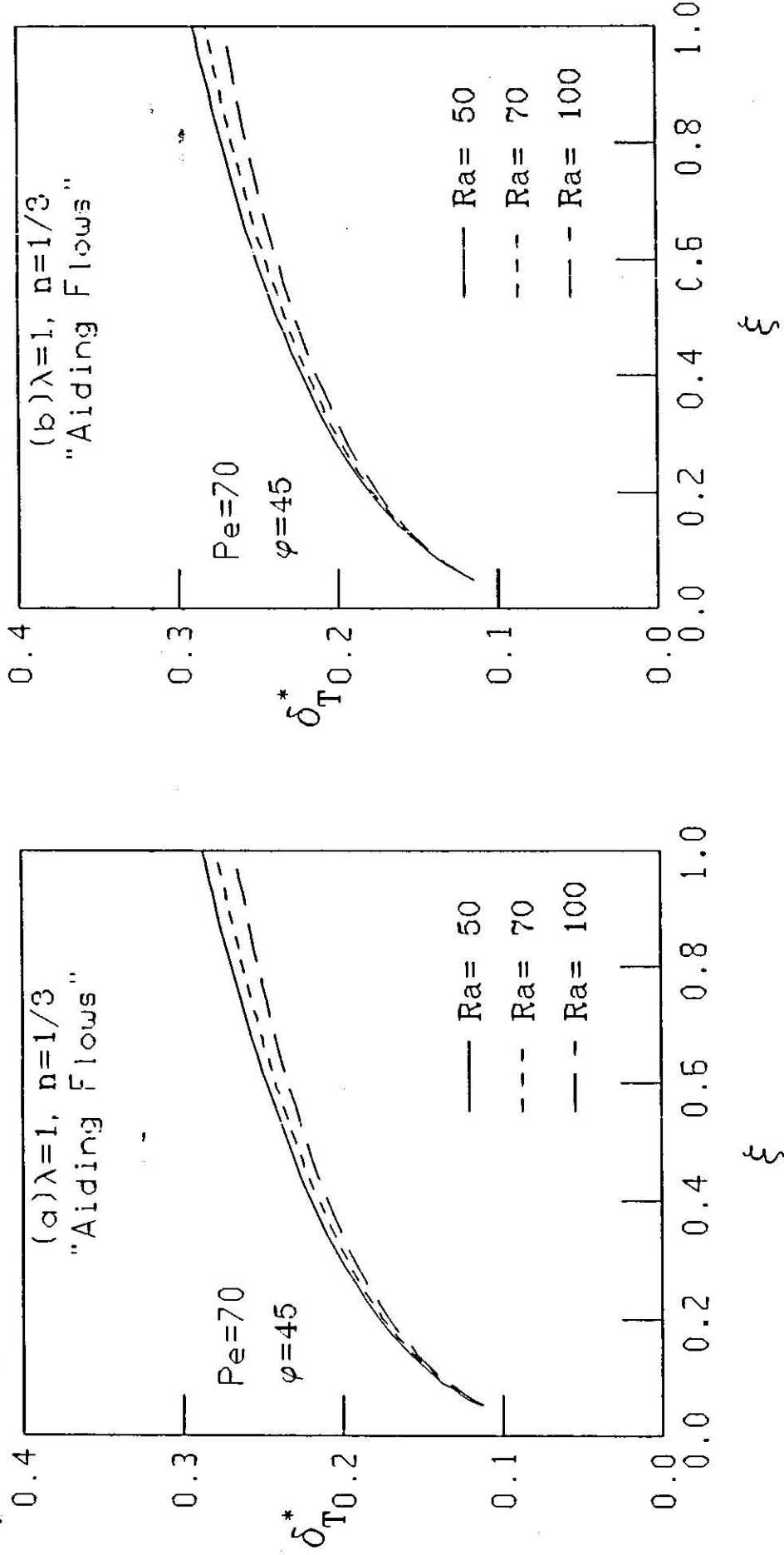
Fig.(5 - 37) Local Thermal Boundary Layer Thickness For Selected
Values of Ra. Linear Wall Temperature Variation.
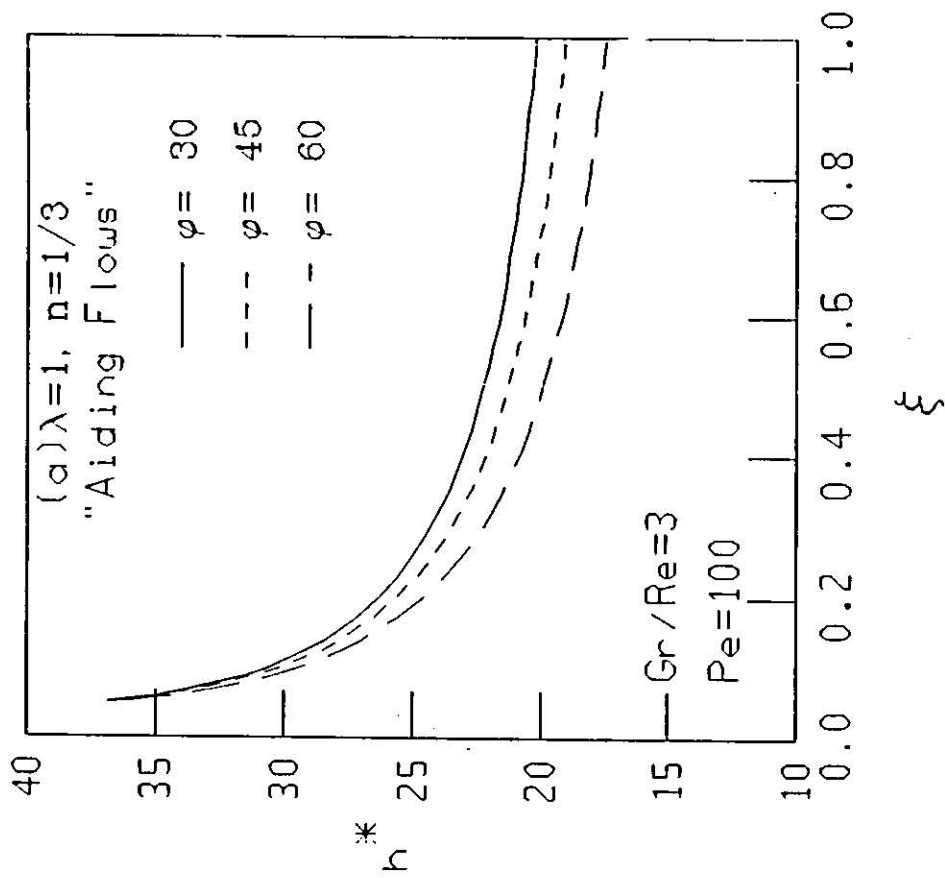(a) Configuration (a) , (b) Configuration (b)
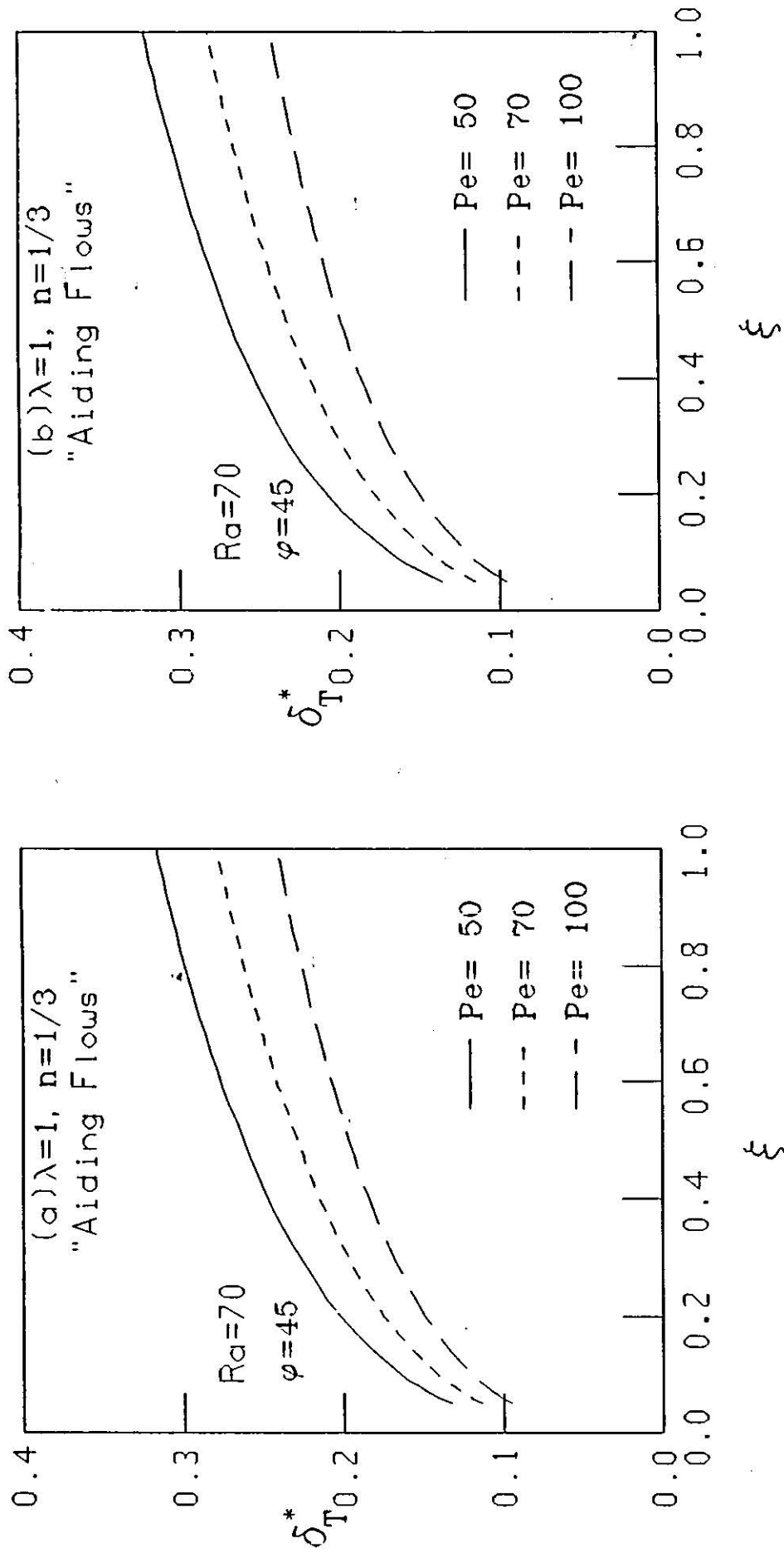
Fig.(5 – 38) Local Thermal Boundary Layer Thickness For Selected
Values of Pe. Linear Wall Temperature Variation.
(a) Configuration (a) , (b) Configuration (b)

Chapter 6

# CONCLUSIONS AND RECOMMENDATIONS

6.1 Conclusions

This work investigates the problem of mixed convection from inclined flat surfaces in porous medium. The following items are concluded:

1. Momentum and thermal boundary-layers are found to be non-similar. Similarity, however, does exist for the special case of $\lambda = n = -1$. The non-similarity is caused by the dependence of the wall temperature and the free stream velocity on the streamwise location and from the retaining of the normal buoyancy component.

2. The present problem involves many parameters. The mixed convection parameter, the Rayleigh number and the Peclet number describes the relative importance of the inertia and buoyancy forces. The analysis involves the inclination and the streamwise location parameters. Also, the analysis admits the general possible variation of the wall temperature and the free stream velocity along the surface.

3. The possible position of the bounding surface over or below the porous medium affects the normal buoyancy component contribution to the problem. Shifting the flow towards free convection (increasing Gr/Re or Ra or decreasing Pe) increases

89

the heat transfer characteristics variations between the two configurations. These variations were found, however, insignificant for the used parameter ranges.

4. The inclination effect comes from the relative magnitudes of the two components of buoyancy. Increasing the inclination increases the normal component of buoyancy and the heat transfer rate decreases.

5. The average Nusselt number and the total heat transfer rate are enhanced by increasing the mixed convection parameter, the Rayleigh number and the Peclet number, and by decreasing the inclination.

6. Maximum heat flux occurs near the tip and decreases as moving downstream in the isothermal walls case, while for the linear variations of wall temperature, it continues to increase as moving downstream.

7. Constant heat flux is never attained for inclined walls. Constant heat flux does, however, exist for vertical walls with wall temperature and free stream variations exponent of one third.

6.2   Recommendations

In the present work, a general investigation of the problem of mixed convection from inclined flat surfaces in porous medium was conducted. Further work in the problem is required and the following are suggestions for further investigations based on the present work:

1. The extension of Darcy's law to account for inertia and boundary effects for high flow rate problems. In this case the momentum equation will contain more terms and will be of third order.

2. The present analysis involves a large number of parameters and it is needed to consider some of these parameters over wider ranges. The selected ranges in the present work may be not enough to describe completely the behaviour of the flow.

3. The conjugate problem is also needed to be investigated. The flow may be mixed or free. The Darcian or non-Darcian models may be considered.

4. In the three previous items or in the present work, the effect of withdrawal and injection of fluid may also be included.

5. The effects of curvature through the study of inclined cylinders is recommended to be investigated. Free or mixed convections may be considered . Also, the analysis may consider Darcy or non-Darcy models. The conjugate problem may also be studied.

6. Experimental works are needed to investigate inclined walls or cylinders in porous medium.

References

1. P. Cheng, *Heat transfer in geothermal systems*, Adv. Heat Transfer, vol. 14, pp. 1-105, (1978).

2. H. Schlichting, *Boundary-layer theory*, McGraw-Hill, New-York, (1968).

3. I. II. Shames, *Mechanics of fluids*, McGraw-IIill, New-York, (1982) .

4. E. M. Sparrow, II. Quack and C. J. Boerner, *Local nonsimilarity boundary -layer solutions*, AIAA Journal, vol. 8, pp 1936-1942, (1970).

5. E. N. Sparrow and H. S. Yu, *Local Non-similarity thermal boundary-layer solutions*, Trans. ASME J. of Heat Transfer , vol. 93, pp. 328-334, (1971).

6. W. J. Minkowycz and E. M. Sparrow, *Local nonsimilar solutions for natural convection on a vertical cylinder*, Trans. ASME J. Heat Transfer, vol.96, pp 178-183, (1974).

7. T. S. Chen and A. Mucolgu, *Boundary effects on forced convection along a vertical cylinder*, Trans. ASME J. Heat Transfer, vol. 97, pp. 198-203, (1975).

8. R. De-Wiest (editor), *Flow through porous media*, Academic Press, New-York, (1969).

9. F. A. L. Dullien, *Porous media, fluid transport and pore structure*, Academic Press, New-York, (1979).

10. K. Vafai, *Convection flow and heat transfer in variable-porosity media*, J. Fluid Mech., vol. 147, pp. 233-259, (1984).

11. V. Prasad and A. Tuntomo, *Inertia effects on natural convection in a vertical porous cavity*, Numerical Heat Transfer, vol. 11, pp. 295-320, (1987).

12. K. Vafai and C. L. Tien, *Boundary and inertia effects on flow and heat transfer in porous media*, Int. J. Heat Mass Transfer, vol. 24, pp. 195-203, (1981).

13. A. Bejan and D. Poulikakos, *The nondarcy regime for vertical boundary layer natural convection in a porous medium*, Int. J. Heat Mass Transfer, vol. 27, pp. 717-722, (1984).

14. N. Kladias and V. Prasad, *Natural convection in horizontal porous layers: effects of Darcy and Prandtl numbers*, Trans. ASME J. Heat Transfer, vol. 111, pp. 926-935, (1989).

15. J. G. Georgiadis and I. Catton, *Prandtl number effect on Benard convection in porous media*, Trans. ASME J. Heat Transfer, vol. 108, pp. 284-290, (1986).

16. P. Cheng, *The influence of lateral mass flux on free convection boundary layers in a saturated porous medium*, Int. J. Heat Mass Transfer. vol 20, pp. 201-206, (1977).

17. W. Minkowycz and P. Cheng, *Local non-similar solutions for free convective flow with uniform lateral mass flux in a porous medium*, Lett. Heat Mass Transfer, vol. 9, pp. 159-168, (1982).

18. I. Pop J. K. Sunada P. Cheng and W. J. Minkowycz, *Conjugate free convection from long vertical plate fins embedded in a porous medium at high Rayleigh numbers*, Int. J. Heat Mass Transfer, vol. 28, pp. 1629-1636, (1985).

19. Jin-Yuan Liu and W. Minkowycz, *The influence of lateral mass flux on conjugate natural convection from a vertical plate fin in a saturated porous medium*, Numerical Heat Transfer, vol. 10, pp. 507-520, (1986).

20. J. Y. Jang and W. J. Chang, *Buoyancy-induced inclined boundary layer flow in a porous medium resulting from combined heat and mass buoyancy effects*, Int. Comm. Heat Mass Transfer, vol. 15, pp. 17-30, (1988).

21. P. Cheng and I-Dee Chang, *Buoyancy induced flows in a saturated porous medium adjacent to impermeable horizontal surface*, Int. J. Heat Mass Transfer, vol. 19, pp. 1267-1272, (1976).

22. J. H. Merkin, *Free convection boundary layers on axi-symmetric and two-dimensional bodies of arbitrary shape in a saturated porous medium* , Int. J. Heat Mass Transfer, vol. 22, pp. 1461-1462, (1979).

23. A. Yucel, *The influence of injection or withdrawal of fluid on free convection about a vertical cylinder in a porous medium*, Numerical Heat Transfer, vol. 7, pp. 483-493, (1984).

24. Jin-Yuan Liu Shagi-Di Shih and W. J. Minkowycz, *Conjugate natural convection about a vertical cylindrical fin with lateral mass flux in a saturated porous medium*, Int. J. Heat Mass Transfer, vol. 30, pp. 623-630, (1987).

25. W. J. Minkowycz and E. M. Sparrow, *Interaction between surface mass transfer and transverse curvature in natural convection boundary layers*, Int. J. Heat Mass Transfer, vol. 22, pp. 1445-1454, (1979).

26. W. J. Minkowycz and P. Cheng, *Free convection about a vertical cylinder embedded in a porous medium*, Int. J. Heat Mass Transfer, vol. 20 , pp 805-813, (1977).

27. A. Nakayama, H. Koyama and F. Kundhara, *Similarity solution for non-Darcy free convection from nonisothermal curved surfaces in a fluid saturated porous medium*, Trans. ASME J. Heat Transfer, vol. 111, pp. 807-810, (1989).

28. Jin-Yuan Liu,W. J. Minkowycz and P. Cheng, *Conjugate mixed convection heat transfer analysis of a plate fin embedded in a porous medium* , Numerical Heat Transfer, vol. 9, pp. 575-590, (1986).

29. U. S. Gill and W. J. Minkowycz, *Boundary and inertia effects on conjugate heat transfer from a vertical plate fin in a high-porosity porous medium*, Int. J. Heat Mass Transfer, vol. 31, pp. 419-427, (1988).

30. P. Ranganathan and R. Viskanta, *Mixed convection boundary-layer flow along a vertical surface in a porous medium*, Numerical Heat Transfer, vol. 7, pp. 305-317, (1984).

31. F. C. Lai, V. Paracad and F. A. Kulacki, *Aiding and opposing mixed convection in a vertical porous layer with a finite wall heat source* , Int. J. Heat Mass Transfer, vol. 31, pp. 1049-1061, (1988).

32. P. Cheng, *Combined free and forced convection flow about inclined surfaces in porous medium*, Int.J. Heat Mass Transfer. vol. 20, pp. 807-814, (1977)

33. B. C. Chandrasekhara and P. M. S. Namboodiri, *Influence of variable permeability on combined free and forced convection about inclined surfaces in porous medium*, Int. J. Heat Mass Transfer, vol. 28, pp. 199-206, (1985).

34. P. Cheng, *Similarity solutions for mixed convection from horizontal impermeable surfaces in saturated porous media*, Int. J. Heat Mass Transfer, vol. 20, pp. 893-898, (1977).

35. W. J. Minkowycz, P. Cheng and R. N. Hirschberg, *Non-similar boundary layer analysis of mixed convection about a horizontal surface over a fluid- saturated porous medium*, Int. Comm. Heat Mass Transfer,vol.11, pp.127-141,(1984).

36. F. C. Lai and F. A. Kulacki, *The influence of surface mass flux on mixed convection over horizontal plates in saturated porous medium*, Int . J. Heat Mass Transfer, vol. 33, pp. 576-579, (1990).

37. Jin-Yuan Liu , W. J. Minkowycz and P. Cheng, *Conjugate mixed convection - conduction along a cylindrical fin in porous medium*, Int. J. Heat Mass transfer, vol. 29, pp. 769-775, (1986).

38. P. Cheng, *Convective heat transfer in porous layers by integral methods*, Lett. Heat Mass Transfer, vol. 5, pp. 243-252, (1978).

39. M. Kaviany, *Boundary-layer treatment of forced convection heat transfer from a semi-infinite flat plate embedded in porous media*, Trans. ASME J. Heat Transfer, vol. 109, pp. 345-349, (1987).

40. R. M. Fand, T. E. Steinberger and P. Cheng, *Natural convection from a horizontal cylinder embedded in a porous medium*, Int. J. Heat Mass Transfer, vol. 29, pp. 119-133, (1986).

41. H. Inaba, M. Sugawara and J. Blumenberg, *Natural convection heat transfer in an inclined porous layer*, Int. J. Heat Mass Transfer, vol. 31, pp. 1365-1374, (1988).

42. N. Seki, S. Fukusako and H. Inaba, *Heat transfer in a confined rectangular cavity packed with porous media*, Int. J. Heat Mass Transfer, vol. 21, pp. 985-989, (1978).

43. V. E. Schroch and A. D. K. Laird, *Physical model of combined forced and natural convection in wet geothermal formations*, Trans. ASME J. Heat Transfer, vol. 101,

pp. 213-219, (1976).

44. W. J. Minkowycz and E. M. Sparrow, *Numerical Solution Scheme For Local Non-similarity Boundary-Layer Analysis*, Numerical Heat Transfer, vol. 1, pp. 69-85, (1978).

45. M. A. Combarnous and S. A. Bories, Adv. Hydrosci., vol. 9, pp. 231-307, (1975).

Appendix A
Non-Similar Transformation

The two governing equations are

$$\frac{\partial^2 \psi}{\partial y^2} = \pm \frac{K \rho_\infty g \beta}{\mu} \left[\cos \phi \frac{\partial T}{\partial y} \mp \sin \phi \frac{\partial T}{\partial x} \right] \tag{A.1}$$

$$\frac{\partial^2 T}{\partial y^2} = \frac{1}{\alpha} \left[\frac{\partial \psi}{\partial y} \frac{\partial T}{\partial x} - \frac{\partial \psi}{\partial x} \frac{\partial T}{\partial y} \right] \tag{A.2}$$

introduce the following dimensionless variables

$$\eta(x,y) = \left(\frac{u_\infty x}{\alpha} \right)^{1/2} \frac{y}{x} = \left(\frac{B}{\alpha} \right)^{1/2} x^{\frac{n-1}{2}} y \tag{A.3}$$

$$\xi(x) = \frac{x}{L} \tag{A.4}$$

$$\psi(x,\eta,\xi) = (\alpha u_\infty x)^{1/2} f(\eta,\xi) = (\alpha B)^{1/2} x^{\frac{n+1}{2}} f(\eta,\xi) \tag{A.5}$$

$$\theta(\eta,\xi) = \frac{T - T_\infty}{T_w - T_\infty} \tag{A.6}$$

with

$$\Delta T = T_w - T_\infty = \pm A x^\lambda$$

Equation (A.6) gives

$$T(x,\eta,\xi) = \pm A x^\lambda \theta(\eta,\xi) + T_\infty \tag{A.7}$$

recalling from the chain rule that if three functions g, f, and k are defined such that

$$g(x,\eta,\xi) = f(x).k(\eta,\xi)$$

then

$$\frac{\partial g}{\partial x} = k\frac{\partial f}{\partial x} + f\frac{\partial k}{\partial x}$$

and

$$\frac{\partial g}{\partial y} = f\frac{\partial k}{\partial y}$$

then, the following chain relations are obtained

$$\frac{\partial}{\partial x} = \frac{\partial}{\partial \eta}\frac{\partial \eta}{\partial x} + \frac{\partial}{\partial \xi}\frac{\partial x}{\partial \xi} + \frac{\partial}{\partial x}\frac{\partial x}{\partial x} \tag{A.8}$$

$$\frac{\partial}{\partial y} = \frac{\partial}{\partial \eta}\frac{\partial \eta}{\partial y} + \frac{\partial}{\partial \xi}\frac{\partial y}{\partial \xi} + \frac{\partial}{\partial x}\frac{\partial x}{\partial y} \tag{A.9}$$

the last two terms on the RHS of Equation (A.9) are zeros and the relation reduces to

$$\frac{\partial}{\partial y} = \frac{\partial}{\partial \eta}\frac{\partial \eta}{\partial y} \tag{A.10}$$

upon substituting Equations (A.3)-(A.7) into Equations (A.8) and (A.10) the transformation is performed as follows

$$\frac{\partial \eta}{\partial x} = \left(\frac{n-1}{2}\right)\left(\frac{B}{\alpha}\right)^{1/2} x^{\frac{n-3}{2}} y \tag{A.11}$$

$$\frac{\partial \eta}{\partial y} = \left(\frac{B}{\alpha}\right)^{1/2} x^{\frac{n-1}{2}} \tag{A.12}$$

$$\frac{\partial \xi}{\partial x} = \frac{1}{L} \tag{A.13}$$

then Equations (A.8) and (A.10) become

$$\frac{\partial}{\partial x} = \left(\frac{n-1}{2}\right)\left(\frac{B}{\alpha}\right)^{1/2} x^{\frac{n-3}{2}} y\frac{\partial}{\partial \eta} + \frac{1}{L}\frac{\partial}{\partial \xi} + \frac{\partial}{\partial x} \tag{A.14}$$

$$\frac{\partial}{\partial y} = \left(\frac{B}{\alpha}\right)^{1/2} x^{\frac{n-1}{2}}\frac{\partial}{\partial \eta} \tag{A.15}$$

upon applying Equations (A.11)-(A.15) obtain the following

$$u = \frac{\partial \psi}{\partial y} = u_\infty f' \tag{A.16}$$

$$-v = \frac{\partial \psi}{\partial x} = \frac{1}{2}\left(\frac{\alpha u_\infty}{x}\right)^{1/2}\left[(n+1)f + 2\xi\frac{\partial f}{\partial \xi} + (n-1)\eta f'\right] \tag{A.17}$$

$$\frac{\partial^2 \psi}{\partial y^2} = u_\infty f''\left(\frac{u_\infty}{\alpha x}\right)^{1/2} \tag{A.18}$$

$$\frac{\partial T}{\partial y} = \Delta T \theta'\left(\frac{u_\infty x}{\alpha}\right)^{1/2}\frac{1}{x} \tag{A.19}$$

$$\frac{\partial T}{\partial x} = \lambda \Delta T x^{-1}\theta + \frac{\Delta T}{L}\frac{\partial \theta}{\partial \xi} + \left(\frac{n-1}{2}\right)\eta\Delta T x^{-1}\theta' \tag{A.20}$$

$$\frac{\partial^2 T}{\partial y^2} = \Delta T\frac{u_\infty}{\alpha x}\theta'' \tag{A.21}$$

A.1   The Momentum Equation

Substitute Equations (A.18)-(A.20) into Equation (A.1) and upon arranging get

$$f'' = \pm\frac{\beta K g A}{\nu B}x^{\lambda-n}$$
$$\left[\theta'\cos\phi \mp \left(\frac{\alpha}{Bx^{n+1}}\right)^{1/2}\sin\phi\left(\lambda\theta + \frac{x}{L}\frac{\partial\theta}{\partial\xi} + \left(\frac{n-1}{2}\right)\eta\theta'\right)\right] \tag{A.22}$$

or

$$f'' = \pm\left(\frac{\beta K g A}{\nu B}L^{\lambda-n}\right)\xi^{\lambda-n}$$
$$\left[\theta'\cos\phi \pm \left(\frac{\alpha}{BL^{n+1}}\right)^{1/2}\xi^{-\left(\frac{n+1}{2}\right)}\sin\phi\left(\lambda\theta + \xi\frac{\partial\theta}{\partial\xi} + \left(\frac{n-1}{2}\right)\eta\theta'\right)\right] \tag{A.23}$$

finally

$$f'' = \pm\Omega\xi^{\lambda-n}\left[\theta'\cos\phi \mp \left(\frac{1}{Pe}\right)^{1/2}\right.$$
$$\left.\xi^{-\left(\frac{n+1}{2}\right)}\sin\phi\left(\lambda\theta + \xi\frac{\partial\theta}{\partial\xi} + \frac{n-1}{2}\eta\theta'\right)\right] \tag{A.24}$$

A.2   The Energy Equation

Substitute Equations (A.10), (A.17), (A.19), (A.20) and (A.21) into Equation (A.2) and upon arranging get

$$\theta'' - \lambda\theta f' + \left(\frac{n+1}{2}\right)f\theta' = \xi\left(f'\frac{\partial\theta}{\partial\xi} - \theta'\frac{\partial f}{\partial\xi}\right)$$
(A.25)

Appendix B

Integral Equations

The governing Equations of the three levels derived in chapter 4 are all of the form

$$\Lambda'' + P_\Lambda \Lambda' = Q_\Lambda \tag{B.1}$$

where the variable Λ is subjected to conditions at $\eta = 0$ and ∞.

Define the integral factor

$$\exp\left(\int_0^\eta P_\Lambda d\eta\right) \tag{B.2}$$

multiply (B.1) by (B.2)

$$\exp\left(\int_0^\eta P_\Lambda d\eta\right) \cdot (\Lambda')' + \exp\left(\int_0^\eta P_\Lambda d\eta\right) \cdot P_\Lambda \Lambda' = \exp\left(\int_0^\eta P_\Lambda d\eta\right) \cdot Q_\Lambda \tag{B.3}$$

or

$$\left[\Lambda' \exp\int_0^\eta P_\Lambda d\eta\right]' = Q_\Lambda \exp\int_0^\eta P_\Lambda d\eta \tag{B.4}$$

integrating

$$\Lambda' = \exp - \int_0^\eta P_\Lambda(\eta^*) d\eta^* \cdot \left[\int_0^\eta Q_\Lambda(\eta^*) \exp\left(\int_0^{\eta^*} P_\Lambda d\eta\right) d\eta^* + c\right] \tag{B.5}$$

where η^* is a dummy variable. Integrating again

$$\mathbf{399031}\Lambda = \int_0^\eta \Lambda'(\eta^*) d\eta^* + \Lambda(0) \tag{B.6}$$

Λ could be either f or θ. To find the constant c in Equation (B.5) integrate Equation (B.5) from $\eta = 0$ to ∞

$$\Lambda(\infty) - \Lambda(0) = \int_0^\infty \exp\left(-\int_0^\eta P(\eta^*)d\eta^*\right) c$$
$$+ \int_0^\infty \exp\left(-\int_0^\eta P(\eta^*)d\eta^*\right) \int_0^\eta Q(\eta^*)\exp\left(\int_0^{\eta^*} P_\Lambda(\eta)d\eta\right) d\eta^* \quad (B.7)$$

If the conditions $\Lambda(\infty)$ and $\Lambda(0)$ are known, use Equation (B.7) to fined c . In the cases where $\Lambda(0)$ and $\Lambda'(\infty)$ are known, c is found as follows;

Substitute the value of ∞ for η in Equation (B.5)

$$\Lambda'(\infty) = \exp - \int_0^{\widetilde{}} P_\Lambda(\eta^*)d\eta^* \cdot \left[\int_0^\infty Q_\Lambda(\eta^*)\exp\left(\int_0^{\eta^*} P_\Lambda(\eta)d\eta\right) d\eta^* + c\right] \quad (B.8)$$

or

$$c = \Lambda'(\infty)\exp - \int_0^\infty P_\Lambda(\eta^*)d\eta^* - \int_0^\infty Q_\Lambda(\eta^*)\exp\left(\int_0^{\eta^*} P_\Lambda d\eta\right) d\eta^* \quad (B.9)$$

The integration formulas used in the numerical computation is suggested in [43] and it was derived by fitting a third- degree polynomial through four points. For the interval $(\eta_{i+1} - \eta_i)$ adjacent to the left -hand boundary of a zone, the integral is computed from

$$\int_i^{i+1} F(\eta)d\eta = \frac{\Delta\eta}{24}(9F_i + 19F_{i+1} - 5F_{i+2} + F_{i+3}) \quad (B.10)$$

For the interval $(\eta_{k+1} - \eta_k)$ adjacent to right-hand boundary of a zone

$$\int_k^{k+1} F(\eta)d\eta = \frac{\Delta\eta}{24}(F_{k-2} - 5F_{k-1} + 19F_k + 9F_{k+1}) \quad (B.11)$$

For the inside interval, e.g. $(\eta_{j+1} - \eta_j)$

$$\int_j^{j+1} F(\eta)d\eta = \frac{\Delta\eta}{24}(-F_{j-1} + 13F_j + 13F_{j+1} - F_{j+2}) \quad (B.12)$$